

IOWA STATE UNIVERSITY  
Digital Repository

---

Retrospective Theses and Dissertations

Iowa State University Capstones, Theses and  
Dissertations

---

1985

# Wind-system performance optimization using microprocessor control

Mehrdad R. Mehrdad

*Iowa State University*

Follow this and additional works at: <https://lib.dr.iastate.edu/rtd>



Part of the [Electrical and Electronics Commons](#)

---

## Recommended Citation

Mehrdad, Mehrdad R., "Wind-system performance optimization using microprocessor control " (1985). *Retrospective Theses and Dissertations*. 7871.

<https://lib.dr.iastate.edu/rtd/7871>

This Dissertation is brought to you for free and open access by the Iowa State University Capstones, Theses and Dissertations at Iowa State University Digital Repository. It has been accepted for inclusion in Retrospective Theses and Dissertations by an authorized administrator of Iowa State University Digital Repository. For more information, please contact [digirep@iastate.edu](mailto:digirep@iastate.edu).

## **INFORMATION TO USERS**

This reproduction was made from a copy of a document sent to us for microfilming. While the most advanced technology has been used to photograph and reproduce this document, the quality of the reproduction is heavily dependent upon the quality of the material submitted.

The following explanation of techniques is provided to help clarify markings or notations which may appear on this reproduction.

1. The sign or "target" for pages apparently lacking from the document photographed is "Missing Page(s)". If it was possible to obtain the missing page(s) or section, they are spliced into the film along with adjacent pages. This may have necessitated cutting through an image and duplicating adjacent pages to assure complete continuity.
2. When an image on the film is obliterated with a round black mark, it is an indication of either blurred copy because of movement during exposure, duplicate copy, or copyrighted materials that should not have been filmed. For blurred pages, a good image of the page can be found in the adjacent frame. If copyrighted materials were deleted, a target note will appear listing the pages in the adjacent frame.
3. When a map, drawing or chart, etc., is part of the material being photographed, a definite method of "sectioning" the material has been followed. It is customary to begin filming at the upper left hand corner of a large sheet and to continue from left to right in equal sections with small overlaps. If necessary, sectioning is continued again—beginning below the first row and continuing on until complete.
4. For illustrations that cannot be satisfactorily reproduced by xerographic means, photographic prints can be purchased at additional cost and inserted into your xerographic copy. These prints are available upon request from the Dissertations Customer Services Department.
5. Some pages in any document may have indistinct print. In all cases the best available copy has been filmed.

**University  
Microfilms  
International**  
300 N. Zeeb Road  
Ann Arbor, MI 48106



8514423

**Mehrdad, Mehrdad R.**

WIND-SYSTEM PERFORMANCE OPTIMIZATION USING MICROPROCESSOR  
CONTROL

*Iowa State University*

PH.D. 1985

**University  
Microfilms  
International**

300 N. Zeeb Road, Ann Arbor, MI 48106



Wind-system performance optimization using  
micropocessor control

by

Mehrdad R. Mehrdad

A Dissertation Submitted to the  
Graduate Faculty in Partial Fulfillment of the  
Requirements for the Degree of  
DOCTOR OF PHILOSOPHY

Department: Electrical Engineering and  
Computer Engineering

Major: Electrical Engineering  
(Computer Engineering)

Approved:

Signature was redacted for privacy.

In Charge of Major Work

Signature was redacted for privacy.

For the Major Department

Signature was redacted for privacy.

For the Graduate College

Iowa State University  
Ames, Iowa

1985

## TABLE OF CONTENTS

	Page
I. INTRODUCTION	1
II. LITERATURE REVIEW	5
A. Aerodynamic Theory of Wind Systems	5
1. Power in the wind	5
2. Wind systems characteristics	6
3. Maximum rotor efficiency	8
4. Wind-system performance	9
B. Wind System Types	12
C. Previous Work on Improving Efficiency of Fixed-pitch Wind Systems	14
D. Scope of the Work	18
III. OPTIMIZING MICROPROCESSOR-BASED CONTROLLER	20
A. Background	20
B. Optimizing Technique Using Field Control	20
C. Controller	22
1. Functional description	22
D. System Development	24
1. Microprocessor	24
2. Field control	25
3. Output voltage transducer	44
4. Analog/digital converter	46
5. Power supply control	47
6. Overspeed brake control	49
7. Wind speed measurement	49
8. Overall schematic diagram and theory of operation	60
9. Control program	66
E. Physical Description	87
F. Installation	89
G. Operation	93

	Page
IV. EXPERIMENTAL PROCEDURE AND RESULTS	96
A. Test Systems	96
1. 10-kW, 23-foot blade Jacobs wind system	98
2. 17.5-kW, 26-foot blade Jacobs wind system	99
B. Method Used for Collection of Performance Data	99
C. Modes of Operation	102
1. Operation in fixed-field mode	102
2. Operation with a synchronous inverter	102
3. Operation in controlled mode	103
D. Results	103
1. Data correction method	103
2. Performance data	104
3. Performance improvement	104
V. CONCLUSIONS	116
VI. SUGGESTIONS FOR FUTURE STUDY	118
VII. BIBLIOGRAPHY	119
VIII. ACKNOWLEDGMENTS	121
IX. APPENDIX A	122
X. APPENDIX B	125

## LIST OF TABLES

	Page
Table 3.1. Field voltage/wind speed relationship for the Jacobs 3-phase alternator with 9 $\Omega$ delta load	27
Table 3.2. Characteristic information for the 17.5-kW, 26' fixed-blade, Jacobs wind energy system	29
Table 3.3. Test data obtained for remote programming resistor $R_p$ and the actual resistors and variable pots used for design of interface for digital control of PMC 60-V variable power supply	40
Table 3.4. Test results of the output-voltage transducer on the Jacobs 17.5-kW alternator	46
Table 3.5. Thermistor specification for anemometer bridge circuit	54
Table 3.6. Anemometer signal frequency and amplitude at various wind speeds	60
Table 3.7. Manufacturer numbers and description of the IC's used	62
Table 3.8. Controller I/O lines assignment	64
Table 4.1. Characteristics of the 10-kW, 23-foot blade Jacobs wind system	98
Table 4.2. Performance data for 10-kW Jacobs wind system operated in fixed-field mode, $V_f = 35$ V	105
Table 4.3. Performance data for 10-kW Jacobs wind system operated in synchronous-inverter mode	106
Table 4.4. Performance data for 10-kW Jacobs wind system operated in controlled mode, hysteresis constant $C = 3$	107

	Page
Table 4.5. Performance data for 17.5-kW wind system operated in fixed-field mode, $V_f = 35$ V	110
Table 4.6. Performance data for 17.5-kW Jacobs wind system operated in controlled mode, hysteresis constant $C = 3$	111
Table 4.7. Performance data for 17.5-kW Jacobs wind system operated in controlled mode, hysteresis constant $C = 2$	114

## LIST OF FIGURES

	Page
<b>Figure 2.1.</b> Characteristic for a hypothetical wind system	7
<b>Figure 2.2.</b> Variation in $C_p$ with TS/WS ratio for a typical wind system	11
<b>Figure 3.1.</b> Block diagram of the microprocessor-based controller	23
<b>Figure 3.2.</b> Alternator field voltage required to obtain rated power at $C_p$ of 0.33 in relation to wind speed	28
<b>Figure 3.3.</b> Delta load configuration	31
<b>Figure 3.4.</b> Interface for digital control of Power/Mate variable power supply	36b
<b>Figure 3.5.</b> Circuit for 20-V and 5-V regulated power supplies	37
<b>Figure 3.6.</b> PMC power supply connections for remote programming	39
<b>Figure 3.7.</b> Picture of the Digital Controller Interface Board for PMC power supply	41
<b>Figure 3.8.</b> Digitally-controllable variable power supply using adjustable regulators	43
<b>Figure 3.9.</b> Circuit diagram for the output voltage transducer	45
<b>Figure 3.10.</b> PMC power supply on/off control interface	48
<b>Figure 3.11.</b> Circuit for digital control of an electric brake system	50
<b>Figure 3.12.</b> Anemometer bridge circuit	53
<b>Figure 3.13.</b> Interface circuit for low-cost anemometer	56
<b>Figure 3.14.</b> Flow chart for the TTL signal to wind speed conversion program	57a

	Page
Figure 3.15. Listing and comments for the TTL Signal-to-Wind-Speed conversion program	58
Figure 3.16. Overall schematic diagram of the microprocessor controller	61
Figure 3.17. Picture of microprocessor board illustrating the physical layout of the IC's	67
Figure 3.18. The flow chart of the control program	68
Figure 3.19. A picture of the completed microprocessor-based controller (top view)	88
Figure 3.20. Drawing of the cable and cinch connector interconnecting the chassis to the metal enclosure	90
Figure 3.21. Interconnection between the controller, the Power/Mate power supply and the output voltage transducer	91
Figure 3.22. A picture showing the rear panel of the controller	92
Figure 3.23. Picture showing the controller, PMC power supply, Ohio Semitronics Wattmeter and three a.c. voltmeters in operation	94
Figure 4.1. A block diagram of the wind energy conversion system	97
Figure 4.2. Data-acquisition system	101
Figure 4.3. 10-kW wind system power output in relation to wind speed	108
Figure 4.4. 17.5-kW wind system power output in relation to wind speed	112
Figure 4.5. 17.5-kW wind system power output in relation to wind speed	115

## I. INTRODUCTION

From the early 1970s, it has been recognized that energy is a factor central to the well being of both the developed and developing world. The present problems of obtaining adequate energy in much of the world is at least in part due to the financial distortions caused by the succession of dramatic rises in the price of all energy sources over the past decade or so. There has been a growing awareness of the finite nature of supplies of the main fossil fuels on which we rely, namely oil, gas and coal. It appears that we will exhaust these valuable resources, produced by nature over millions of years, in a matter of decades in the case of oil and gas and in a few hundred years in the case of coal [2].

It is, therefore, not surprising that there has been a considerable surge of interest and activity worldwide in searching for more efficient ways of using existing energy sources, and in developing new ones, including nuclear fusion, solar, wind, wave, and tidal energy. In many parts of the world, there is a growing awareness that some of the above alternative energy sources could have an important role to play in the production of electricity by the end of the century. However, there are many technical and economic problems which are yet to be overcome. Economics need to be improved for nearly all of them before they can be competitive on a large scale with most conventional sources. Some of these energy sources also present substantial environmental problems.

Among the alternative energy sources named above, one of the most promising is wind.

Man has used wind energy in one form or another for hundreds of years. The earliest use was for the propulsion of ships but nearly two thousand years ago in Persia, China and Japan, windmills are believed to have been widely used [22]. In the thirteenth and fourteenth centuries, windmills of the traditional Dutch type came into widespread use for grinding grain. The first modern windmills were developed in the late nineteenth century for pioneer agricultural use in Australia and the United States. These were originally developed for water pumping and were generally of the multi-bladed type still familiar in many parts of the world. An excellent review of the early development of wind energy has been given by Minchinton [18].

The development of the internal combustion engine and steam cycle for electricity production led, in the early part of this century, to a rapid decline in the use of the wind as a source of power in most parts of the world but some windmills were used for electricity production before rural electrification programs made electricity available in most rural areas.

In the past few years, the increasing importance of fuel savings has been responsible for a revival of interest in wind energy, in particular wind-generated electricity. Research is proceeding both on large and small-scale wind generating systems [4]. Hundreds of wind-energy conversion systems (WECS) are being used for production of electricity in "wind farms," particularly on the West Coast. Clusters of units are grouped together in good wind regimes to provide supplemental generation capacity for the electrical utilities. In these applications, tax con-

siderations and utility buy-back policies have enhanced the economic aspects.

In many other areas of the country, particularly in The Great Plains, winds are available that also can produce substantial amounts of power. These winds can provide a free, nonpolluting, and inexhaustible source of energy that, if not used, is wasted. Therefore, there has been a considerable interest in the economic possibilities of medium-sized wind systems of capacity between 10 and 50 kW, which can be used either alone or in conjunction with some other source of power, to supply small communities in thinly populated districts and rural areas [28]. In these rural areas, however, wind regimes and tax considerations generally are not as favorable, and economic feasibility depends greatly on WECS that extract the maximum amount of energy from variable winds. This study is concerned with the possibility of optimizing the performance of medium sized WECS. However, optimizing the performance of such wind systems to extract the maximum amount of energy from the wind is difficult because of a combination of factors. First, wind speed always varies unpredictably. Second, typical generator load characteristics are incompatible with the output characteristics of typical wind-driven rotors. As a result, a simple system in which a wind-driven rotor drives a generator is, at best, optimally efficient over a limited range of wind speeds. Deviations in windspeed from this limited range result in a drop in the efficiency of the wind systems and a consequent decrease in power output. Therefore, to obtain good wind/en-

ergy conversion efficiency over the normal range of wind speeds, it is important to control a wind system so that it runs at optimum rotational speed (i.e., the speed at which the power that is extracted from the wind is a maximum) [22].

In this dissertation, a technique for optimizing the efficiency of wind energy conversion systems has been developed that is based only on the measurement of the wind system output voltage without the requirement for direct measurement of the wind speed or rotational speed of the alternator.

To implement the developed optimizing technique, a microprocessor-based controller system has been designed and built which allows adaptation to different types of wind systems by software.

---

The controller system has been applied to two typical wind systems and substantial performance improvements have been achieved. It is hoped that the improvement in performance achieved can make a contribution to economic feasibility of wind energy conversion systems.

## II. LITERATURE REVIEW

Several approaches for improving wind energy conversion system (WECS) performance have been suggested in the past indicating that the basic problem of improving performance has been well recognized. These approaches are discussed in this chapter; however, to understand WECS performance and optimization, an elementary theory of wind-system performance and its relation to wind power and impeller rotational speed will first be presented.

### A. Aerodynamic Theory of Wind Systems

#### 1. Power in the wind

The equation for calculating the theoretical power in the wind can be derived from the basic kinetic energy equation [10].

$$KE = \frac{1}{2} MV^2 \quad (1)$$

where

M = mass

V = mass velocity

Since the mass flow of air per unit time is:

$$\dot{M} = \frac{\text{mass}}{\text{unit time}} = \rho AV \quad (3)$$

where

$\rho$  = air density

A = intercepted area

V = velocity of the wind

and power is defined as:

$$P = \frac{\text{energy}}{\text{time}} \quad (3)$$

The resulting equation for theoretical wind power is:

$$P_w = \frac{1/2 MV^2}{\text{unit time}}$$

$$P_w = 1/2 MV^2$$

$$P_w = 1/2 \rho AV^3 \quad (4)$$

Using the value for the average density of air in central Iowa [25], and SI units, equation (4) becomes:

$$P_w = 0.605 AV^3 \quad (5)$$

where,

$P_w$  = theoretical wind power in watts

$A$  = intercepted area in  $\text{m}^2$

$V$  = velocity of the wind in  $\text{m/s}$

## 2. Wind systems characteristics

All wind systems have certain characteristics related to wind speed.

At some low value of wind speed, usually from 6 to 8 mph, a wind system can begin to produce power. This is known as the cut-in wind speed, when the rotor accelerates enough for the generator to begin producing

power [22]. Above this speed, the wind system should generate power proportional to the wind speed cubed, according to equation (5). At some higher speed, usually 25 to 35 mph, wind loads on the rotor blades will be approaching the maximum strength of the wind system, and the generator will be producing its maximum or rated power. A maximum useful wind speed, sometimes called the rated wind speed, will have been reached. At some very high wind speed in the range of 60 to 100 mph, complete destruction of the wind system could result if it were to continue generating power. The characteristic for a hypothetical wind system is illustrated in Figure 2.1.

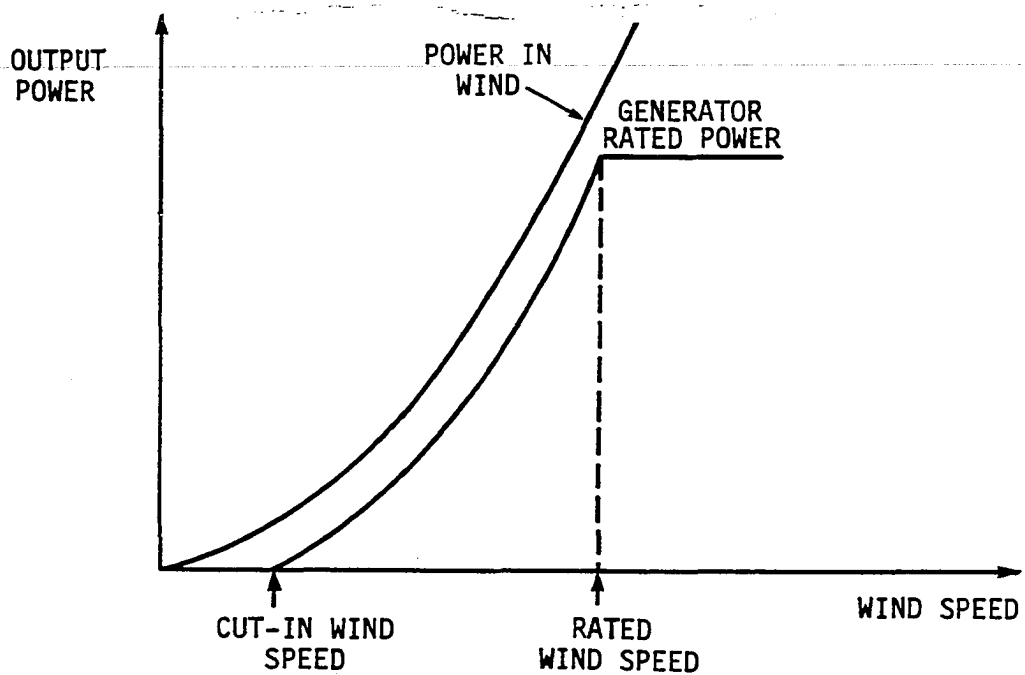


Figure 2.1. Characteristic for a hypothetical wind system

### 3. Maximum rotor efficiency

All of the theoretically available power in the wind cannot be extracted by an ideal rotor. The analysis of maximum possible efficiency for lift-type rotors was originally done by Betz, of Göttingen, in 1927, as cited by Golding [10]. The following brief outline covers the more essential points.

The rotor extracts power from the airstream by slowing down the free-stream wind speed  $V_1$  to a lesser speed  $V_2$  far down-stream of the rotor blades. Therefore, the power absorbed by the rotor ( $P_r$ ) is equal to the rate of change of kinetic energy in the wind or the difference in wind energy upstream and downstream of the rotor.

$$P_r = 1/2 \dot{M} (V_1^2 - V_2^2) \quad (6)$$

If  $V_2$  equals zero in the above equation, one might expect that power would be maximized. But no air would flow through the rotor in this case, and the power is zero. The mass flow through the rotor is just the air density times the rotor area times the average wind speed at the rotor, or:

$$\dot{M} = \rho A \left( \frac{V_1 + V_2}{2} \right) \quad (7)$$

substituting (7) in (6) yields:

$$P_r = 1/4 \rho A (V_1 + V_2) (V_1^2 - V_2^2) \quad (8)$$

It can be shown that the power absorbed by the rotor is maximum when  $V_2 = 1/3 V_1$ , i.e. when the final wind speed  $V_2$  is one-third of the up-

wind speed  $V_1$ . Substituting  $V_2$  by  $1/3 V_1$  in (8) gives:

$$\begin{aligned} P_{r_{\max}} &= 1/2 \rho A V_1^3 (16/27) \\ P_{r_{\max}} &= 1/2 \rho A V_1^3 (0.59) \end{aligned} \quad (9)$$

Thus, the maximum power which can be extracted by an ideal rotor is 59.3% of the theoretical power in the wind. This theoretical value is known as Betz limit.

#### 4. Wind-system performance

In a typical wind system when the rotor drives an electric generator, through gearing, the wind system extracts substantially less power than the maximum Betz limit. This is because of the aerodynamic imperfections and mechanical and electrical power losses associated with a real wind system.

The performance of a wind system as related to power output is a function of the efficiency at which the system extracts energy from the windstream. This is known as the "coefficient of performance" [28], and can be expressed as:

$$C_p = \frac{P_o}{P_w} \quad (10)$$

where

$C_p$  = coefficient of performance

$P_o$  = power output

$P_w$  = power in wind

In practice,  $C_p$ 's of practical wind systems may not be greater than about 0.4 (instead of 0.593) and may be less [10, ]. The actual value of  $C_p$  of a wind system depends upon the type and detailed design of the system. Also, for a given design,  $C_p$  is dependent upon the rotational velocity of the airfoil, measured at its radial extremity or tip, in relation to the free flow wind speed. This relationship is commonly referred to as the tip-speed/wind speed ratio (TS/WS), or simply the tip-speed ratio,  $\lambda$ , and it is given by

$$\lambda = \frac{\omega r}{V} \quad (10)$$

where

$\lambda$  = impeller tip-speed ratio

$\omega$  = rotational angular velocity in radians/s

$r$  = radius of impeller blade in m

$V$  = velocity of the wind in m/s

By using the tip-speed ratio, impeller performance can be considered in a more generalized discussion without the knowledge of impeller diameter and rotational speed. Typical values of the tip speed range from 1 to 15 for different rotor types [22].

The effects of variations in TS/WS ratio on  $C_p$  for a typical fixed-pitch horizontal-axis wind system is shown in Figure 2.2. The  $C_p$  against tip-speed ratio curve is one of the primary characteristics of a wind system impeller [13], and together with equation (4) and knowledge of load characteristics enables predictions to be made

of the steady-state behavior of the wind-power system. As it can be seen from the curve in Figure 2.2., a single maximum in  $C_p$  occurs when the tip-speed ratio takes a particular value  $\lambda'$ . Therefore, the impeller speed should vary as

$$\omega = \frac{\lambda' v}{r} \quad (1)$$

if the impeller is to extract the maximum power from the wind. If the impeller is controlled so as to maintain tip-speed ratio at  $\lambda'$ , the output power from the wind system is maximized.

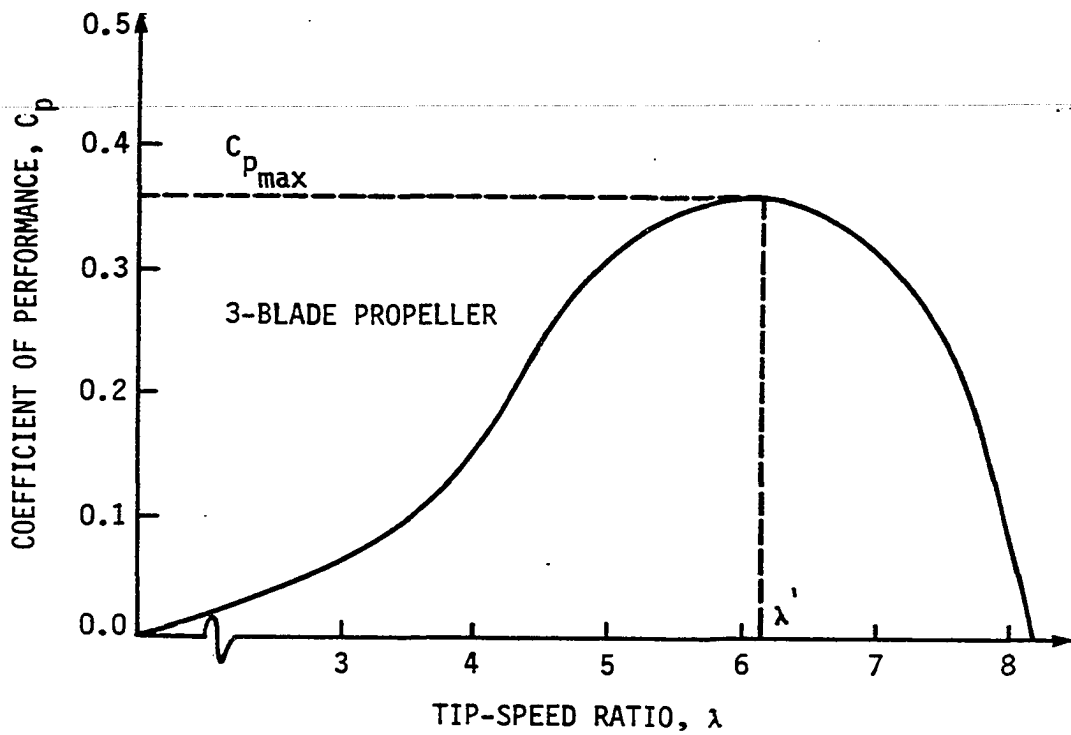


Figure 2.2. Variation in  $C_p$  with TS/WS ratio for a typical wind system

### B. Wind System Types

Two main classes of wind systems which may be distinguished are:

- a) wind systems having the effective moving surfaces of their rotors in the direction of the wind (vertical axis machines) and
- b) wind systems whose rotors move in a plane, or planes, perpendicular to the direction of the wind (horizontal-axis machines)

In several studies and reviews of the possible types of wind systems, it is indicated that the horizontal-axis machines can attain higher coefficients of performance than vertical-axis machines and prove more economical for power production [10,13,28]. This is because, in vertical-axis machines, the rotor surfaces which move with wind during one-half of their revolution about their vertical axis, must move against the wind during the other half revolution and this involves an increased loss of power. Furthermore, the rotor surface must always move at less than the speed of the wind, thus the speed of revolution of the rotor is low compared to speed requirement of electrical generators and this implies the need for gearing with higher step ratios than for the horizontal-axis machines.

Among the horizontal-axis machines, two types of wind systems have generally been used in the past to harness wind energy for various purposes. The two types of wind systems include systems with fixed-pitch impellers and systems with variable-pitch impellers.

The variable-pitch impeller has been used previously both to control rotational speed of the impeller and to increase the amount of energy extracted from the wind. Control of rotational speed using a

variable-pitch impeller has been used in some previous design approaches to provide a blade tip speed that is proportional to the wind speed [11]. These approaches generally may improve wind system's performance but result in designs that are more complicated than those of fixed-pitch machines and still may not extract maximum energy from the wind [10]. In addition, variable-pitch impellers are more expensive, and the increased complexity of design increases the probability of failure and damage to the system, and possible injury to individuals in high winds. Thus, for optimum reliability, simplicity, and cost, it is desirable to use fixed-pitch or fixed-geometry wind systems if such systems can be made to operate in a safe and efficient manner.

The fixed-pitch impellers usually consist of two to four blades which are shaped similar to a mirror image of airplane propeller blades. To provide maximum energy output from a fixed-pitch system, it is desirable to operate at maximum impeller efficiency for the particular wind speed available. As illustrated in Figure 2.2., maximum impeller efficiency occurs if the rotational speed of the impeller in relation to the wind speed, the TS/WS ratio, can be held constant. However, because wind speed always varies unpredictably, the maximum impeller efficiency for a fixed-pitch wind system occurs only during a narrow range of wind speeds. Therefore, although the fixed-pitch wind system is more desirable from the standpoint of cost and reliability, the fixed-pitch wind system does not provide optimum output power since it operates most efficiently only at its design pitch [10]. Several approaches have

been attempted previously to overcome this problem. These approaches are discussed in the following section.

### C. Previous Work on Improving Efficiency of Fixed-pitch Wind Systems

In 1980, Pal Dharam and Huang [21] developed an automatic load matching device for applying loads to wind driven generators in an attempt to obtain maximum efficiency for the particular wind speed available by matching the load to the generator's capacity. This device was designed to selectively switch five different loads to the output of a wind driven generator's rotor, where each load was chosen to correspond to a range of speeds of the wind driven generator's rotor. However, this device has a limited effectiveness in obtaining maximum efficiency because load matching technique involves following the generator's output versus wind speed characteristics over its entire range. This would require an infinitely variable load which is impossible to obtain.

In 1981, Lawson-Tancred [15] proposed a method for matching the power available from the wind to power delivered to the load using fixed-pitch turbines. He described an arrangement wherein a fixed-pitch impeller was connected to drive an electric generator via an energy converter that effected a torque reaction on the impeller proportional to the square of the rotational speed of the impeller. He suggested that the energy converter in the above arrangement may be of a type having continuously variable torque characteristics, such as a variable-

angle swash-plate pump. The swash-plate angle could then be controlled by a signal output from an impeller-speed sensing device. The above technique proposed by Lawson-Tancred requires conversion of energy to an intermediate form, which can increase costs and also can decrease efficiency significantly.

The idea of matching the power available from a fixed-pitch impeller to the power delivered to the load was previously proposed in 1941 by Claytor [7]. Claytor suggested a device which consisted of a wind-driven generator connected to an electric motor of larger capacity which operated a water pump. The nature of the interconnection of the generator and electric motor was to ensure increase of power delivered to the load in proportion to increase of power in the wind. However, Claytor's device required the use of a closely matched generator/motor combination which significantly increased capital costs of the system. Moreover, the motor efficiency resulted in further decreases in the overall efficiency of the wind system.

Claytor has been given credit for another idea which he developed in 1939 for improving the performance of fixed-pitch wind driven generators [6]. In this case, he described a wind-driven generator control system in which shunt resistors were switched in and out of the field circuit, in accordance with wind speed. Varying the shunt resistor in the field circuit produced a modified generator loading curve which approximated the locus of the peaks of the impeller curves. However, where control is attempted in accordance with wind speed, match-

ing of the generator load curve and the impeller curve is imperfect because wind speed and impeller speed correspond to each other only under steady-state conditions.

Alberts [1], in 1944, described a system in which the field current of a wind-driven generator is controlled through a variable resistance. The resistance varied in accordance to the variations in impeller speed. The system of Alberts is at least theoretically capable of producing a better match between the generator load curve and the impeller curve because field current is controlled in accordance with impeller speed rather than directly by wind speed as was the case in Claytor's device. However, in practice, maximum efficiency cannot be achieved strictly by sensing the rotational speed of the impeller.

Moran and Korzeniewski [19], in 1978, described a method to improve the efficiency of fixed-pitch wind systems by matching the generator load curve to impeller characteristics. Moran and Korzeniewski suggested a system in which a generator load curve was matched to a wind-driven impeller characteristic. This system included an impeller speed-responsive tachometer which cooperated with appropriate circuitry for incrementally controlling the field current in the generator.

In 1976, Bright [5] also described a field control system for a wind-driven electrical generator. Bright employed a tachometer coupled to the impeller shaft for generating an output signal representative of wind velocity. This signal was applied to a field-control circuit,

thereby adjusting the field current of the generator.

The primary problem with the systems of Moran et al. and Bright was that the field current control of the generator was strictly in accordance with the rotational speed of the impeller. Of course, as it is illustrated by the  $C_p$  curve for fixed-pitch impeller shown in Figure 2.2., efficiency of a wind system is dependent on both wind and impeeller speeds.

Bolton and Nicodemore [4], in 1979, examined the possibility of achieving optimum performance by leaving the impeller, generator and load without control means under normal conditions and designing them so that efficient operation occurs naturally. The authors examined a wind-driven self-excited generator supplying resistive loads and concluded that a natural match can be obtained between the power/speed characteristics of the generator and the impeller if the generator loading on the impeller can be arranged to vary as the square of the impeller rotational speed. They suggest that this can be achieved by a careful choice of generator magnetization characteristic. However, choosing a generator with proper magnetization characteristic to match the power/speed characteristics of an impeller, in practice, requires the design of a specific generator strictly for a chosen impeller and is not economically feasible. Furthermore, such a system cannot be entirely free of control means since special measures for starting and overspeed protection are necessary.

As a result of a wind research conducted in cooperation with the

Department of Energy, Soderholm and Andrew [27], in 1982, developed a method of operating a wind machine at maximum efficiency. The objective of Soderholm's method was to maintain a constant, predetermined tip speed/wind speed ratio by control of alternator field voltage. This method was implemented by the use of analog circuits. Tip-speed and wind-speed signals applied to a comparison circuit provided an input to a field voltage control circuit that varied in magnitude in relation to the covarying wind speed and tip speed. Use of this field control and some of the operational improvements obtained with specific wind machines have been described by Soderholm [25].

#### D. Scope of the Work

---

This research work has concentrated on developing a method and apparatus for optimizing the efficiency of fixed-pitch wind-driven alternators.

An optimizing technique has been developed which is based on the maximization of the output voltage of the alternator. A controller system using a microprocessor has been designed which implements this technique.

The validity of this optimizing technique has been tested by assessing the performance improvement of two typical wind systems. Three sets of performance data have been obtained for each of the two wind systems. One set corresponds to the results obtained by application of the method presented in this dissertation and the other two sets cor-

respond to the results obtained by application of the fixed-field and synchronous-inverter methods, respectively. Observations are made based on the comparison of the results. The demonstrated improvement in overall performance of wind-driven alternators should make a contribution to the economic feasibility of WECS and help in reducing use of nonrenewable energy resources.

---

### III. OPTIMIZING MICROPROCESSOR-BASED CONTROLLER

#### A. Background

When wind-driven alternators supply a load that is proportional to the field voltage, the loading of the WECS may be varied by controlling the output voltage of the alternator and thus the rotational speed of the impeller. Changes in the field voltage applied to a wind-driven alternator were found capable of producing substantial changes in impeller speed by the variation of the output voltage of the alternator.

In a typical test of a 10-kW wind system, propeller rotational speed varied from 148 to 183 rpm for alternator field voltages ranging from 45 to 25 volts. These data indicate how impeller speed of rotation may be changed by varying alternator output voltage using field control.

#### B. Optimizing Technique Using Field Control

The field control principle described has previously been applied to wind driven alternators to determine the possibility of improving performance; however, the principal objective has been to maintain a TS/WS ratio at an optimum constant value. This requires the measurement of both the wind speed and the impeller rotational speed. Furthermore, holding the TS/WS ratio constant, at best, results in  $C_p$ 's equal to an assumed  $C_p$  which is derived from the ratio of the WECS expected power output at maximum rated rpm and the theoretical power in the wind at maximum rated speed. Also, the TS/WS ratio of an impeller can vary substantially due

to slight changes in the airfoils' design pitch or to icing of the blades. Under these conditions, the  $C_p$  drops further below the assumed  $C_p$  level.

The technique developed here, however, is based only on the measurement of the alternator output voltage without the requirement for direct measurement of the wind speed or rotational speed of the alternator. The field control principle is used to maintain the voltage output of the alternator at an optimum value. Because power output of the wind system is a function of output voltage from the alternator with a voltage-responsive load, maximum power will be obtained if the voltage output of the alternator is maintained at its maximum value. With this technique, optimum performance is achieved under all conditions regardless of the variations of the TS/WS ratio. The above technique is accomplished by taking periodic samples of output voltage and determining if incrementing or decrementing the field voltage will produce a higher voltage than the previous sample taken before the field voltage change. For example, if incrementing the field voltage produces an increase in output voltage, the field voltage is again incremented and the output voltage checked to see if a further increase in output voltage is obtained. If so, further increments of field voltage are made until a decrease in output voltage is obtained that would indicate that the rotational speed of the impeller had been reduced below the optimum value or that the wind speed had been reduced and that the load presented to the wind system needs to be reduced.

The basic implementation of the optimizing technique is summarized

in the steps below:

1. Measure wind speed.
2. Verify that wind speed is within specified limits.
3. Determine approximate field voltage needed for the measured wind speed and apply this value to the alternator field.
4. Sample the alternator output voltage.
5. Verify that the alternator output voltage is within specified limits (or initiate shut down).
6. Increment the field voltage to a higher value.
7. Determine if output voltage increases by a specific amount.
8. If so, cycle back to Step 6.
9. If not, decrement the field voltage to a lower value.

---

10. If output voltage increases, decrement the field voltage again.
11. If decrementing the field voltage reduces output voltage, cycle back to step 6.

### C. Controller

A controller system using a microprocessor has been designed that implements the described optimizing technique and allows adaptation to different types of wind systems and modification of control parameters by software.

#### 1. Functional description

A block diagram of the controller system is illustrated in Figure 3.1. The heart of the controller is a microprocessor. The main input signal to the controller is the alternator output voltage. This

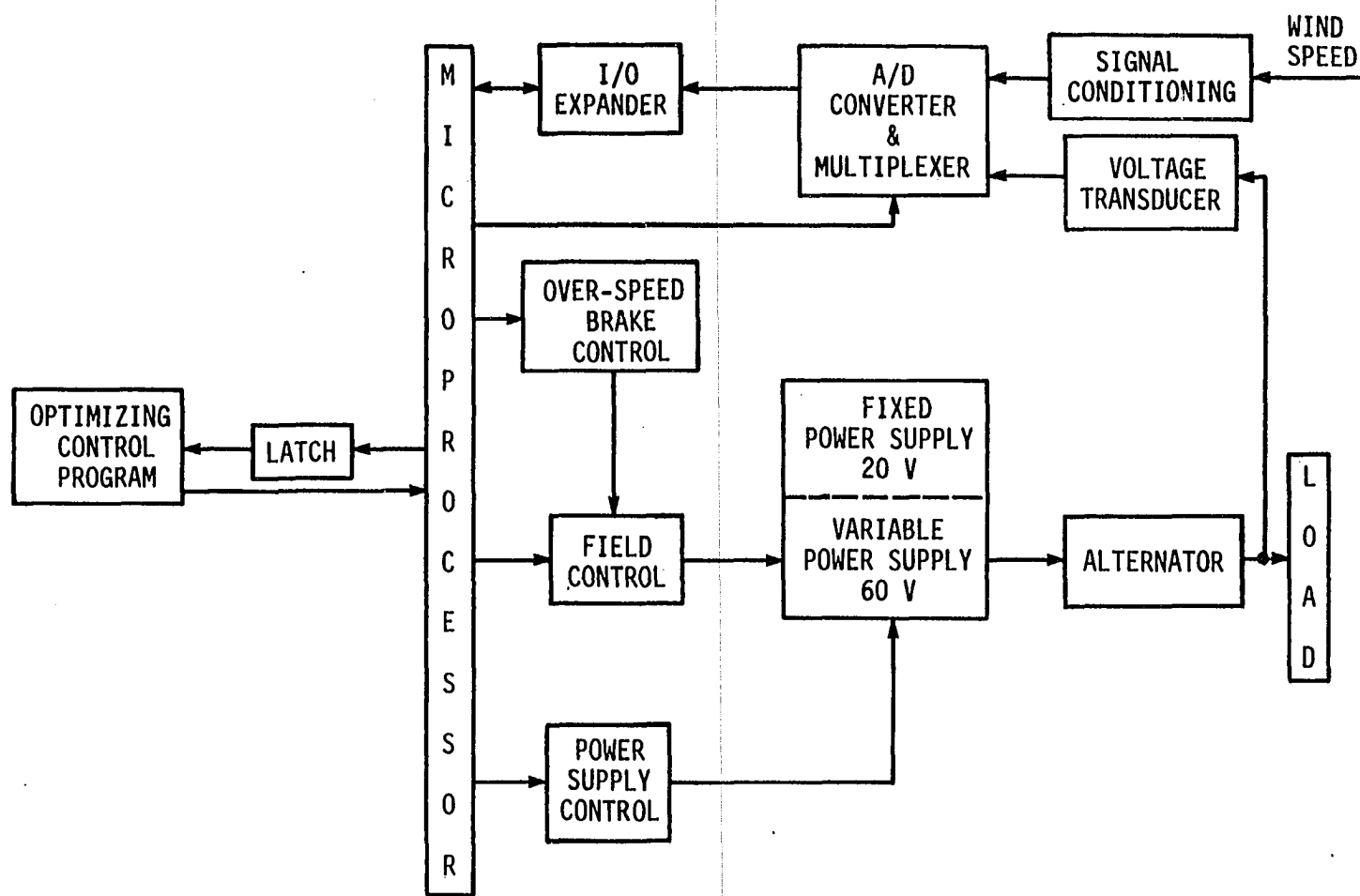


Fig. 3.1. Block diagram of the microprocessor-based controller.

signal is translated to TTL levels using a voltage transducer and then digitized by means of an A/D converter. A control program, written to implement the developed optimizing algorithm, is stored in the controller memory. The control program, in response to the output voltage signal, generates the proper code for the field control which then adjusts the field voltage for optimum efficiency. The function of the over-speed brake control is to provide protection in over-speed or over-voltage conditions. The function of the power supply control is to avoid unnecessary power consumption at low wind conditions.

A wind speed signal is also provided as an input to the controller. Although no measurement of wind speed is necessary for optimizing the efficiency, a knowledge of the approximate wind speed can help speed up the optimization process and can provide for additional useful control functions such as brake application for rotational over-speed at high wind speeds.

#### D. System Development

In the following subsections, the research involved in developing the primary logic/functions of each block, shown in the basic block diagram of Figure 3.1, will be described.

##### 1. Microprocessor

The 8035 microprocessor from the MCS-48 family of single-chip microcomputers was chosen because of the following reasons [17,30]:

1. It is virtually a self-contained single-chip system intended for dedicated system controllers.
2. A large variety of conditional jump and table look-up instructions are provided.
3. It includes a software-controlled 8-bit Counter/Timer.
4. Twenty-seven programmable (I/O) lines are available with provision for expansion.
5. On-board oscillator and clock circuits are available.
6. Only a single 5-V power supply is needed.
7. It is relatively low in cost, approximately \$6.00.
8. It can be operated with external memories, making development convenient.

In addition, the 8035 microprocessor was found attractive because programming support and development for the MCS-48 family are provided by the Hewlett Packard (HP) 64000 minicomputer system available at the Electrical Engineering and Computer Engineering Department of Iowa State University. The HP 64000 system includes assembler and text editor programs and an EPROM programmer which makes it possible to create and edit programs in MCS-48 assembly language and generate the machine code equivalence for programming of EPROMS.

Operation with external memories provides a simple way for controller adaptation to different wind systems and/or different climatic locations.

## 2. Field control

a. Design procedure      The first step in obtaining the proper parameters for the development of an optimizing field control is a de-

termination of the alternator output-voltage/field-voltage characteristics. If data are not available from the manufacturer, a plot may be obtained by running the alternator on a motoring dynamometer or other speed-controllable power source. From knowledge of the wind system gear ratio, impeller diameter, alternator rotational speed and wind speed for rated power output, the approximate TS/WS ratio for the wind system may be obtained. Using this information and the coefficient of performance required to obtain the specified power output at rated wind speed, estimated power output and rotational speed over the normal range of wind speeds can be calculated. The basic formula for the kinetic energy (5) in the wind multiplied by the wind system efficiency ( $C_p$ ) is used for calculation of the estimated power output. The alternator rotational speed for each wind speed is determined from the system gear ratio and the calculated TS/WS ratio.

By operating the alternator over a range of speeds and measuring the required field voltage to produce the proper power output, data for the required field voltage in relation to wind speed can be obtained. The above procedure was carried out for a 17.5-kW Jacobs wind system. The data obtained are shown in Table 3.1. A plot of the field voltage versus wind speed is shown in Figure 3.2. The calculations of the required parameters for the above design procedure are shown below. The characteristic information for the 17.5-kW Jacobs wind system is shown in Table 3.2.

Table 3.1. Field voltage/wind-speed relationship for the Jacobs 3-phase alternator with  $9 \Omega$  delta load (gear ratio 6.16:1,  $C_p = .33$ , TS/WS ratio 6.7)

Wind speed (mph)	Generator rpm	Power output (W)	Output voltage (V)	Field voltage (V)
8	356	454.4	39.7	24.0
9	400	657.0	47.3	26.2
10	445	887.5	55.4	28.5
11	489	1181.3	64.0	29.9
12	534	1433.7	72.9	31.1
13	578	1949.9	82.2	32.3
14	623	2435.4	91.9	33.9
15	667	2995.4	101.9	35.3
16	711	3635.3	112.2	36.9
17	756	4360.4	122.9	39.3
18	800	5176.1	133.9	40.6
19	845	6087.6	145.2	42.5
20	889	7100.3	156.8	44.6
21	934	8219.4	168.7	47.4
22	978	9450.4	180.9	50.3
23	1023	10798.6	193.4	53.2
24	1067	12269.2	206.2	56.0
25	1112	13867.7	219.2	59.0
26	1156	15599.3	232.5	61.9
27	1201	17469.3	246.0	64.9

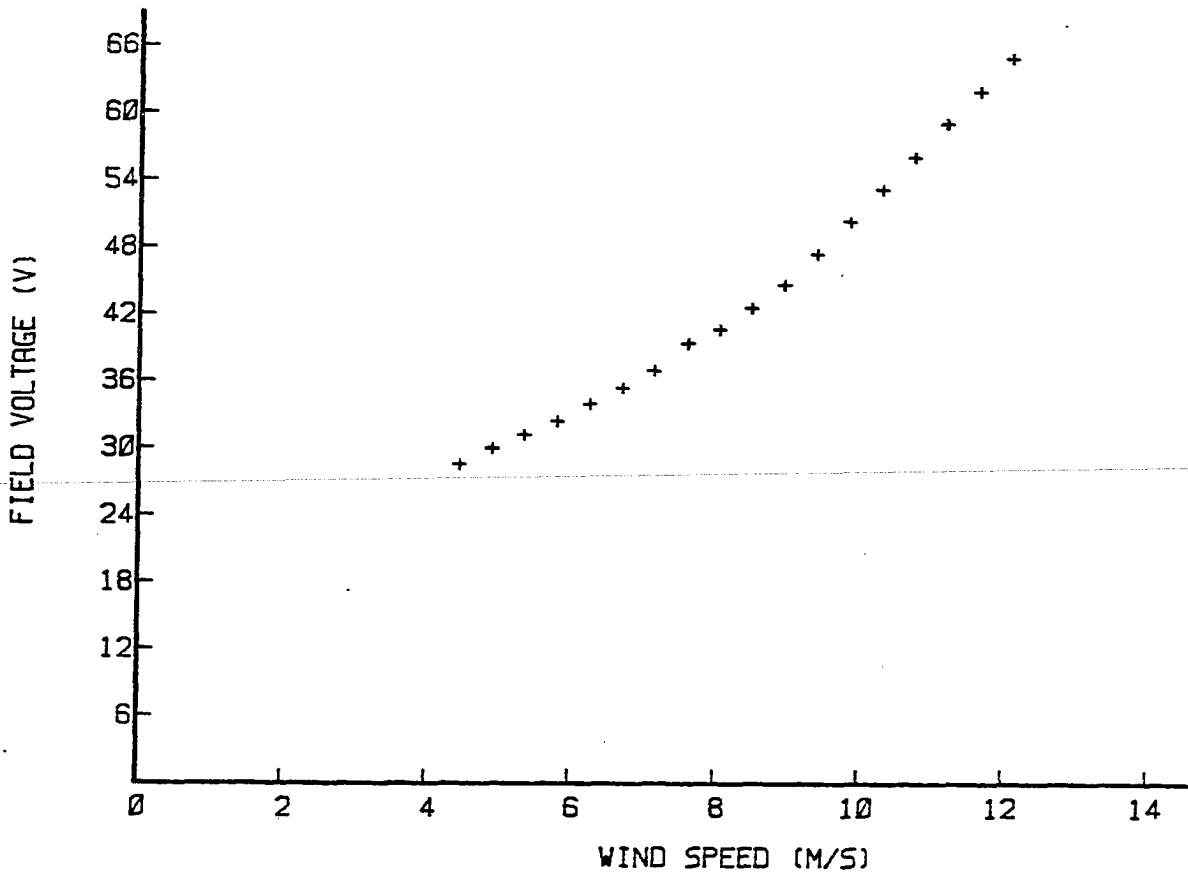


Figure 3.2. Alternator field voltage required to obtain rated power at  $C_p$  of 0.33 in relation to wind speed

Table 3.2. Characteristic information for the 17.5-kW, 26' fixed-blade, Jacobs wind energy system

Rated power output	17.5 kW
Alternator rated speed	1200 rpm
Rated wind speed	27 mph
Gear ratio	6.6:1
Blade diameter (D)	26 ft
Output voltage (at full power)	246 volts (rms)
Alternator field resistance	61 ohms

Data in Table 3.2, available from the manufacturer, was used to determine the values of TS/WS, P and  $R_{eff}$  at full power. Calculations are shown below:

Calculation of TS/WS ratio:

$$TS = \text{Tip Speed}$$

$$TS = \text{Alternator rpm/Gear ratio}$$

$$TS = 1200/6.16$$

$$TS = 195 \text{ rpm}$$

$$TS \text{ at } 195 \text{ rpm} = 195 (\pi D)$$

$$TS \text{ at } 195 \text{ rpm} = 195(\pi)(26)$$

$$TS \text{ at } 195 \text{ rpm} = 15928 \text{ ft/min}$$

$$15928 \text{ ft/min} (60/5280) = 181 \text{ mph}$$

$$TS/WS = \text{Tip Speed/Wind Speed Ratio}$$

$$TS/WS = \frac{181}{27}$$

$$TS/WS = 6.7$$

$$\begin{aligned} P &= \frac{1}{2} \rho A V^3 \\ &= 0.605 A V^3 \end{aligned}$$

where

$A$  = area ( $\text{m}^2$ ) and,

$V$  = wind speed ( $\text{m/s}$ )

$\rho$  = air density ( $\text{kg/m}^3$ )

or,  $P = 5.02 \times 10^{-3} A V^3$

where

$A$  = area ( $\text{ft}^2$ ) and,

$V$  = wind speed ( $\text{mph}$ )

Therefore,

$$\begin{aligned} P &= 5.02 \times 10^{-3} (\pi \times 13^2) (27)^3 \\ &= 52.5 \text{ kW} \end{aligned}$$

$$\text{Indicated } C_p = \frac{17.5 \text{ kW}}{52.5 \text{ kW}}$$

$$= 0.33$$

Calculation of effective load resistance needed at full power:

$$\text{Rated } P = \frac{\sqrt{3} V_o^2}{R_{\text{eff}}} \quad (1)$$

where

$P$  = rated power output (watts)

$V_o$  = output voltage at full power (volts)

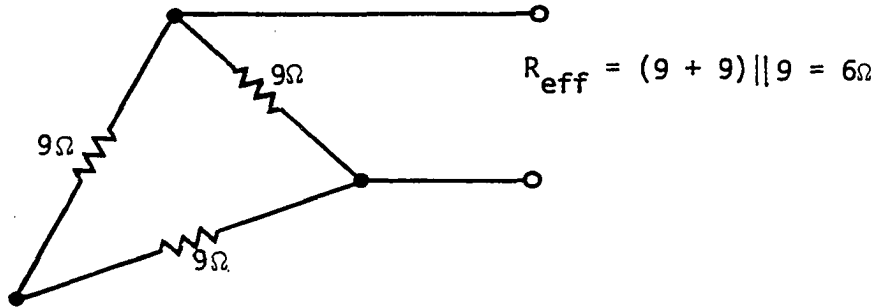
$R_{\text{eff}}$  = effective load resistance (ohms)

$$17.5 \text{ kW} = \frac{\sqrt{3} (246)^2}{R_{\text{eff}}} \quad (1)$$

Therefore,

$$R_{\text{eff}} = 6 \Omega$$

Resistance per leg of  $9 \Omega$  was used in a delta load configuration using resistor racks to construct the  $6 \Omega$  effective load. Each  $9 \Omega$  leg consists of two  $45 \Omega$  and two  $30 \Omega$  resistors placed in parallel.



The  $9\Omega$  load per leg consists of two  $30\Omega$  and two  $45\Omega$  resistors placed in parallel.

Figure 3.3. Delta load configuration

EXAMPLE: For a 20-mph wind speed,

$$\text{Tip speed} = 20 \text{ (TS/WS)}$$

$$= 20(6.7)$$

$$= 134 \text{ mph}$$

$$\text{Tip speed} = 134 \left(\frac{5280}{60}\right) \left(\frac{1}{26\pi}\right)$$

$$= 144 \text{ rpm}$$

$$\text{Alternator rpm} = 144 \text{ (gear ratio)}$$

$$= 144(6.16)$$

$$= 889 \text{ rpm}$$

$$\text{Power output} = 5.02 \times 10^{-3} \times A V^3 \times C_p$$

$$= 5.02 \times 10^{-3} \pi \left(\frac{26}{2}\right) (20)^3 (0.3)$$

$$= 7100 \text{ watts}$$

Output voltage can be calculated from the formula shown below:

$$P = \frac{\sqrt{3} \times V^2}{R_{\text{eff}}} \quad (2)$$

where

P = alternator output power (watts)

V = alternator output voltage (volts)

$R_{\text{eff}}$  = effective load resistance (ohms)

Therefore,

$$V = \sqrt{\frac{PR_{\text{eff}}}{\sqrt{3}}} \quad (3)$$

$$= \sqrt{\frac{7100 \times 6}{\sqrt{3}}}$$

$$= 157 \text{ volts}$$

In order to establish a mathematical relationship between wind speed and alternator field voltage, the statistical methods of Least Squares and Curvilinear Regression Analysis were applied to the data of Table 3.1. (Calculations are shown in Appendix A along with a Fortran program designed to determine the constants a, b, and c for the equation:  $Y = a + bX + cX^2$ ).

The following relationship was found:

$$Y = 21.31 + 0.07X + 0.0569X^2 \quad (4)$$

where

$Y$  = field voltage (volts)

$X$  = wind speed (mph)

In order to control the alternator field voltage digitally, it is first needed to store the field voltage/wind speed data of Table 3.1 in the microprocessor-based controller memory. Two methods are possible:

1. Table 3.1 can be directly stored in the memory and a look-up table technique may be employed to access the data in it.
2. The relationship developed by means of The Least Squares and Curvilinear Regression Analysis can be implemented in the software and the proper field voltage may then be calculated for each sampled wind speed.

Method one was chosen over method two, and used in the actual design of the controller because, as it will be shown later, the micro-

processor used has simple instructions permitting easy access to a look-up table. Implementation of method two would require a multiplication and/or a squaring routine which occupies more memory space and increases the controller response time.

b. Digitally-controllable variable power supply and voltage regulator Data shown in Table 3.1 indicate that in order to maximize the alternator power output for different rpm settings, the field voltage needs to vary in the range of 24 to 65 volts. Thus, the need arises for a digitally-controllable variable power supply or regulator by which the microprocessor can control and adjust the alternator field voltage.

Before designing the circuit that can accomplish the above task, a nominal field voltage step had to be determined. A large number of field voltage steps would be desirable; however, increasing the number of steps results in a decreased step size. On the other hand, changes of the field voltage by the selected step size must be capable of producing an appreciable change in the wind system response. Therefore, realizing the trade-off, a nominal field voltage step of 1.5 V was selected for the following reasons:

1. Data in Table 3.1 show that the required increase or decrease in the field voltage for a 1-mph variation in the wind speed is at least 0.9 and at most 3.0 volts.
2. The variation in the pattern of the field voltage data shown in Table 2.3 can be described in a reasonable detail by a step size of 1.5 volts.

3. Dividing the field voltage range into 1.5-V steps results in 32 separate steps which is a reasonable number of steps in terms of design considerations.

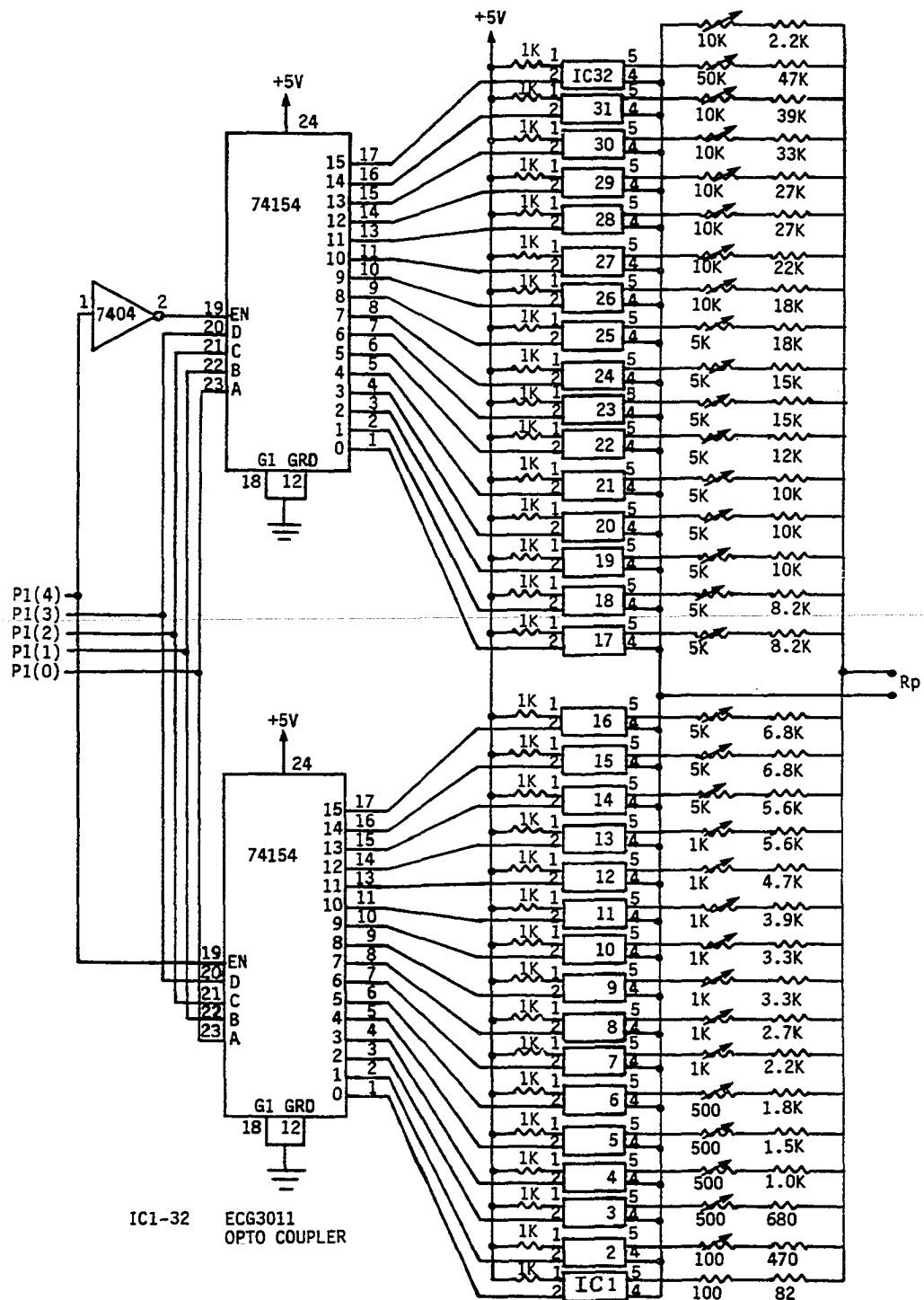
Two circuits were designed to accomplish the above purpose.

The first circuit shown in Figure 3.4 is designed to allow digital control of an existing 60-V variable power supply made by Power/Mate Corporation (PMC), model BPA 60F, shown in Figure 3.23. Because the value of required field voltage exceeds the maximum 60-V limit of this power supply, but never goes below 24 V, it was decided to build a separate 20-V regulated fixed power supply and place it in series with the PMC power supply. Series addition of the 20-V regulated fixed power supply to the PMC 60-V variable power supply produces an 80-V variable power supply which can satisfy all the field voltage requirements and in the meantime helps to reduce the difficulties of overheating present when working with high-voltage regulators. The circuit for the 20-V regulated fixed power supply is shown in Figure 3.5. Also, shown in Figure 3.5 is the 5-V power supply obtained by use of a 5-V regulator placed in series with the 20-V regulated power supply. The 5-V power supply is necessary for the microprocessor and all of the other Integrated Circuits (IC's) requiring a 5-V d.c. source. It was then necessary to design a digital control interface that would vary the output of the 80-volt variable power supply through 32 steps, at 1.5-V intervals.

In the PMC power supply, provisions are made to permit remote adjustment of output voltage by means of an external resistance  $R_p$  shown

**Figure 3.4. Interface for digital control of Power/Mate variable power supply**

---



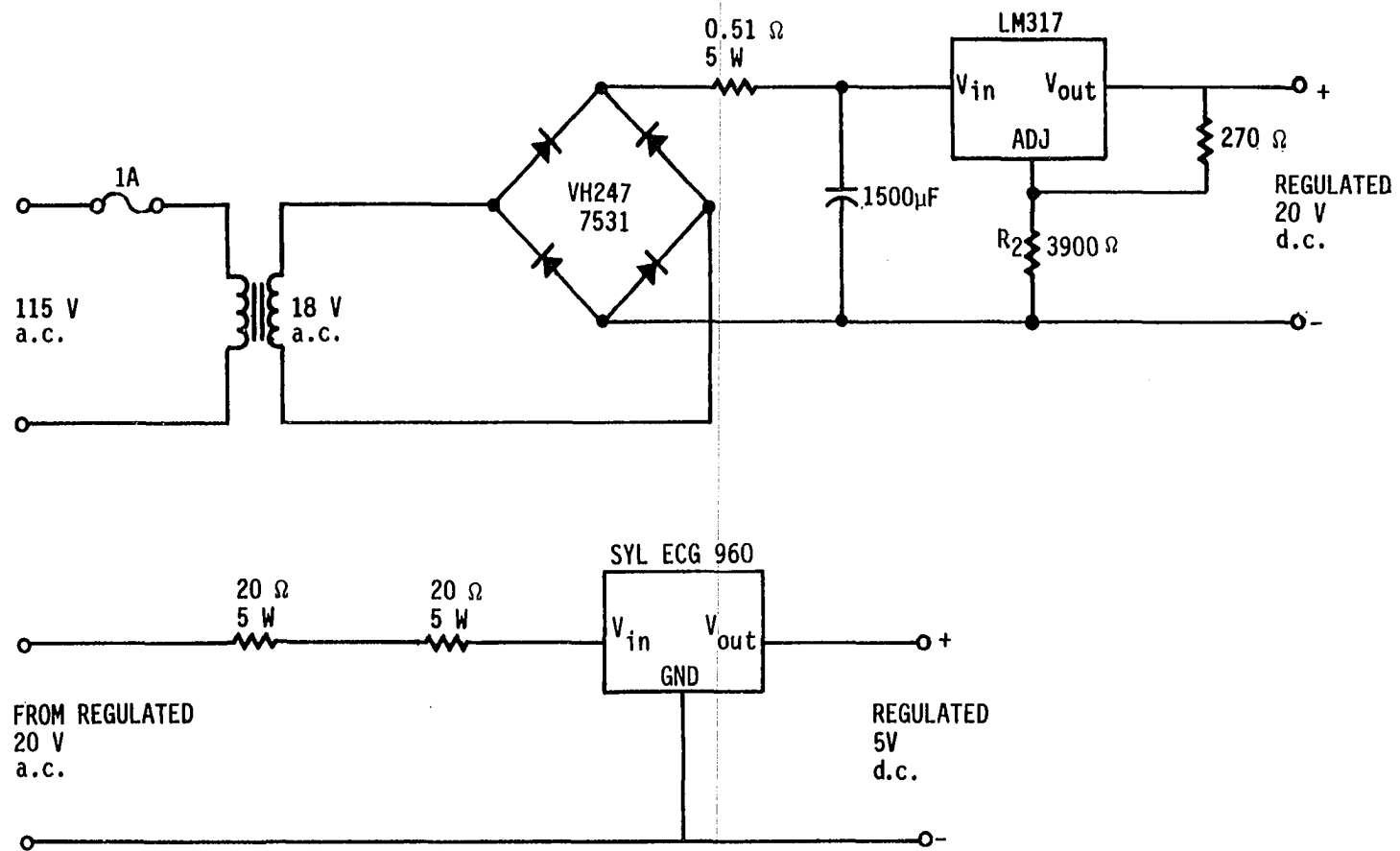
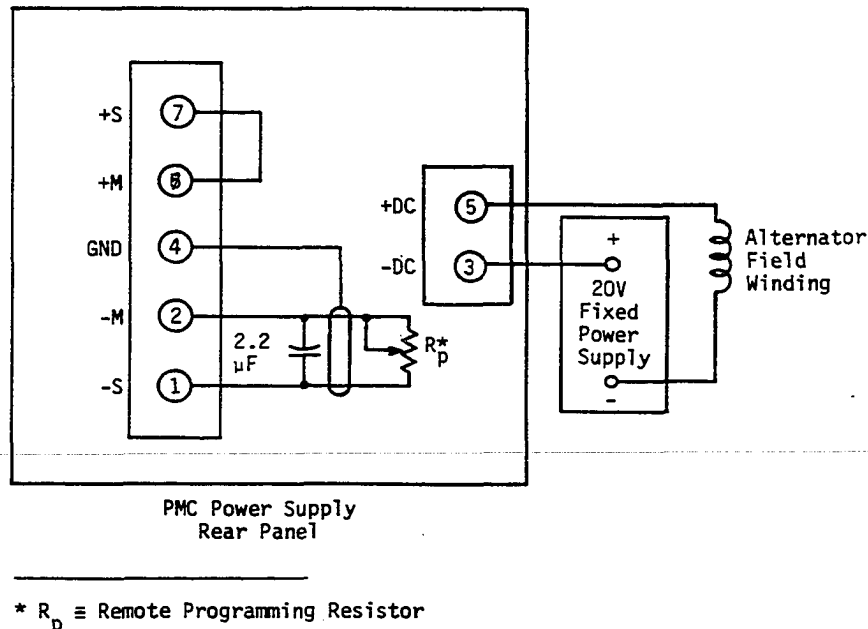


Figure 3.5. Circuit for 20-V and 5-V regulated power supplies

in Figure 3.6. A test was performed on the PMC power supply to determine the required values of  $R_p$ 's for a desired set of output voltages. Resistances needed are listed in Table 3.3 along with the actual sizes of resistors and variable pots used. Five input/output (I/O) port lines from the microprocessor were assigned to select between any one of the 32 voltage values. Four of these I/O lines are used to select among any one of the 16 output lines from each of two 4 by 16 decoders. The fifth I/O line is used to select between the two decoders, thus, allowing 32 possible control lines as shown in Figure 3.4.

Each of the 32 control lines from the two 4 x 16 decoders in turn activates an opto-isolator. The opto-isolators then place the proper  $R_p$  across the (-S) and (-M) terminals (remote programming) of the PMC power supply. The opto-isolators are intended to isolate the TTL circuits from the high voltages associated with the PMC power supply. All  $R_p$ 's when selected, are placed in parallel with the series combination of R97 and R98. The series combination of resistors R97 and R98 are necessary to protect the power supply when none of the 32 control lines are activated. A picture of the digital controller interface board for controlling the PMC power supply is shown in Figure 3.7. The digital controller was calibrated by adjusting the variable pots to obtain a step size of 1.5 V with a minimum output voltage of 22.4 V and a maximum output voltage of 68.9 V.

The programmed output voltage from this controllable power supply



\*  $R_p$  ≡ Remote Programming Resistor

Figure 3.6. PMC power supply connections for remote programming

Table 3.3. Test data obtained for remote programming resistor  $R_p$  and the actual resistors and variable pots used for design of interface for digital control of PMC 60-V variable power supply

Steps	Field voltage (V)	Resistance needed ( $\Omega$ )	Discrete resistor ( $\Omega$ )	Variable resistor (pot) ( $\Omega$ )
0	20.0	0	0	0
1	22.4	120	82	100
2	23.9	560	470	100
3	25.4	900	680	500
4	26.9	1270	1000	500
5	28.4	1650	1500	500
6	29.9	2070	1800	500
7	31.4	2500	2200	1 K
8	32.9	2960	2700	1 K
9	34.4	3430	3300	1 K
10	35.9	3750	3300	1 K
11	37.4	4500	3900	1 K
12	38.9	5100	4700	1 K
13	40.4	5730	5600	1 K
14	41.9	6420	5600	5 K
15	43.4	7160	6800	5 K
16	44.9	7960	6800	5 K
17	46.4	8840	8200	5 K
18	47.9	9800	8200	5 K
19	49.4	10790	10 K	5 K
20	50.9	11950	10 K	5 K
21	52.4	13260	10 K	5 K
22	53.9	14770	12 K	5 K
23	55.4	16430	15 K	5 K
24	56.9	18300	15 K	5 K
25	58.4	20400	18 K	5 K
26	59.9	23030	18 K	10 K
27	61.4	26030	22 K	10 K
28	62.9	29830	27 K	10 K
29	64.4	33030	27 K	10 K
30	65.9	40000	33 K	10 K
31	67.4	46900	39 K	10 K
32	68.9	57900	47 K	50 K

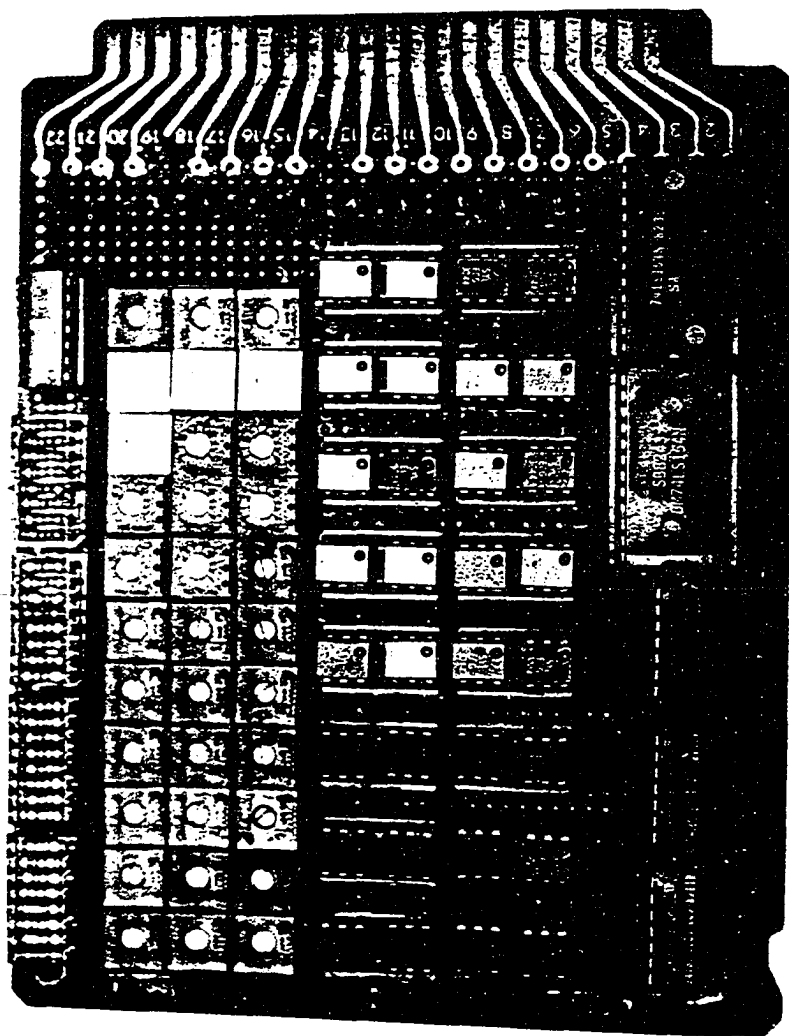


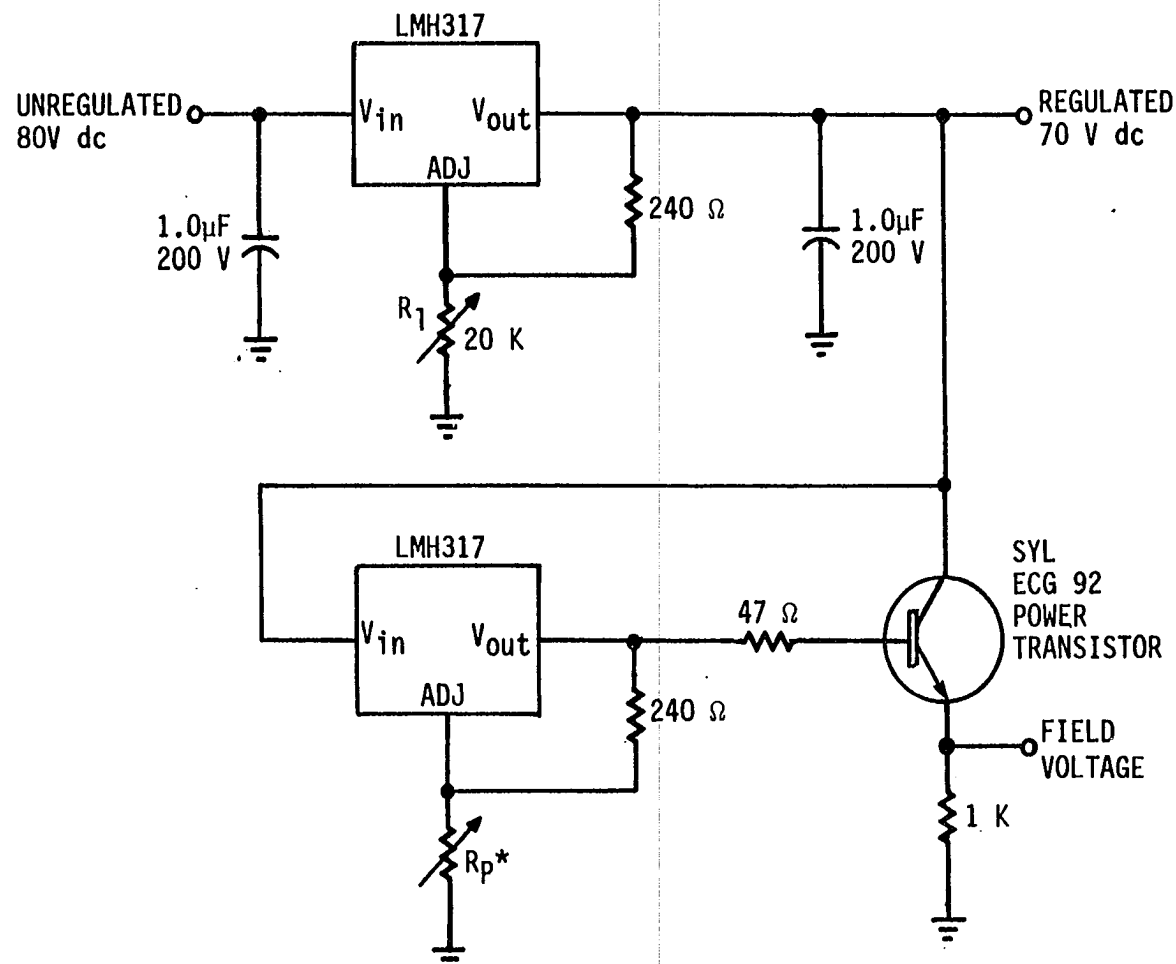
Figure 3.7. Picture of the Digital Controller Interface Board for PMC power supply

was applied across the alternator's field winding as the required field voltage. Because the field winding of the alternator is measured to be  $61 \Omega$ , the amount of current drawn from the power supply can reach levels of over 1 amp. Therefore, a separate 2-amp fuse was used for this circuit.

The second circuit, shown in Figure 3.8, was designed to allow digital control of the alternator field voltage without using the PMC power supply needed in previous circuit. In this circuit the I/O ports from the microprocessor were directly connected to a high voltage adjustable regulator. Here, there is a one-to-one relationship between I/O lines and the number of voltage steps obtained. Thus, in order to reduce the number of I/O lines required, the digital controller of Figure 3.4 was tied to the "Adjust" input of the high-voltage adjustable regulator obtaining the desired 32 voltage levels by use of 5 I/O lines as before.

Exact values of the resistors  $R_2$  in the circuits of Figures 3.5 and 3.8 were calculated using the formula derived below [18]:

$$\begin{aligned}
 V_{\text{out}} &= V_{\text{ref}} + \left( \frac{V_{\text{ref}}}{R_1} \right) R_2 + I_{\text{adj}} R_2 \\
 &= V_{\text{ref}} \left( 1 + \frac{R_2}{R_1} \right) + I_{\text{adj}} R_2
 \end{aligned} \tag{5}$$



\* $R_p$  IS PROVIDED FROM CIRCUIT OF FIGURE

43

Figure 3.8. Digitally-controllable variable power supply using adjustable regulators

$R_1 = 240 \Omega$  (typical value used)

$I_{adj} \approx 100 \mu A \approx 0$

$V_{ref} \approx 1.25 V$  fixed (determined in operation)

Therefore,

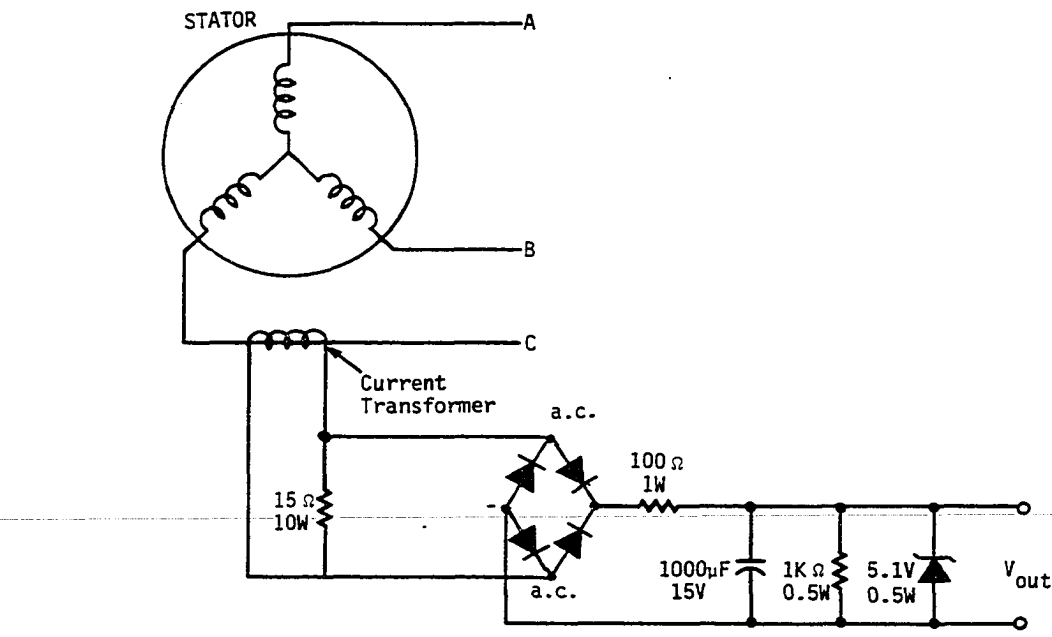
$$V_{out} = 1.25 \left(1 + \frac{R_2}{240}\right) \quad (6)$$

The first circuit, Figure 3.4, was used in the controller design because of convenience.

### 3. Output voltage transducer

As it can be seen from Table 3.1, the alternator output voltage may vary anywhere from approximately 40 to 246 a.c. volts. In order to maximize the alternator's output voltage, a knowledge of its value at any one time becomes necessary. However, this value must first be digitized before it can be used in the optimizing control program.

A transducer circuit, Figure 3.9, was first designed to translate the output voltage of the alternator down to values below 5 volts. The output from this transducer was then digitized by use of an analog-to-digital converter. The transducer uses a standard current transformer with a turns ratio of 100:5. The current transformer is placed on one of the 3-phase lines of the alternator and this results in an a.c. signal out of the current transformer that is proportional to the output voltage of the alternator. This a.c. signal is then fed through a bridge rectifier and a resistor divider network to obtain the desired 0 to 5-V d.c. voltage proportional to the alternator output voltage.



Current Transformer - Standard 100:5 Ratio  
 Bridge - VH247 7531  
 Zener - ECG 5010A

Figure 3.9. Circuit diagram for the output voltage transducer

Table 3.4. Test results of the output-voltage transducer on the Jacobs 17.5-kW alternator

Alternator output voltage (V)	Transducer output voltage (V)
50	.5
80	1.2
120	2.4
180	3.7
210	4.3
220	4.5
230	4.7

Results of a test run using this transducer on the Jacobs three-phase alternator are shown in Table 3.4.

#### 4. Analog/digital converter

Both of the input signals to the controller, i.e., the alternator output voltage and the wind speed, are analog signals which must first be translated to levels between 0 and 5 volts before they can be digitized to be used in the control program of the controller. An ADC0809 8-bit microprocessor compatible A/D converter was used for the following reasons [18]:

1. It is microprocessor compatible with latched TRI-STATE output.
2. It contains 8-channel analog signal multiplexer, which eliminates the need for an additional A/D converter or a separate multiplexer.
3. It has a relatively fast conversion time (100 microseconds typical with a clock frequency of 640 KHz).

4. It requires one 5-V power supply and is relatively low cost.

### 5. Power supply control

In order to avoid unnecessary power consumption at low wind conditions, it was desirable to have the ability to turn the PMC power supply on or off through program control. The circuit shown in Figure 3.10 was built to accomplish this task. An I/O line P2(7) was used to drive an optocoupler through a TTL buffer. The optocoupler in turn drives an 8-Amp triac which connects the 120 volts, 60 Hz a.c. power to the PMC power supply. The optocoupler's light-emitting diode is rated at 1.2 V at 10 mA, therefore, the value of resistor  $R_{in}$  was calculated to be:

$$R_{in} = \frac{(5 - 1.2) \text{ K}\Omega}{10 \text{ mA}}$$

$$= 380 \Omega$$

The 8-Amp triac requires a minimum of 30 mA on the gate to operate. Assuming a typical gate current of 50 mA, the power dissipated in each of the 180 and 1.2-K  $\Omega$  resistors may be approximated.

$$\text{For } 180 \Omega, \quad P = 180(50 \text{ mA})^2$$

$$= 0.45 \text{ watts}$$

$$\text{For } 1.2 \text{ K } \Omega, \quad P = 1.2 \text{ K } (50 \text{ mA})^2$$

$$= 3 \text{ watts}$$

Actual resistors used are 180  $\Omega$  (1 watt) and 1.2 K (5 watt).

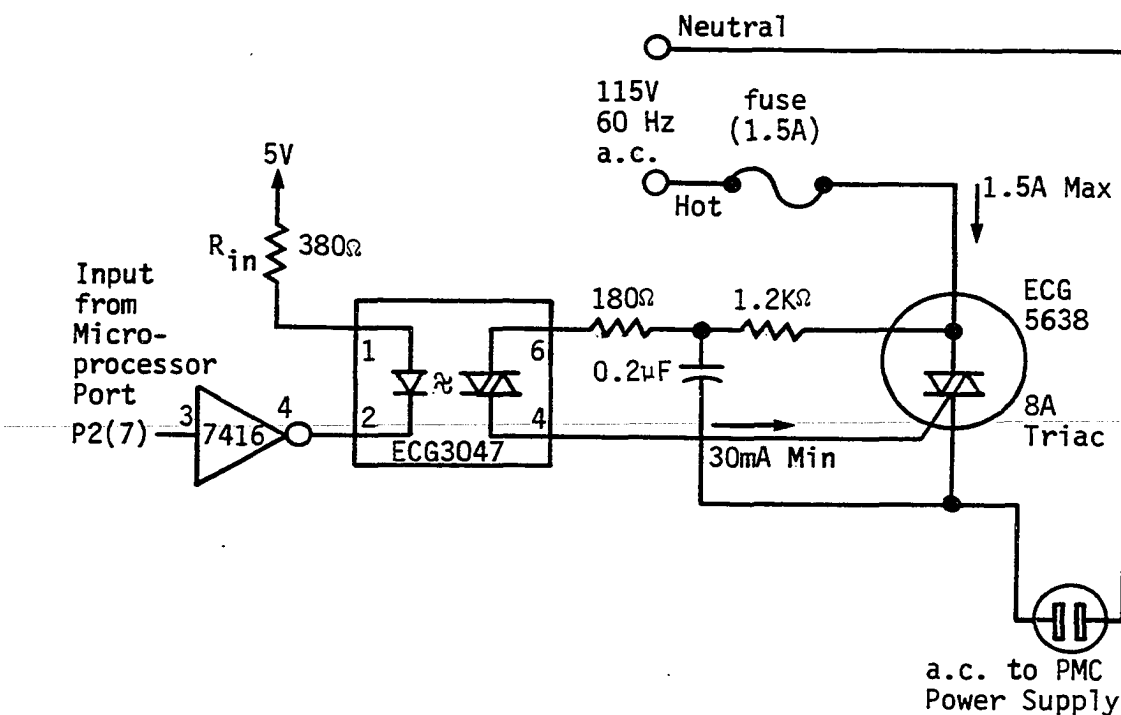


Figure 3.10. PMC power supply on/off control interface

## 6. Overspeed brake control

Two conditions dictate the activation of the brake system.

1. Wind speeds greater than maximum wind-speed rating of the wind machine.
2. Alternator output voltages greater than the rated output voltage of the alternator.

As shown in Figure 3.11, provisions are made for addition of a digital-controlled brake system. This is done by allowing software control of the a.c. power via the system controller. Because an electrically-operated brake system was not used on the WECS, a 120-V lamp was used to verify operation of the brake function.

A second method for overspeed protection is provided through the application of maximum field voltage to the alternator field winding. An increase in the field voltage represents an increase of the loading on the wind system and consequently reduces the system speed. This technique is discussed in more detail in section D9.

## 7. Wind speed measurement

Before discussing the various methods of measuring wind speed, it should be noted that in the proposed optimizing technique a knowledge of the wind speed is not absolutely necessary because the field control's objective is to keep the alternator output voltage at its maximum value. Although this can be accomplished by monitoring the alternator output voltage alone, a knowledge of the wind speed, even an approximate value of it, can have three advantages in the overall control of a wind system.

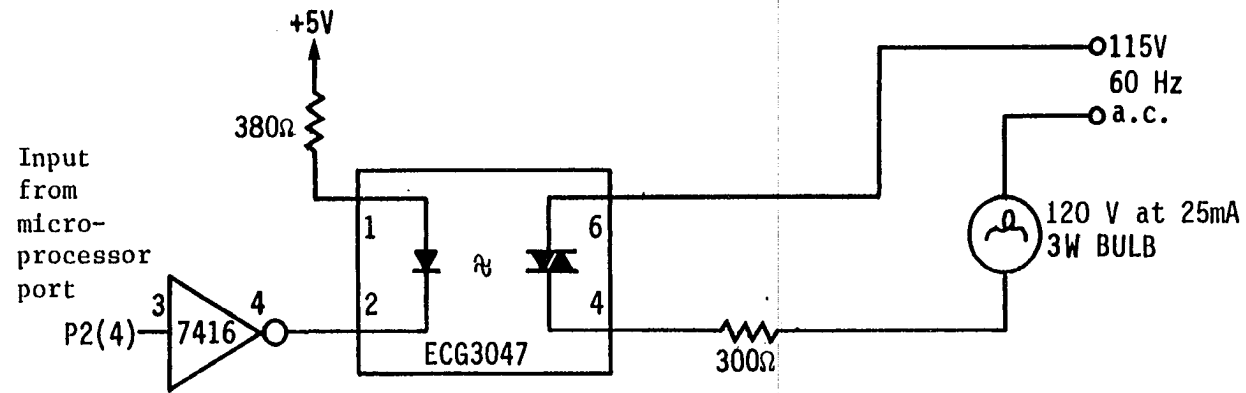


Figure 3.11. Circuit for digital control of an electric brake system

1. Power conservation: At wind speeds below which the wind system cannot produce any power, the system's power supply is shut off to conserve energy. The minimum wind speed varies for different wind systems, so provisions are made in the control program of the microprocessor-based controller for adjusting its value.
2. System protection: At wind speeds above the maximum rating of the wind system, a brake mechanism can be activated to protect the system from damaging high winds and overspeed conditions.
3. Field voltage initialization: An appropriate initial field voltage value needed for the alternator field can be determined and thus speed up the decision process.

Three techniques were studied for measurement of wind speed:

- a. Use of thermistors.
- b. Use of cup or anemometer.
- c. Use of a program controlled low-cost anemometer.

a. Wind speed measurement using thermistors Thermistors have a negative temperature coefficient of resistance (NTC): i.e., as the temperature goes up, the thermistor resistance goes down. Their behavior can be approximated according to the following formula:

$$\frac{R_0(T)}{R_0(T_0)} = e^{B\left(\frac{1}{T} - \frac{1}{T_0}\right)} \quad (7)$$

where

$R_0(T)$  is the resistance at absolute temperature  $T$ .

$R_0(T_0)$  is the resistance at absolute temperature  $T_0$ .

$e = 2.718 \dots$

B is constant (nearly) which depends on the thermistor material.

The value of B (material constant) is given by the manufacturer and is generally determined from measurements at 0°C and 50°C. When a thermistor is directly heated by passage of current through it, its equilibrium condition will be reached when it dissipates heat at the same rate at which it absorbs it [29]. Based on the attainment of this condition, when two thermistors are placed in a bridge circuit and enough power is applied to heat them far above room temperature, an equilibrium point in the bridge circuit is reached which is sensitive to the environment of both thermistors as shown in the circuit of Figure 3.12. When one of the thermistors is sealed in a reference chamber, and the other is exposed to the open air, the circuit acts as an anemometer. The two thermistors must be matched, that is, they must be within close resistance limits at the mid-operating-range temperature and should also be of the same type. For a linear output scale, values of the two resistors forming the lower legs of the bridge must be equal to each other and approximately equal to or higher than the thermistor resistances.

Because it is desired to use the available 5V power supply as the power source for the bridge circuit, the sensor thermistor must be picked such that at balanced bridge condition it has half of the source or 2.5 volts across it. Furthermore, it is assumed that the bridge balance condition occurs at a maximum temperature of 130° F. Then, assuming a dissipation constant of  $0.4\text{mw}/^{\circ}\text{C}$ , we can calculate:

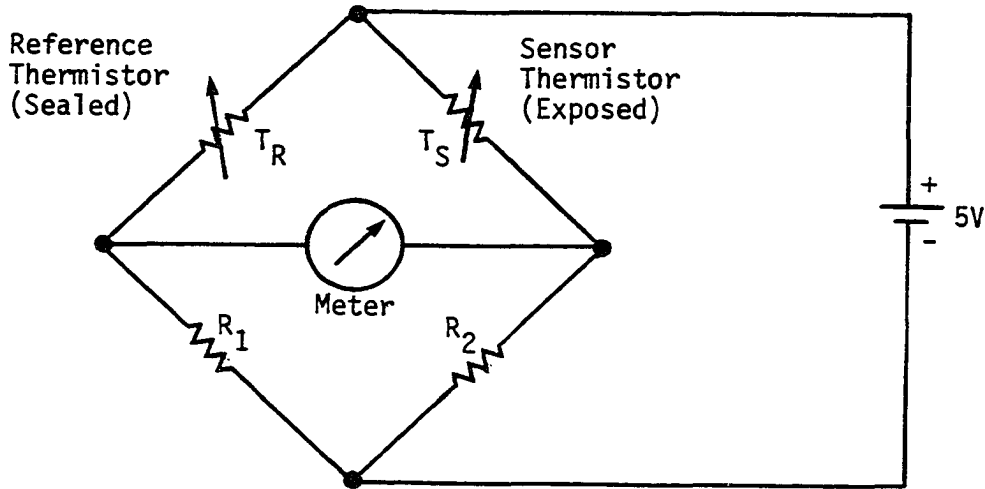


Figure 3.12. Anemometer bridge circuit

$$130^{\circ}\text{F} = 54.4^{\circ}\text{C},$$

$$[(54.4 - 25)^{\circ}\text{C}][0.4 \text{ mW}/^{\circ}\text{C}] = 11.76 \text{ mW}$$

$$P = V^2/R,$$

$$11.75 \text{ mW} = (2.5)^2/R,$$

$$\text{Therefore, } R = 531 \text{ ohms at } 130^{\circ}\text{F}$$

Using the Fenwal Electronics Thermistor Manual [9], the thermistors listed in Table 3.5 were found to best fit the above requirements. In order to keep the self-heating problem associated with the reference thermistor small, a larger reference thermistor with the same resistance ratio and of the same type as the sensor thermistor was chosen. Specifi-

cation for the thermistors are shown in Table 3.5.

The resistors on the lower legs of the bridge may be 10 K variable pots. The bridge may be calibrated against a known anemometer at various wind speeds. The output voltage from this bridge anemometer can then be fed through an A/D converter and the digitized wind speed signal can then be used in the control software.

Table 3.5. Thermistor specification for anemometer bridge circuit

Thermistor	Manufacturer type	Resistance at 25°C (K Ω)	Resistance ratio 0°C to 50°C	Dissipation constant (mW/°C)
Sensor	GB35j1	5	7.04	0.4
Reference	GB41j1	10	7.59	0.4

b. Use of cup anemometer In this technique, the a.c. signal output of the cup anemometer is translated into an equivalent d.c. voltage by means of a Frequency-to-Voltage (F/V) converter. This voltage is then fed into an A/D converter which generates a digital representation of the wind speed. If the cup anemometer contains a d.c. generator which produces an analog signal directly proportional to the wind speed, then there is no need for a F/V converter.

c. Use of a program controlled low-cost cup anemometer This approach uses the capabilities of the available microprocessor to minimize the cost of wind-speed measurement. With this approach, the need

for the F/V and A/D converters become unnecessary. However, as it is shown in Table 3.6, because the a.c. signal output level of the low-cost cup anemometer used is very small (under 1.5 volt peak to peak) for the desired range of wind speeds, an interface circuit shown in Figure 3.13 has been designed which amplifies and translates this signal into a TTL compatible signal. The translated TTL signal from the above circuit is then fed through a monostable multivibrator and tied directly to one of the input ports of the microprocessor. The actual conversion of the TTL signal to a proper wind speed is accomplished by means of a software program stored in the microprocessor-based controller memory. Figure 3.14 shows the flow chart for the TTL signal to wind speed conversion program. A commented listing for the TTL signal to wind-speed conversion program is shown in Figure 3.15.

This program takes advantage of the microprocessor's on-board timer which is started upon detecting a TTL-high signal coming from the anemometer through the interface circuit. The program then waits for the next TTL high to stop the timer. The timer runs with a frequency in kilo Hertz range as compared to the anemometer signal frequency which is in the tens-of-Hertz range. Thus, a very good resolution can be achieved. Associated with this timer is a timer register (R6) which stores the timer's count. The true wind speed is then obtained by applying a correction factor to the contents of the time register. To obtain the proper correction factor, the anemometer was placed in a wind tunnel and the frequency of its output signal was measured for different

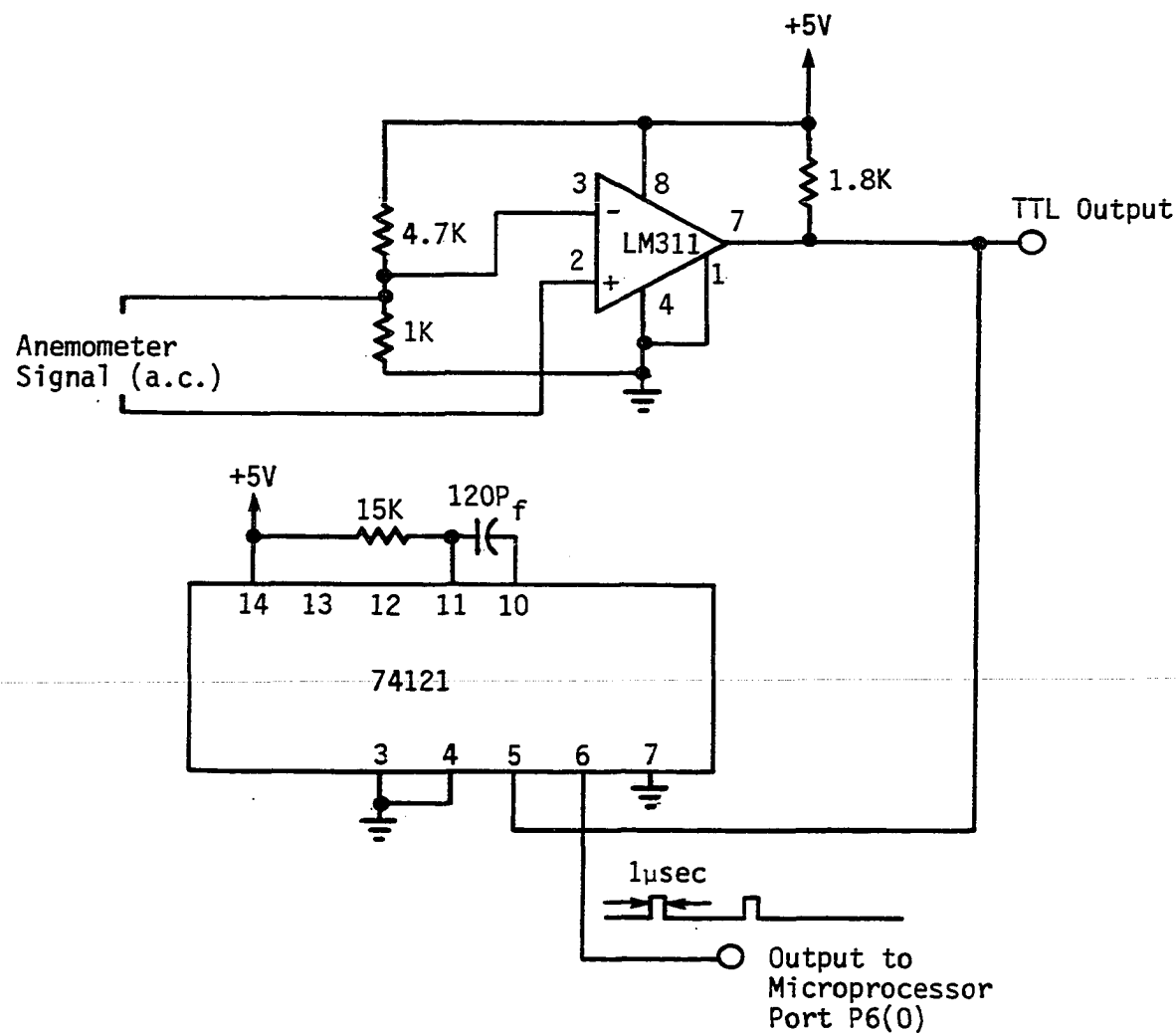
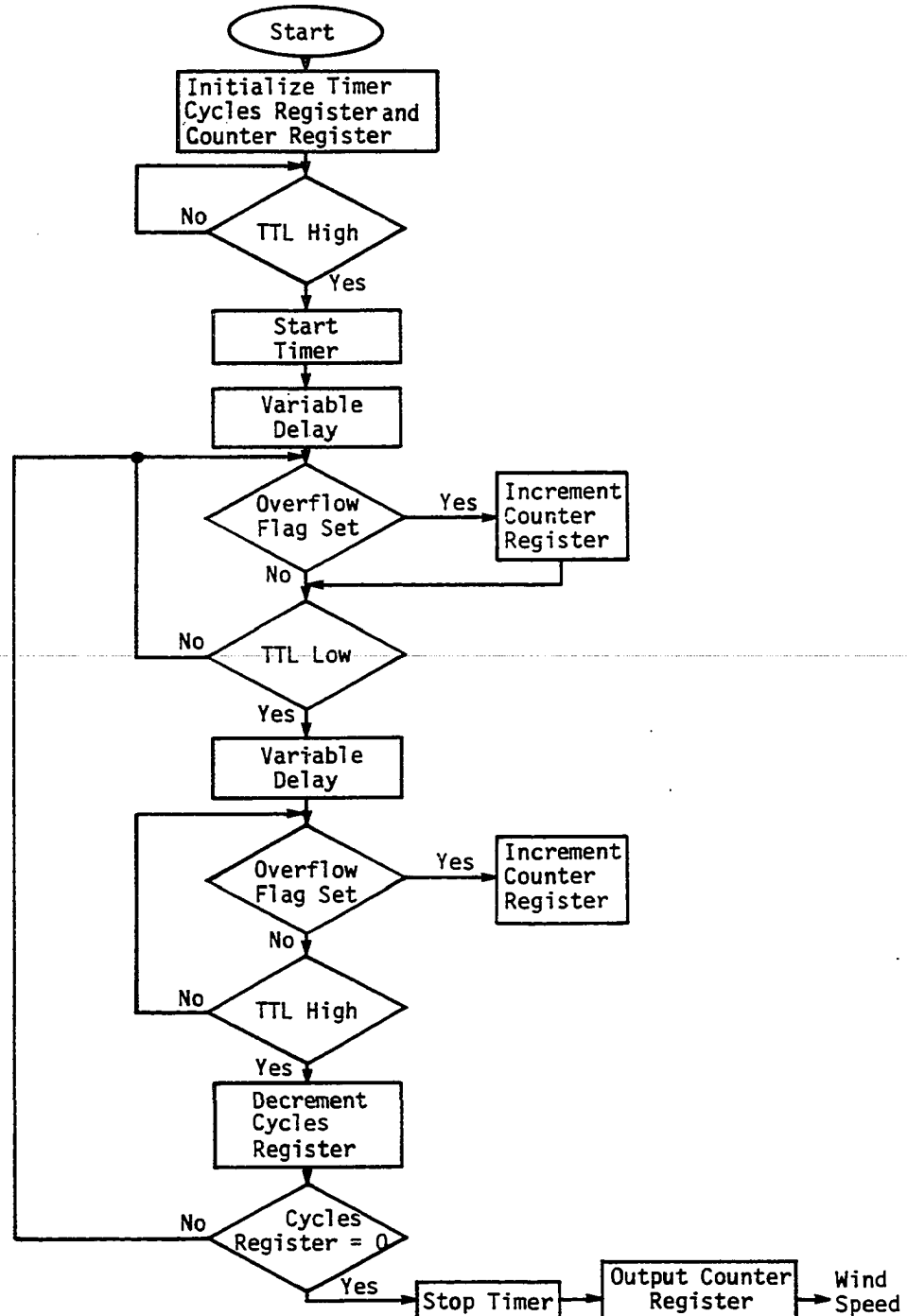


Figure 3.13. Interface circuit for low-cost anemometer

**Figure 3.14.** Flow chart for the TTL signal to wind speed conversion program



"8048"

```

ORG OOH
JMP START
ORG 10H
START SEL RBO
CLR A
MOV T,A      ;CLEAR TIMER REGISTER
MOV R6,A      ;CLEAR COUNTER REGISTER (R6)
MOV R5,#10H   ;SET UP FOR 10 CYCLES OF THE ANEMOMETER SIGNAL
WAIT  JT1 BEGIN ;DETECT THE FIRST PULSE (TTL-HIGH) FROM
                ;ANEMOMETER
        JMP WAIT    ;START TIMER
BEGIN STRT T
HERE CALL DELAY
OUTLOOP JTF INLOOP
        JNT1 CHECK   ;DETECT TTL-LOW
        JMP OUTLOOP
INLOOP INC R6      ;INCREMENT COUNTER REGISTER
        JT1 OUTLOOP
CHECK CALL DELAY
OUT  JTF IN
        JT1 CH       ;CHECK FOR NEXT TTL-HIGH
        JMP OUT
IN   INC R6
        JNT1 OUT

```

Figure 3.15. Listing and comments for the TTL Signal-to-Wind-Speed conversion program

```

CH      DJNZ R5,HERE ;10 CYCLES OF ANEMOMETER SIGNAL ARE COUNTED
        STOP TCNT
        MOV A,R6
        OUTL P1.A ;R6 CONTAINS THE VALUE CORRESPONDING TO MEASURED
                  ;WIND SPEED
        JMP START

        MOV R4,#10H ;DELAY ROUTINE OF APPROXIMATELY 50  $\mu$ sec IS
DELAY    DJNZ R4,DELAY ;NEEDED TO AVOID COUNTING THE SAME TTL HIGH TWO
        RETR      ;TIMES. NOTE: TTL-HIGH FROM THE ANEMOMETER
                  ;MUST BE GREATER THAN 10  $\mu$ SEC BUT LESS THAN 20.98
                  ;MSEC TO PRODUCE CORRECT RESULTS. THIS IS BECAUSE
                  ;A TTL-HIGH INPUT FROM THE ANEMOMTER IS CHECKED
                  ;EVERY 10  $\mu$ SEC AFTER THE EXECUTION OF THE
                  ;FOLLOWING INSTRUCTIONS:
                  ;WAIT      JT1 BEGIN 2 CYCLES
                  ;          JMP WAIT   2 CYCLES
                  ;THEREFORE, ASSUMING A 6 MHZ CLOCK:
                  ;4(2.5  $\mu$ SEC /CYCLE) = 10  $\mu$ SEC
                  ;THUS, MAKING THE TTL-HIGH SIGNAL FROM ANEMOMETER
                  ;GREATER THAN 10  $\mu$ SEC ENSURES THE DETECTION OF
                  ;ALL TTL HIGH SIGNALS.
                  ;COUNTER OVERFLOW FLAG IS SET ONCE EVERY
                  ;20.48 MSEC.

```

Figure 3.15. continued

fixed wind speeds. This is shown in Table 3.6. Generally, this frequency increased linearly with the wind speed, thus, suggesting a constant correction factor. One important advantage of this technique is that a filtering of the wind gusts and small variations in the wind can be implemented within the program. The program can be easily modified so that any number of cycles of the anemometer signal can be counted before the timer stops. The timer register contents is then averaged over the number of cycles. Increasing the number of cycles governs the degree of filtering of the wind gusts.

Table 3.6. Anemometer signal frequency and amplitude at various wind speeds

Wind speed (mph)	Anemometer signal	
	Frequency (Hz)	Amplitude (volts peak-peak)
5	1.67	0.32
10	5.88	0.70
15	9.09	1.0
20	12.5	1.4

A cup anemometer was used for measurement of wind speed because of availability.

#### 8. Overall schematic diagram and theory of operation

The overall schematic diagram of the microprocessor-based controller is shown in Figure 3.16. The numbers and description of ICs used are listed in Table 3.7.

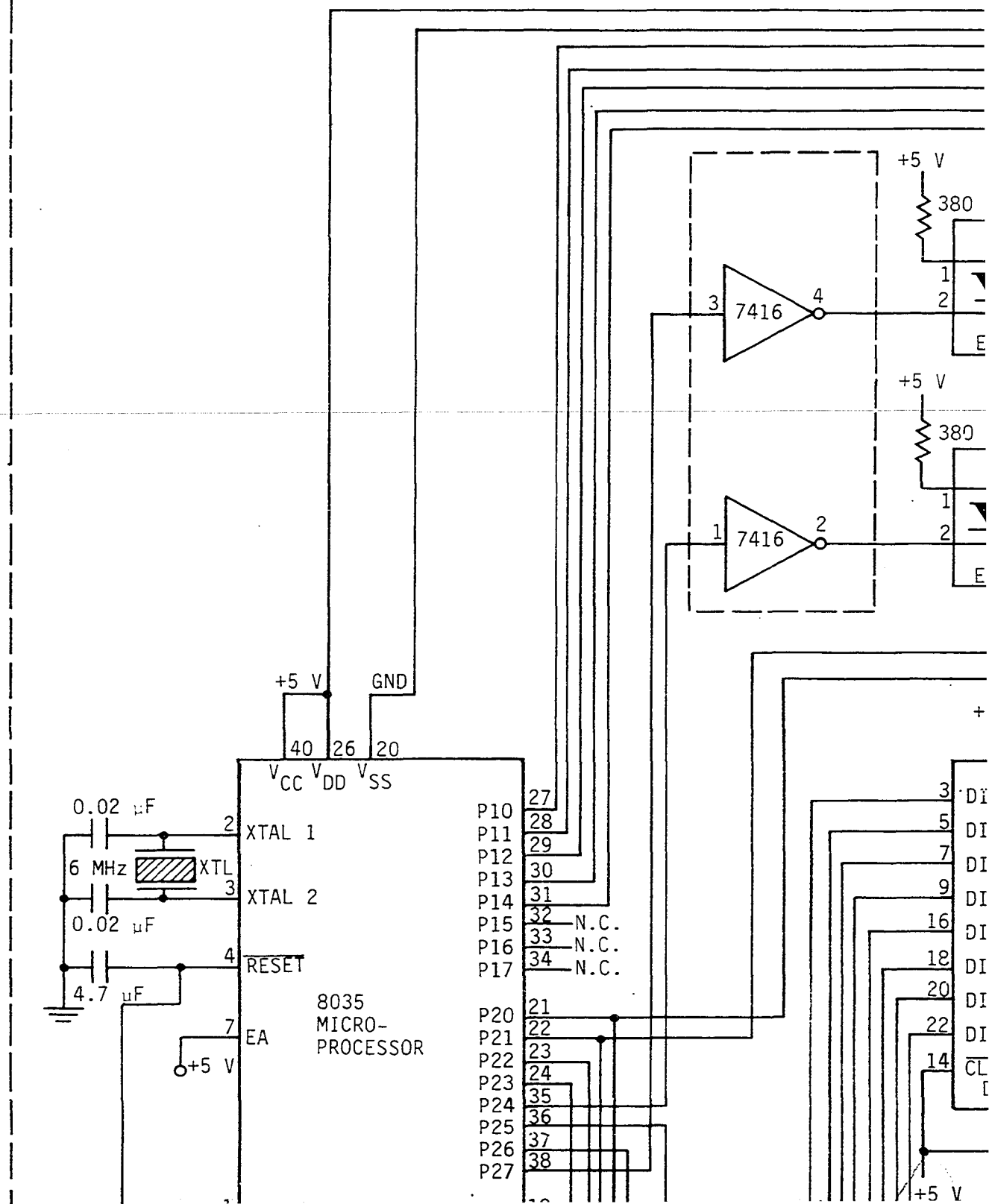
In order for the 8035 processor to operate in the external program memory mode, the external access (EA) input, pin (7), of the microproc-

**Figure 3.16.** Overall schematic diagram of the microprocessor controller

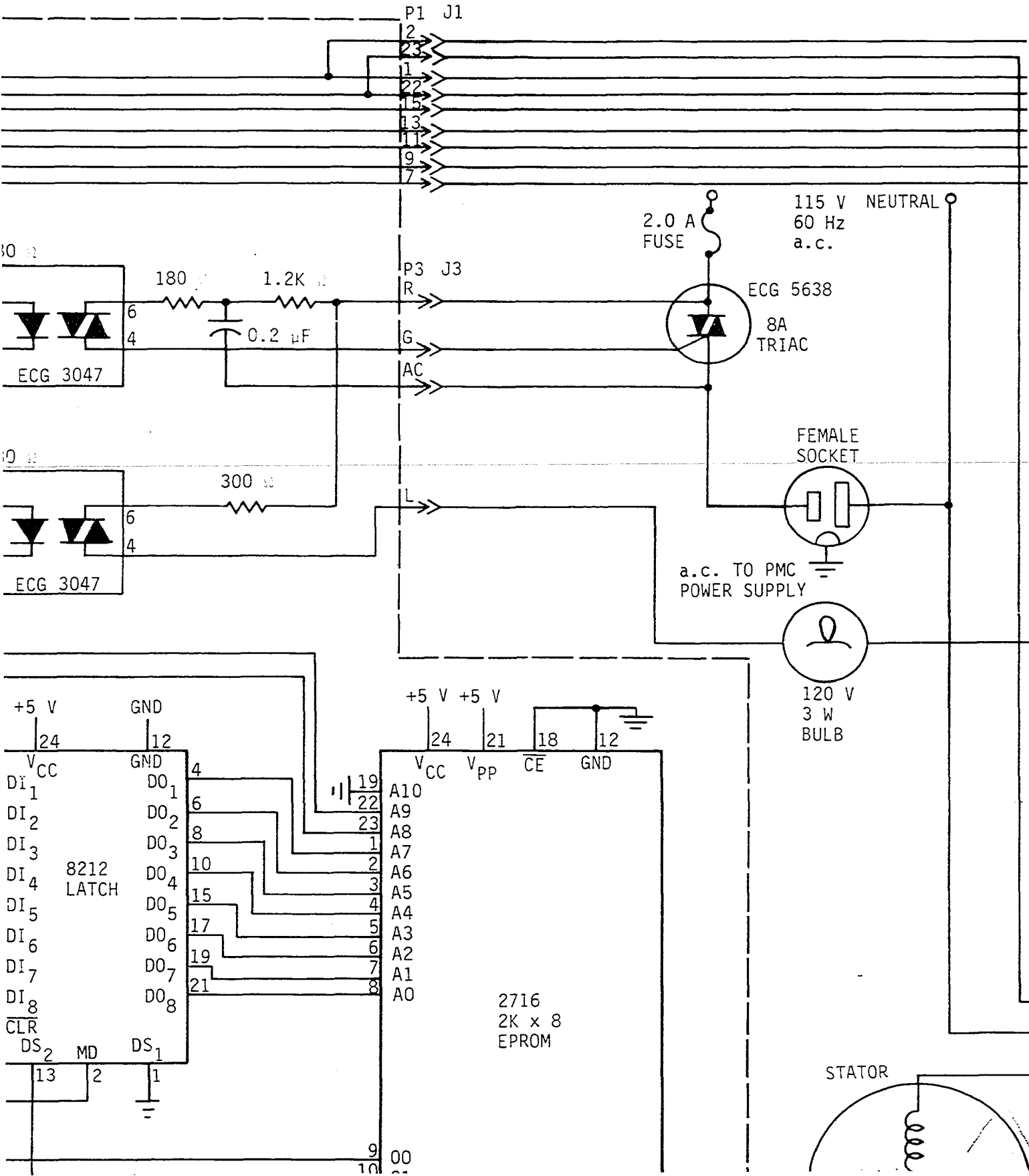


618

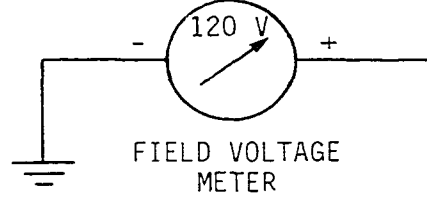
MICROPROCESSOR BOARD



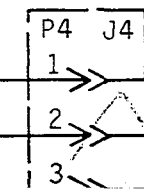








A





J2 P2

7

5

11

13

15

17

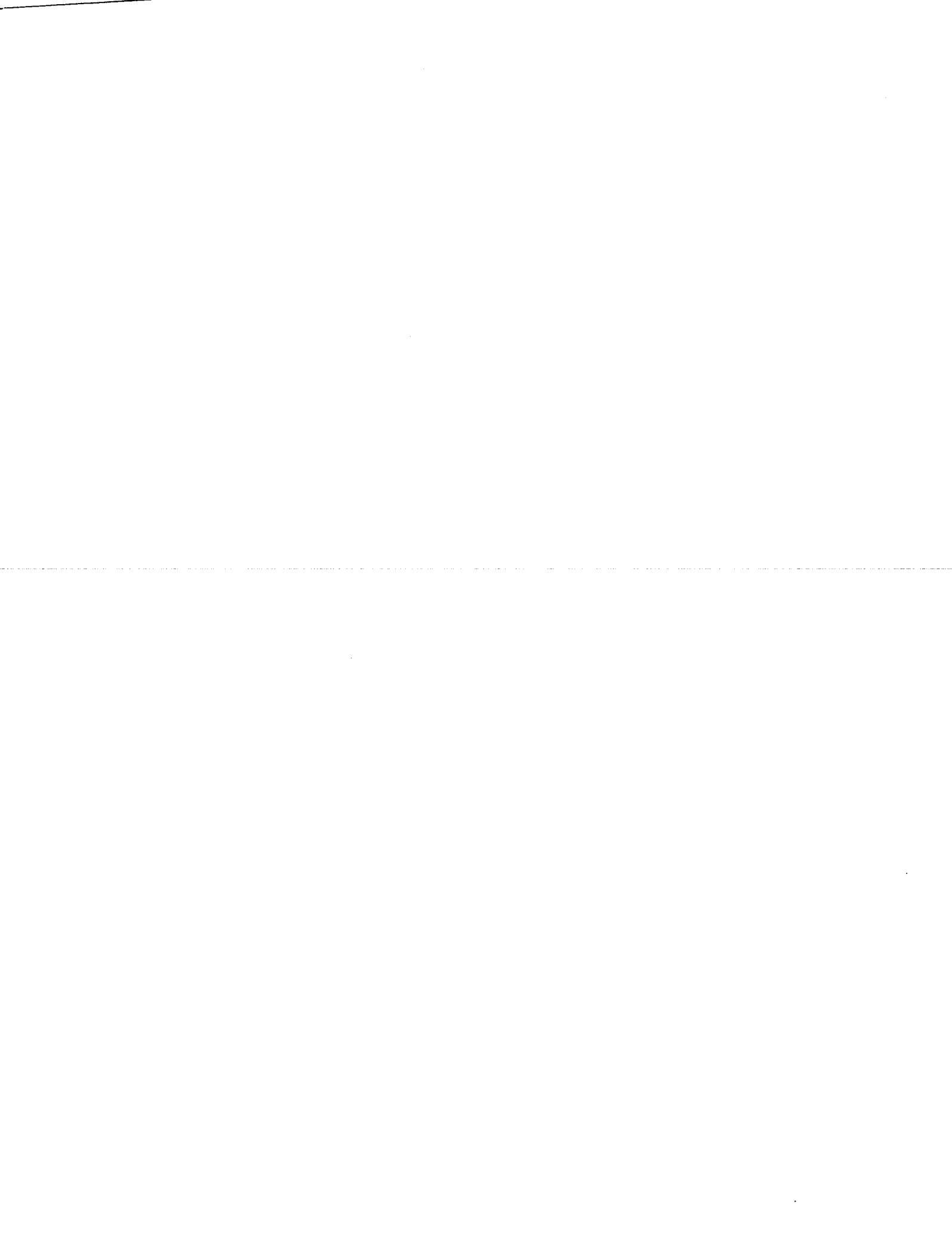
19

4-PIN CINCH  
CONNECTOR

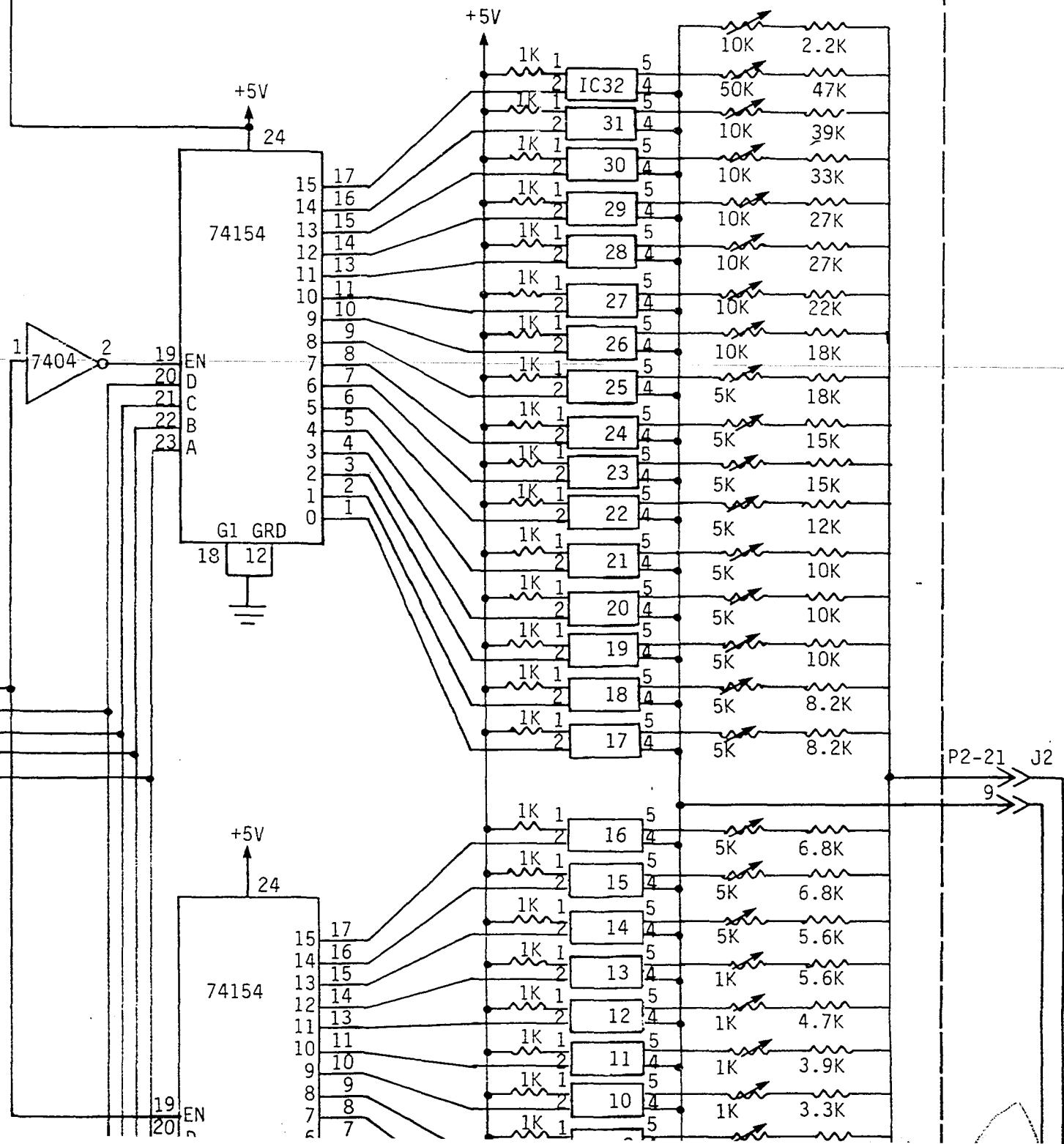
J5 P5

4

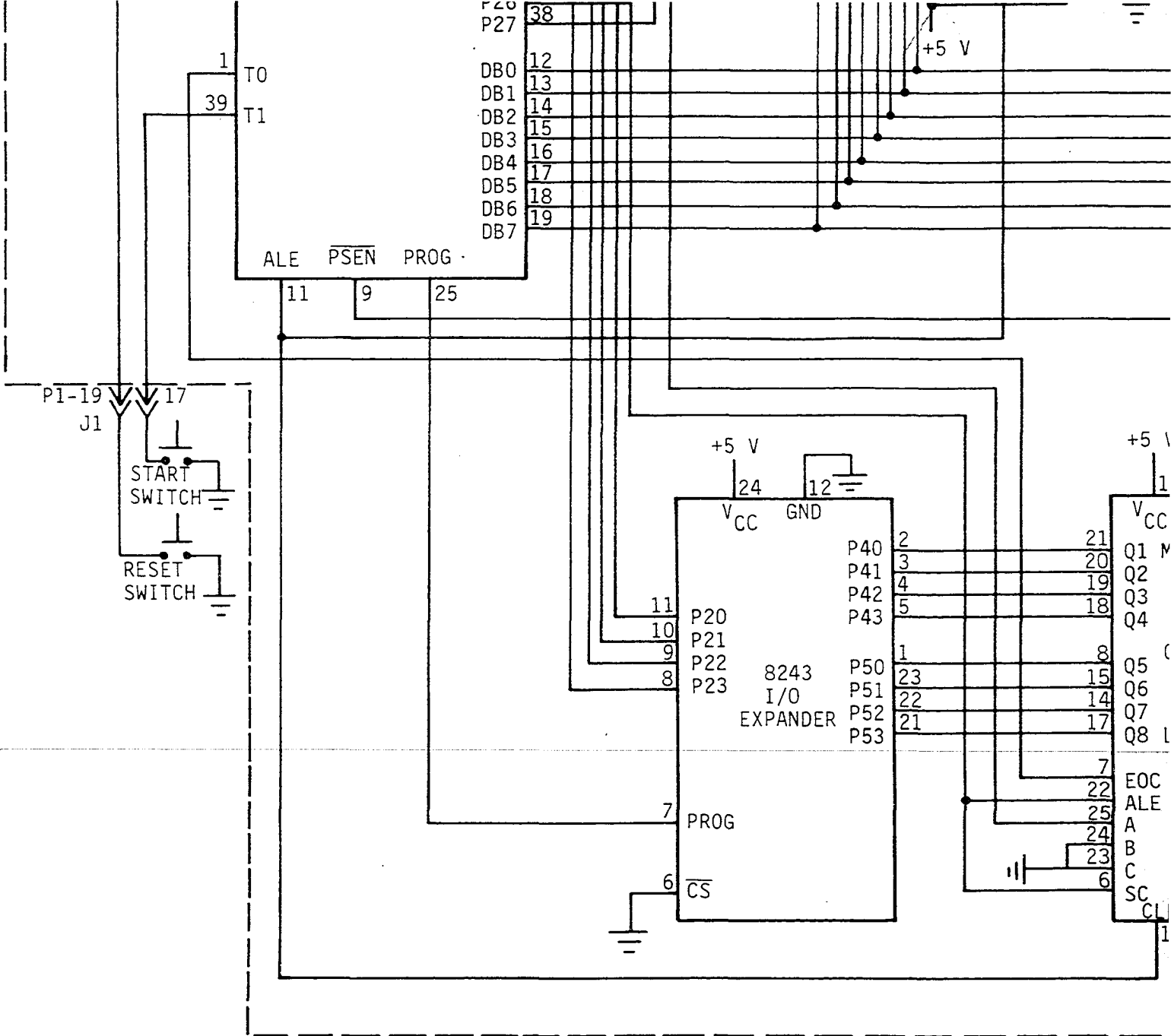
+5 7



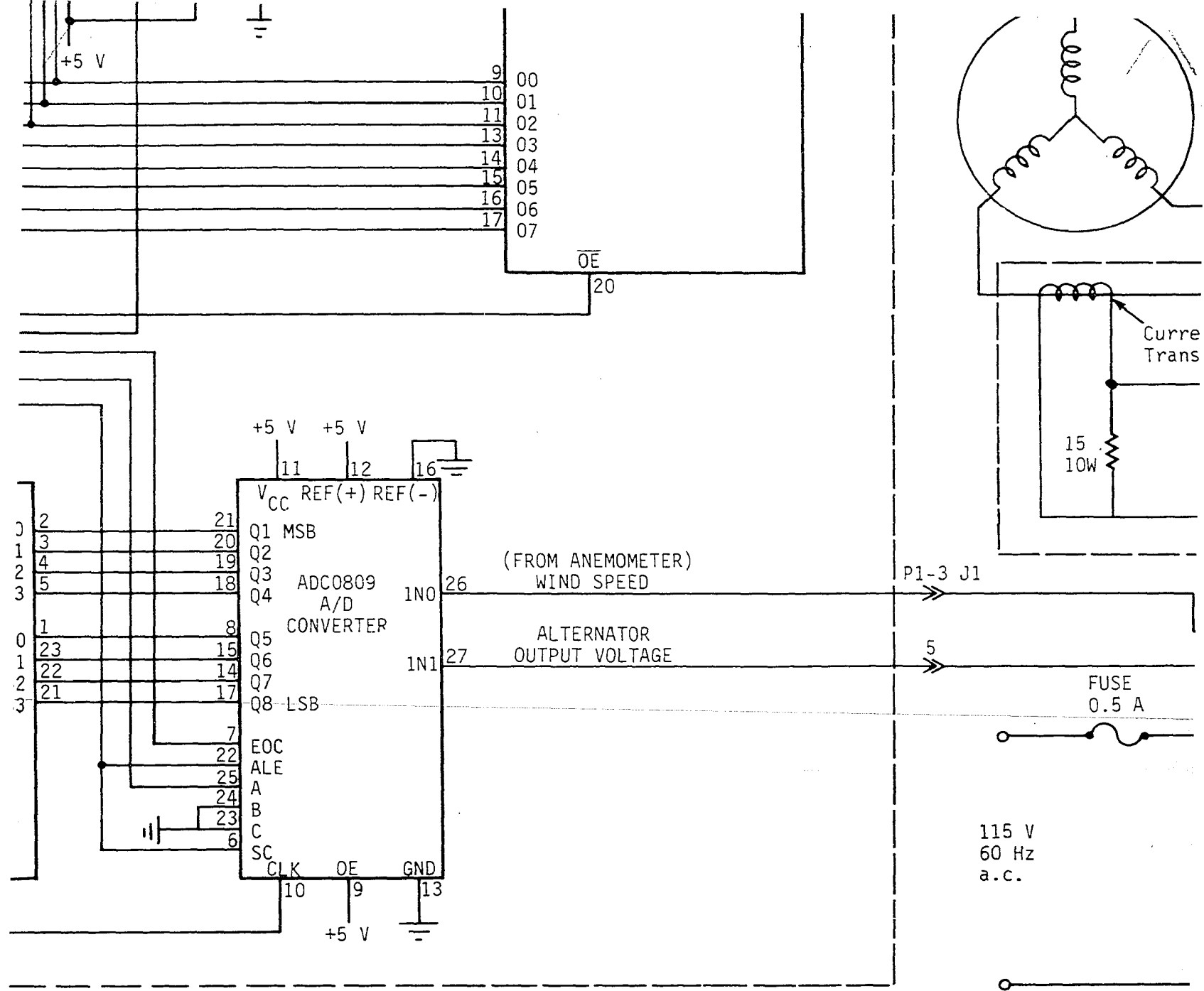
## FIELD CONTROL BOARD



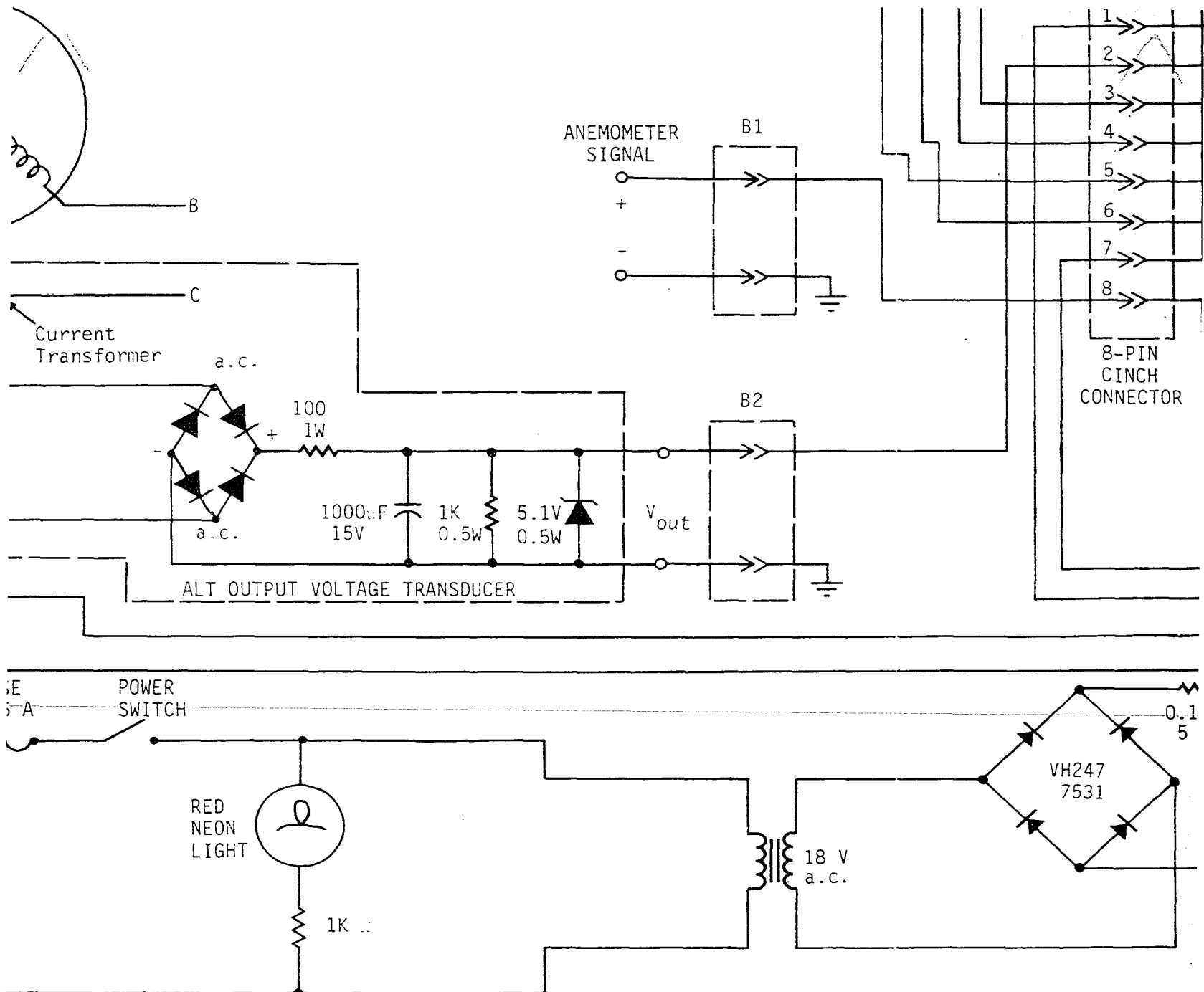




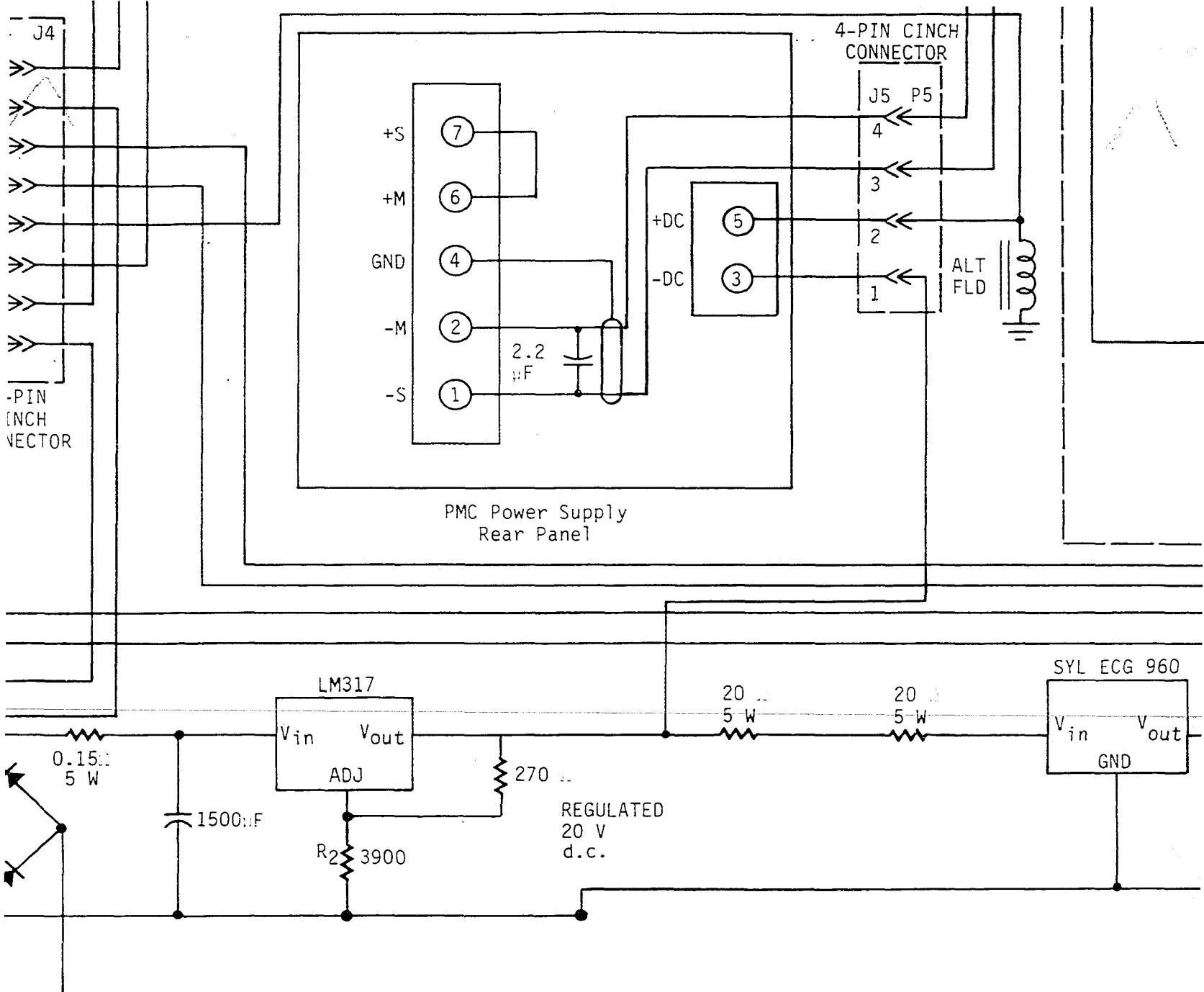














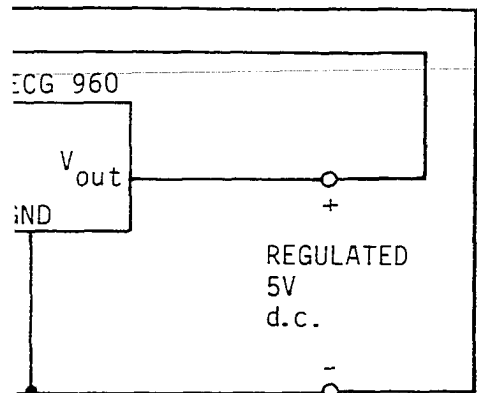
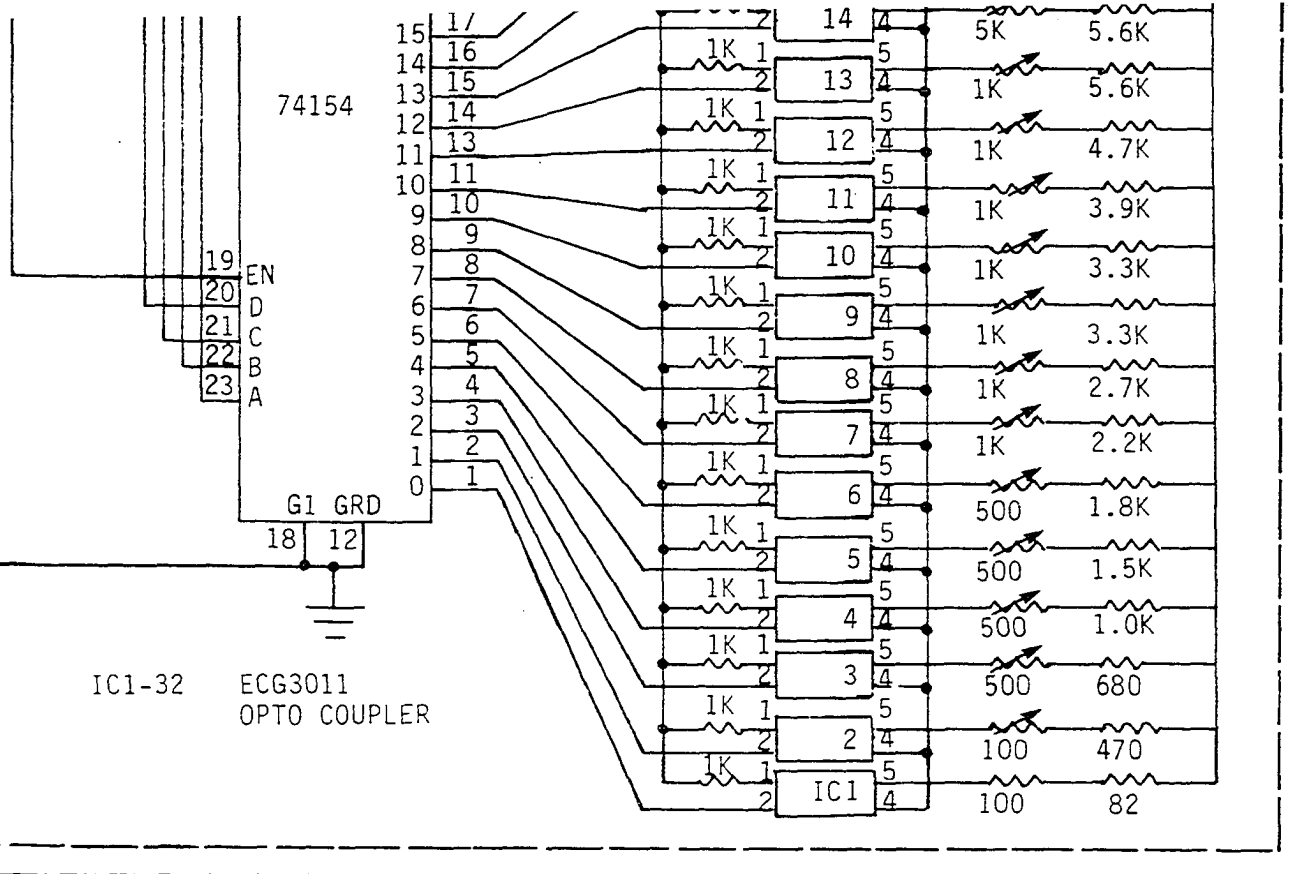




Table 3.7. Manufacturer numbers and description of the IC's used

Manufacturer's type #	Function
8035	Microprocessor
9212	8-bit latch
2716	EPROM (2K bytes)
8243	I/O expander
74154	4 x 16 decoder
7404	Hex inverter
ECG 3047	Optoisolator (Triac)
7416	Hex inverter (open collector)
LM311	Comparator
74121	Monostable multivibrator
ADC 0809	8-bit A/D converter
ECG 5638	8A triac
LM317	3-terminal adjustable regulator
ECG 960	5-V regulator
ECG 3044	Optoisolator (NPN darlington)
LMH317	High voltage 3-terminal adjustable regulator
ECG 92	Power transistor (NPN-si)
Bourns 411 4R-002-RC	Resistor network (thirteen 1kΩ)

essor must be activated ( $EA=5V$ ). This allows all program memory fetches to reference the external memory. The bus port of the microprocessor connects directly to the data output lines of the external memory. The lower 8 bits of the address for the EPROM need to be latched; therefore, an "8212" 8-bit latch was employed for this purpose. The Address Latch Enable (ALE) output signal, pin (11), of the microprocessor provides the required strobe signal for the "8212" 8-bit latch. The lower half of port 2, P2(0-3), provides the upper 4 bits of the memory address and since port 2 lines are stable for the duration of the program memory fetch, they do not have to be latched. The Program Store Enable (PSEN) output signal, pin (9), from the microprocessor is used to activate the chip select input, pin (18), of the EPROM. I/O port lines assignment for the controller are summarized in Table 3.8.

The 27 I/O lines provided in the 8035 microprocessor consist of an 8-bit data bus, ports 1 and 2, each 8 bits wide, and 3 testable input lines, T0, T1 and INT. However, the bus port cannot be used as a latched I/O port when the bus is also used to access external memory. This is because the next instruction, if external, will be fetched improperly. In order to allow for various necessary control functions for the controller, more I/O lines were needed. Thus, an 8243 I/O expander was used. The 8243 contains four 4-bit I/O ports which are designated as ports 4-7. All communications between the microprocessor and the 8243 occur through port 2 lower four bits, P2(0-3), with timing provided by

Table 3.8. Controller I/O lines assignment

IC	Designation	Function
8035 (processor)	D0-D7 (data bus)	Bidirectional port. Contains the 8 low order program counter bits during an external program memory fetch, and receives the addressed instruction under the control of PSEN.
	P1(0-4) (port 1)	Contain the 5-bit control code for field control.
	P2(0-3) (port 2)	Contain the 4 upper program counter bits during an external program memory fetch. Also used for communication with the 8243 I/O expander under the control of an output pulse on the PROG pin of the processor.
	P2(4)	Contains the control code for the "BRAKE" light.
	P2(5)	Contains the address for selection between channels 0 and 1 of the A/D converter.
	P2(6)	Contains the Start-Conversion signal for the A/D converter.
	P2(7)	Contains the control code for the PMC power supply ON/OFF.
	T(0)	Contains the End-of-Conversion signal from the A/D converter.
	T(1)	Contains the start signal from the "START" push-button switch.
8243 (I/O expander)	P4(0-3) & P5(0-3)	Contain the 8-bit digitized wind speed or alternator output voltage signal from the A/D converter.

Table 3.8. continued

IC	Designation	Function
ADC0809 (A/D converter)	ch 0 (channel 0)	Receives the wind speed analog (0-5v) signal.
	ch 1 (channel 1)	Receives the alternator output voltage analog (0-5v) signal.

an output pulse on the program (PROG), pin (25), of the microprocessor. A high to low transition of the PROG line indicates that address is present while a low to high transition indicates the presence of data.

A specific input channel of the 8-channel multiplexer on-board the A/D converter is selected by means of the address lines A, B and C of an address decoder. Because only 2 of the 8 input channels are needed, address lines B and C were grounded allowing address line A to select between two input channels 0 and 1. The wind speed and the alternator output voltage signals were tied to input channels 0 and 1, respectively. A TTL-low signal on address line A selects input 0 and a TTL-high selects input 1. The address is latched into the decoder on the low-to-high transition of the ALE output signal from the microprocessor. The A/D converter is reset on the positive edge of the Start-Conversion (SC) pulse and the conversion is begun on the falling edge of the Start-Conversion pulse. End-of-Conversion (EOC) signal will go low between 0 and 8 clock pulses after the rising edge of the Start-Conversion pulse. Therefore, conversion will be completed when End-of-Conversion signal goes back high again.

### 9. Control program

A control program written in the MCS-48 assembly language was developed to accomplish the objectives of the proposed optimizing technique. This program was edited and assembled using the Hewlett Packard 64000 minicomputer system. The machine code generated was stored on a 2716 EPROM. The programmed EPROM was then placed in the socket provided on the microprocessor board shown in Figure 3.17. The control program was designed following a "top-down" program design approach thus allowing simpler modification and debugging. A flow chart of the control program is provided in Figure 3.18.

An assembly listing of the control program including the equivalent machine codes and comments is provided in Appendix B.

---

a. Description of the flow chart for the control program Efforts have been made to make the flow chart for the control program easy to follow and self-explanatory; however, a description of program flow and the function of each block may be helpful. For this purpose, a brief description of the block functions is given:

Initialize The program starts by first performing an initialize routine. The function of initialize is to establish the proper configuration for the microprocessor I/O ports.

Sample V<sub>o</sub> Next, a sample of the alternator output voltage ( $V_o$ ) is obtained. This is done for two reasons:

1. To establish a basis for comparison against later samples of output voltage.

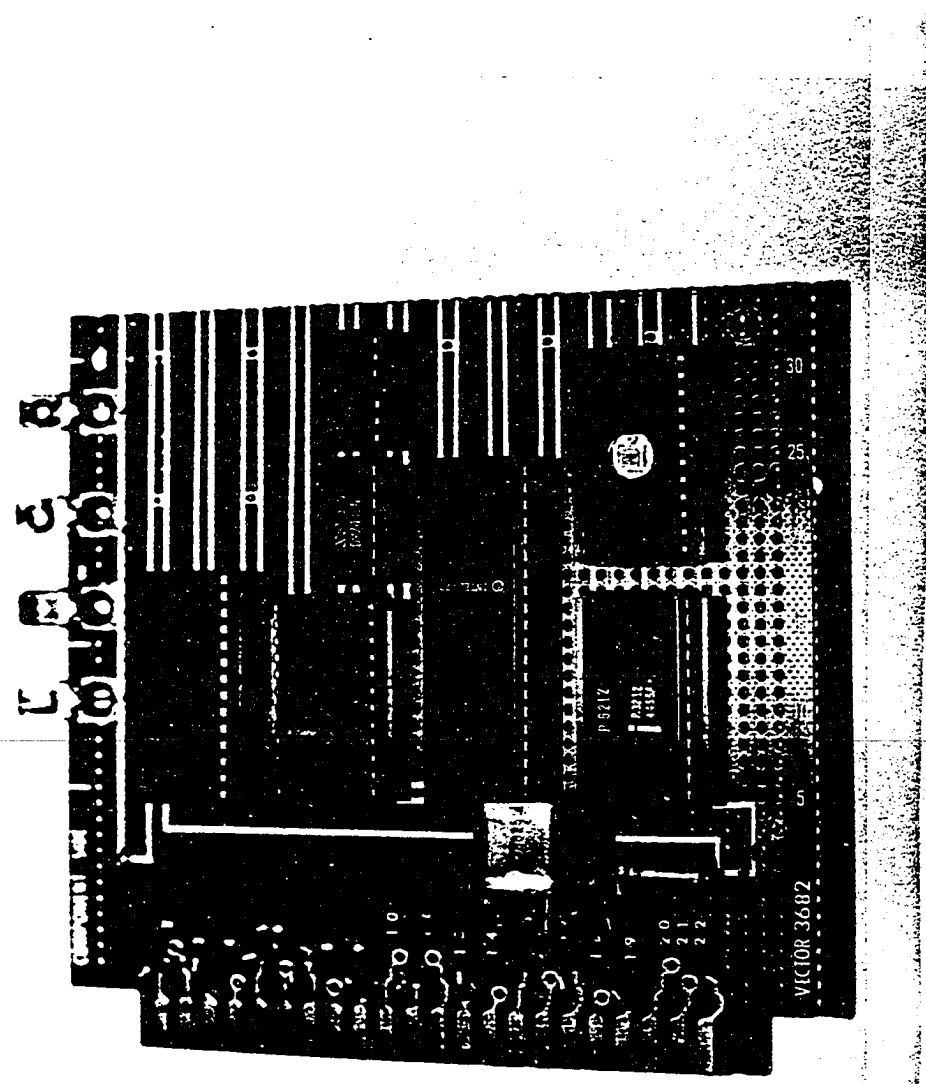
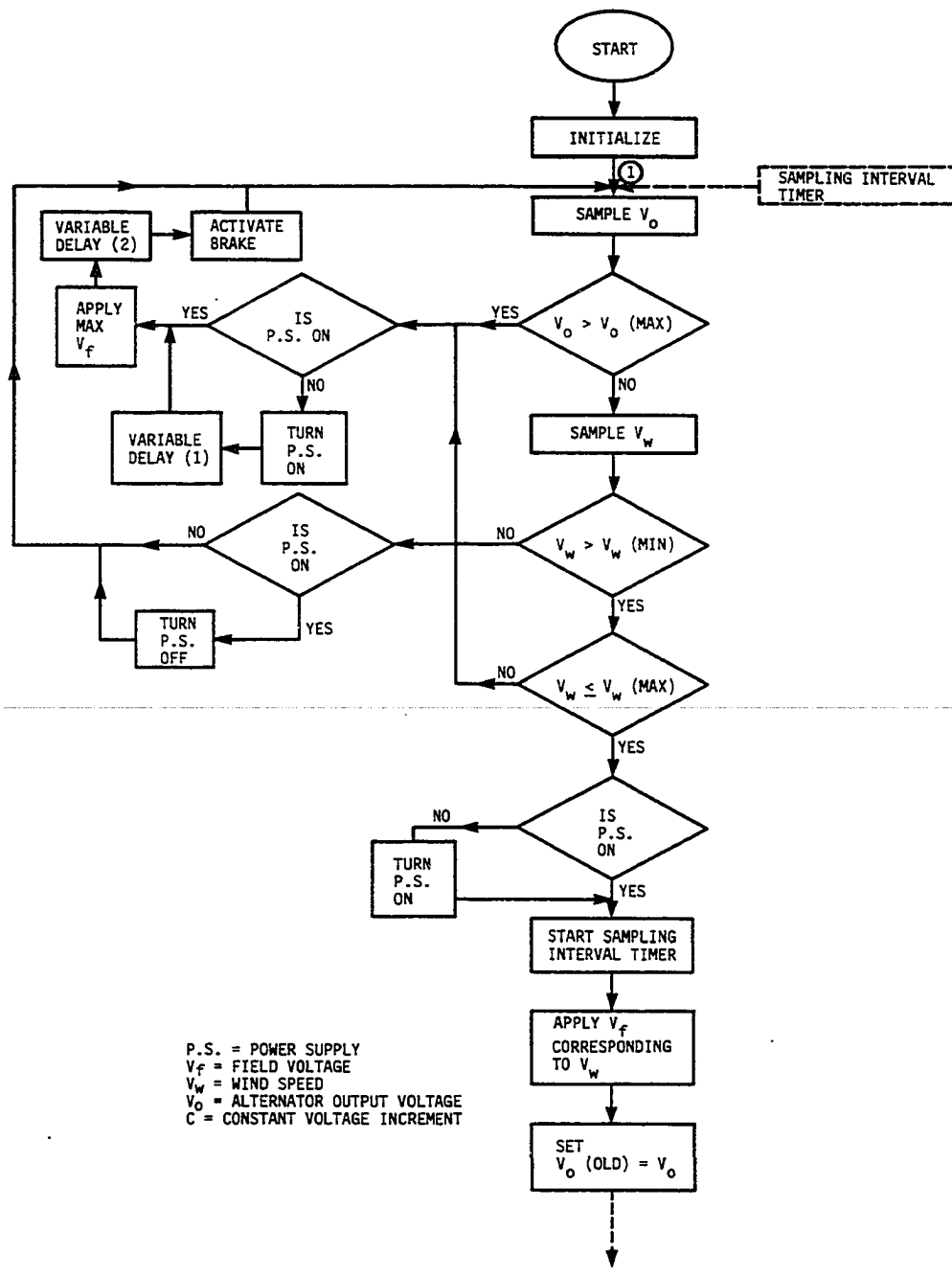


Figure 3.17. Picture of microprocessor board illustrating the physical layout of the IC's



Flow chart of the control program

Figure 3.18. The flow chart of the control program

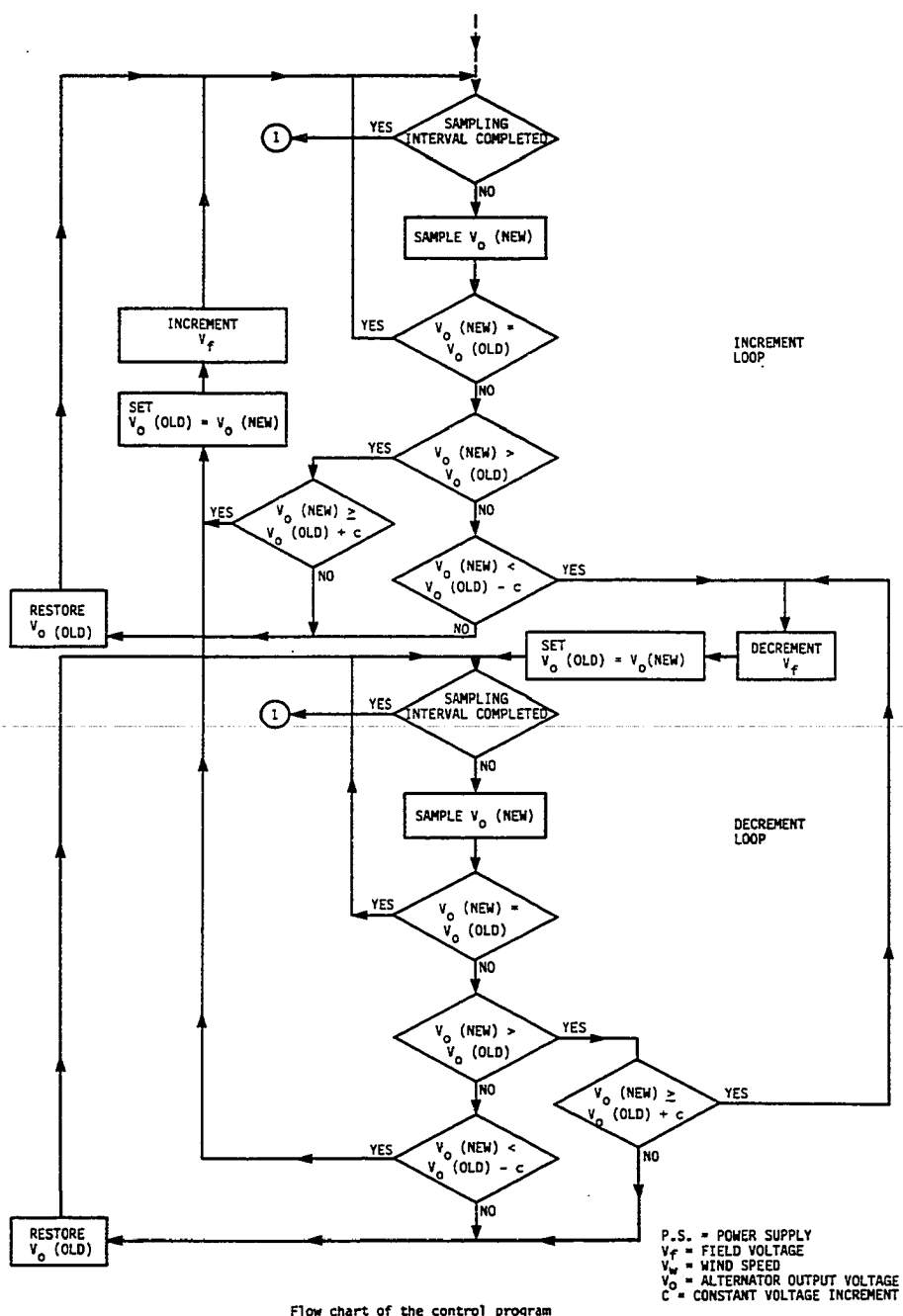


Figure 3.18. continued

2. To check for output voltages exceeding the maximum rating of the wind system. If the value of  $V_o$  is greater than the maximum rating, then, the power supply should be turned on as part of the brake procedure.

Is P.S. on and turn P.S. on It is possible for the power supply (P.S.) to not have been turned on previously. If it has already been turned on, the program continues; if not, the power supply is turned on.

Variable delay (1) Because the microprocessor executes program instructions in microseconds, some delay is necessary after turning the P.S. on to allow for its output voltage to stabilize before continuing with program execution.

Apply max field voltage Maximum voltage available from the power supply is applied to the alternator field as part of the shut-down procedure. This is equivalent to increasing the load on the system and causes a decrease in the system speed.

Variable delay (2) The purpose of variable delay (2) is to allow for the system speed to decrease before the brake is activated. This helps in reducing both brake wear and mechanical shock on the system.

Activate brake The brake mechanism may be activated to protect the system from damaging high winds and over-speed conditions.

Sample  $V_w$ ,  $V_w > V_w(\min)$  AND  $V_w \leq V_w(\max)$  A sample of wind speed ( $V_w$ ) is obtained to check for minimum wind speed at which the power supply is turned on and also to check for wind speeds greater

than the maximum wind speed rating of the system so that the maximum field voltage ( $V_f$ ) and brakes can be applied to shut down the system. If the  $V_w$  sample taken falls within the acceptable  $V_w$  range for the wind system, the control program continues. The power supply is turned on at this point if it has not been turned on before.

Start sampling interval timer To ensure safe operation of the wind system, it is necessary to check the limits of  $V_o$  and  $V_w$  periodically. This is accomplished by an adjustable timer routine controlling the on-board microprocessor counter.

Apply  $V_f$  corresponding to  $V_w$  Proper  $V_f$  corresponding to the  $V_w$  sample previously taken is obtained from a look-up table stored in memory and applied to the alternator field. Note: Data in the look-up table are the results obtained from a separate test run on the alternator, described in the section under Field Control.

Set  $V_o$  (old)= $V_o$  The output voltage sample obtained initially is assigned to a storage register as the value for comparison and designated the "old output voltage sample,"  $V_o$  (old). The rest of the flow chart consists of an increment and a decrement loop.

Sampling interval completed Whenever the timer interval, previously set by the sampling interval timer, is completed, the program branches to step (1) at the beginning of the flow chart and continues from there.

Sample  $V_o$  (new) A new sample of alternator output voltage,  $V_o$  (new), is obtained to be compared with the old sample. Based on the

result of the comparison tests that follow,  $V_f$  will either be incremented or decremented.

$V_o$  (new)= $V_o$  (old)       $V_o$  (new) is compared with  $V_o$  (old). If they are equal, it can be concluded that no adjustment of the field voltage value is necessary.

$V_o$  (new)> $V_o$  (old)+C      If  $V_o$  (new) is greater than  $V_o$  (old) by a fixed amount "C," it can be concluded that the wind speed has increased and alternator field voltage must be adjusted for optimum control. Note: The fixed voltage increment "C" produces a hysteresis effect for the field-voltage adjustment. It eliminates the changes on the field voltage that could exist due to very small changes in the alternator output voltage.

---

Set  $V_o$  (old)= $V_o$  (new)       $V_o$  (new) is assigned to the storage register designating  $V_o$  (old). This is done so that the next output voltage sample taken will be compared to the most recent old sample.

Increment  $V_f$        $V_f$  is incremented in an attempt to maximize the wind system output voltage.

$V_o$  (new)< $V_o$  (old)-C      If  $V_o$  (new) is not less than  $V_o$  (old) by a fixed amount "C," then  $V_o$  (old) is restored and no adjustment of the  $V_f$  value is necessary. Otherwise, two conclusions can be drawn:

1. Wind speed has decreased causing a drop in alternator output voltage.
2. The proper field voltage for the particular wind speed has been exceeded and further increments in the value of field voltage will cause the alternator output voltage to decrease rather than increase.

Decrement  $V_f$  For either of the above two conditions, the proper solution is to decrement the field voltage. The rest of the flow chart consists of the decrement loop, the description of which is very similar to the above increment loop. The same comparison tests are performed but the resulting control action is to decrement the field voltage rather than to increment it.

b. Control program description The assembly listing of the control program, including comments, is provided in Appendix B. The control program consists of a main body and a set of subroutines following the approach of "top-down" program design. Each subroutine when called upon by the main body performs the specific task it is designed for and then transfers the control to the main program. Each subroutine may be called upon more than once during each cycle of the program execution. Once the control program is started, it will perform its objective, i.e., maximizing the output voltage continuously. The control program execution may be interrupted by resetting the processor externally. At overspeed conditions, when wind speed exceeds the maximum rating of the wind system, the control program departs from its main cycle and executes the brake routine. During this time, the control program continuously monitors the wind speed and resumes execution of the main cycle as soon as the wind speed drops below the maximum rating. The same holds true in the case of the alternator output voltage exceeding its maximum rated limit. During the time when the necessary brake procedures are being performed, the control program continuously monitors

the alternator output voltage. When the alternator output voltage no longer exceeds the maximum rated limit, the control program resumes execution of the main cycle. At under-speed conditions, when wind speed drops below the minimum required limit, the control program initiates a shut-down procedure to conserve energy; however, it continues to monitor the wind speed. When the wind speed increases above the required minimum limit, the control program again resumes execution of the main cycle.

The control program together with the microprocessor-based controller form a closed loop real time control system in which the microprocessor is able, through the field control, to optimize the performance of the wind system.

---

In order to describe the operation of the control program, each of the subroutines will be looked at separately. First, the objective of each subroutine will be defined and then the actual program instructions constituting each subroutine will be commented on individually. In reading the following subroutine descriptions, refer to Table 3.8 for the description of the I/O port line assignments. The execution of the main body of the control program begins when a hardware reset is invoked by depressing a momentary push-button switch located on the front panel. This provides a means for initialization for the processor. The program counter is set to zero, thus, the first instruction to be executed after reset initialization is placed in location 0. A jump instruction at location 0 causes the first ten memory locations to be

skipped. This is because these locations are preassigned to special functions and must not be overwritten. In particular, a time/counter overflow causes a jump to subroutine at location 7, where a jump to the timer subroutine is stored. At location 10, a cell to subroutine START is stored. All of the subroutines, first of which is the START subroutine, are stored starting at memory location 200 Hex.

1) START subroutine By executing the register-bank-select instruction (SEL RB1), resident data memory locations 24-31 of the 8035 microprocessor are assigned as the working registers in place of data memory locations 0-7 and are then directly addressable. This second bank of working registers is used as an extension of the first bank of working registers. The value 21 Hex (21H) is assigned to register R2 of register bank 1. The Hex value 21 is equivalent to 4.0-mph wind speed shown in the calculations below. Thus, the minimum wind speed at which the power supply is turned on is set at 4.0 mph. Later, in the POWER-ON subroutine, the minimum wind speed at which the power supply is turned off will be set at 3.4 mph. This eliminates the problem of continuous power supply turn on and off when wind speed stays near 4.0 mph.

2) Calculations of the wind-speed calibration value The anemometer used for measuring the wind speed is calibrated for 40 mv/mph. Thus, a 4-mph wind is represented by  $4 \text{ mph} * 40 \text{ mv/mph} = 160 \text{ mV}$ . However, to achieve better resolution and simplify future calculations, all wind speed values in the program are multiplied by the constant 4.0.

Therefore,

$$\begin{aligned}4 \text{ mph} &= 160 \text{ mV} \times 4 \\&= 640 \text{ mV}\end{aligned}$$

The A/D converter used is an 8-bit, 5-volt converter, thus

$$\begin{aligned}5 \text{ V} &\equiv (2)^8 \\&\equiv 256 \text{ counts}\end{aligned}$$

Therefore,

$$\begin{aligned}640 \text{ mV} &= \frac{0.640 \times 256}{5} \\&= 33 \text{ counts} \\&= 21 \text{ H}\end{aligned}$$

---

The two general purpose user accessible flags F0 and F1 are cleared. These flags are later tested by conditional jump instructions to decide on the state of the power supply and the brake control system. The I/O Port line P2(4) is assigned to digitally activate an electrical brake system. Writing a "1" out to P2(4) turns the brake light on for operation check. The I/O Port lines P1(0-3) are assigned to adjust the field voltage. Writing all "0"s out to P1(0-3) will set the field voltage to zero. Input pin T1 of the microprocessor is used to detect when the "START" momentary push button switch has been depressed. T1 is tied to 5V supply through a 4.7K resistor. Depressing the "START" push button switch will ground T1. Therefore, JT1 DETECT instruction is used to test the state of the input pin T1.

3) INTLZ subroutine     Four different initialization subroutines INTLZ(1-4) are designed to complement the SAMPLE subroutine described ahead. Execution of each of these four subroutines prior to the SAMPLE subroutine will cause a sample to be taken from any of two input channels of the A/D converter. Furthermore, the initialization subroutines determine the conditions in which a sample is taken. These conditions are the state of the power supply and the brake control system. Execution of each of the initialization subroutines will result in two bytes of control code to be stored in registers R0 and R1 of the register bank 1. As an example, the INTLZ4 subroutine is described below.

4) INTLZ4 subroutine     This subroutine, when executed before the SAMPLE subroutine, prepares the controller to take a sample from channel 1 of the A/D converter and keeps the power supply and brake off. This is done by storing control bytes 6FH and 2FH in registers R0 and R1 of the register bank 1 and then later in the SAMPLE subroutine; the contents of the registers R0 and R1 of the register bank 1 are recalled and output to port 2.

5) SAMPLE subroutine     The SAMPLE subroutine begins by recalling the two bytes of control code previously stored in R0 and R1 of register bank 1, by one of the initialization subroutines. These control codes are then output to port 2. This causes the proper channel of the A/D converter to be selected and starts the conversion process. P2(5) is assigned to select between channels 0 and 1. P2(6) is as-

signed to start the conversion process. P2(4) and P2(7) determine the status of the brake and power supply. A delay of 1 second is added at this point to allow for completion of the conversion process and to establish a sampling rate of 1 second. The End-of-Conversion (EOC) signal from the A/D converter is connected to test input T0 of the microprocessor. Test input T0 is then tested by a conditional jump instruction to determine whether the conversion process has been completed. A high signal on T0 indicates end of conversion. The digitized sample is then transferred from the A/D converter to register R3 of the processor through the 8243 I/O expander. Communication between the processor and the I/O expander is done through the four I/O port lines P2(0-3). The digitized sample is thus transferred to register R3 of the processor four bits at a time. The "SWAP" instruction is used to switch the two nibbles of information from the A/D converter in the accumulator. The contents of the accumulator are then saved in register R3.

6) OVBRAK, OSBRAK and MINWIND subroutines The titles of these subroutines stand for "over-voltage brake," "overspeed brake" and "minimum wind," respectively. Their functions are very similar in that each compares the value of either output voltage sample or the wind speed previously taken with a fixed value. The fixed values are maximum alternator output voltage rating, maximum allowable wind speed, and minimum acceptable wind speed, respectively. Although there is no compare instruction in the 8035 microprocessor, this operation can be implemented by subtraction using two's complement addition, and by using the condi-

tional jumps on the resulting carry or absence of carry. Specifically in the case of OSBRAK subroutine, the wind speed sample has been previously taken and stored in the accumulator. The two's complement of the accumulator is first generated using the complement and increment instructions on the accumulator. Next, the fixed value 3BH, equivalent to 29 mph, maximum allowed wind speed, is added to the accumulator. At this point, control is transferred to the main program and if no carry has been produced as the result of the above addition, the conditional jump instruction "JNC BRAKE" will transfer control of the program to the BRAKE subroutine. In general, in two's complement subtraction, a carry produced indicates that the result is positive and no carry indicates that the result is negative. Therefore, in the above three subroutines, if the sample value stored in the accumulator is less than or equal to the fixed value being compared with, a carry is produced, otherwise, if the sample value is greater than the fixed value being compared with, no carry is produced.

7) BRAKE subroutine      The function of the brake subroutine is to activate the brake mechanism to protect the wind system from over-speed and over-voltage conditions. Two conditions will result in the execution of the BRAKE subroutine.

1. When output voltage exceeds the rated output voltage of the alternator.
2. When the wind speed exceeds a maximum limit of 29 mph.

The BRAKE subroutine begins by first calling the PWRON subroutine which turns on the power supply. This is done because it is possible

for the power supply to not have been turned on prior to this time. The maximum voltage available from the power supply is then applied to the alternator field by outputting the control code 1FH to port 1. This is equivalent to increasing the load on the system and causes a decrease in the system speed. Next, the DELAY subroutine is called to execute a 10-second delay. The purpose of this delay is to allow for the system speed to decrease before the brake is activated. Next, the control code 9FH is output to port 2. This applies the a.c. power to the brake mechanism. Finally, the control codes OFFH and OBFH are stored in registers R0 and R1 of register bank 1. This ensures that the brake remains active until the condition that caused the activation of brake mechanism is no longer true.

8) PWRON subroutine      This subroutine when executed turns on the power supply. It is possible for the power supply to have been turned on previously, therefore, the PWRON subroutine will be by-passed using the conditional jump instruction "JFO CONTNU" on the user flag F0. If the power supply has not been turned on previously, then, the setting of flag 0 is complemented and the control code 8FH is output to port 2. This turns the power supply on, and complementing of flag 0 ensures that the PWRON subroutine will be by-passed if it is called again. Because the microprocessor executes program instructions in microseconds, some delay is necessary after turning the power supply on to allow for its output voltage to stabilize before continuing with program execution.

Therefore, the DELAY subroutine is called to execute a five second delay. Next, the value 1CH is assigned to register R2 of the register bank 1. The Hex value 1C is equivalent to 3.4 mph wind speed. This is the minimum wind speed for which the power supply will be turned off. As discussed earlier under START subroutine, this eliminates the problem of continuous power supply turn on and off when wind speed stays near 4.0 mph.

9) PWROFF subroutine Initially in this (power off) subroutine, the setting of flag 0 is checked to examine the state of the power supply. A 0 setting indicates that the power supply has already been turned off, therefore, the instruction "JMP GOON4" is executed to by-pass the PWROFF subroutine. A 1 setting indicates that the power supply is on and must be turned off. Therefore, the control code 00H is output to ports 1 and 2 to reduce the field voltage down to zero and shut the power supply off. The control code 21H is stored in register R2 of the register bank 1, setting the minimum wind speed, at which the power supply should turn on, at 4.0 mph. This is discussed in more detail under START subroutine.

10) SAMINT, TIMER and INTCHK subroutines The three subroutines "sampling interval," "timer," and "interval check," form an adjustable timer routine which makes periodic checks on the limits of alternator output voltage and wind speed as part of a safety procedure. This is done by making use of an 8-bit on-board counter in the 8035 microprocessor.

In the SAMINT subroutine, the Hex value assigned to register R7 designates the sampling interval in seconds. Therefore, the sampling interval can be adjusted by merely changing this Hex value to the desired value. The instruction STOP TCNT ensures that the counter is stopped since it may have been started previously. The counter is present by clearing the accumulator and by the "MOV T,A" instruction. Once started by the "STRT T" instruction, the counter will increment to its maximum count, FFH, and sets the overflow flag when it is full. The counter continues its count until stopped by the "STOP TCNT" instruction. The increment from maximum count to zero (overflow) results in the generation of an interrupt request. The timer interrupt request may be enabled or disabled independently of external interrupt by the "EN TCNTI" and "DIS TCNTI" instructions. If enabled, the counter overflow will cause a subroutine call to location 7 where a jump to TIMER service routine is stored. Therefore, the last two instructions before returning from the SAMINT subroutine are the "EN TCNTI" and "STRT T" instructions. The timer interrupt is reset when a call to location 7 is executed. Therefore, the timer interrupt request is enabled immediately in the TIMER subroutine. The source of the input to the counter is an internal clock which is derived by passing the 400 kHz Address Latch Enable (ALE) clock signal through a divide by 32 prescaler. The prescaler is reset during the "STRT T" instruction. The resulting 12.5 kHz clock increments the counter every 80 microseconds (6 MHz crystal is used). A delay of 20 ms (256 counts) can be obtained

by detection of each overflow. Therefore, register R6 is used to accumulate 50 overflows to achieve a delay of exactly 1 second. Furthermore, the value of register R7, previously assigned in the SAMINT subroutine, is decremented for each 1-second delay. Finally, in the INTCHK subroutine, the content of R7 is checked. A 0 in R7 indicates that the sampling interval time has been completed. At this time, the control is transformed to BEGINI to do the periodic check on the limits of output voltage and wind speed.

11) FLDVOL subroutine      The title of this subroutine stands for "field voltage." The function of it is to determine the proper field voltage corresponding to the wind speed sample previously taken and apply it to the alternator field winding. As it was decided previously under the digitally controllable variable power supply, five I/O port lines from the microprocessor are assigned to select between 32 field voltage settings. A specific field voltage setting can be established by outputting a 5-bit control code to port 1 of the microprocessor. Therefore, all 32 possible 5-bit codes are stored in the form of a "look-up" table in page 3 of the external program memory. This information is stored in page 3 of memory because the instruction "MOVP3 A,@A," in the 8035, allows easy access to data "look-up" tables. The FLDVOL subroutine is designed so that the address of each memory location, in which a 5-bit control code is stored, corresponds to the value of the wind speed requiring that control code. The following calculations were done to determine the proper memory locations in the look-

up table to store the 5-bit control codes. The normal operating wind speed range is assumed to be approximately between 5 and 28 mph and the anemometer is calibrated for 40 mV/mph. Therefore, a 28-mph wind can be represented by 1.12 volts. To simplify the programming, this value was multiplied by the constant 4 so that a 28-mph wind is represented by 4.5 volts. But 5 volts from the 8-bit A/D converter is represented by  $2^8$  or 256 counts. Therefore,

$$\begin{aligned} 28 \text{ mph} &= 4.5 \text{ v} \\ &= 230 \text{ counts} \\ &= \text{E6H} \end{aligned}$$

$$\begin{aligned} 5 \text{ mph} &= 0.75 \text{ v} \\ &= 38 \text{ counts} \\ &= \text{26H} \end{aligned}$$

$$\begin{aligned} \text{Total range} &= 230 - 38 \\ &= 192 \text{ counts} \end{aligned}$$

$$\begin{aligned} \text{number of counts/step} &= \frac{192}{32} \\ &= 6 \text{ H} \end{aligned}$$

Therefore, for 32 different field voltage settings, each 5-bit control code must be stored 6 memory locations apart from another. The first 5-bit control code was stored in the 38th memory location in page 3 (location 325H) and represents the field voltage corresponding to a 5-mph wind speed. The last 5-bit control code was stored in the 230th

memory location in page 3 (location 3E5H) and represents the field voltage corresponding to a 28-mph wind speed. The FLDVOL subroutine begins by using register R2 as an index register to point to memory locations containing the field voltage control codes. The address of the first 5-bit code, i.e., (25H) is first loaded into R2 and then access to each memory location containing a 5-bit control code is accomplished by adding a constant 6H to the contents of R2. Because the address of these memory locations correspond to the measured wind speed, the contents of register R2 and the sampled wind speed are compared for a match. The content of R2 is incremented by the constant 6H, each time, until it becomes greater than or equal to the sampled wind speed. The instruction "MOVP3 A,@A" extracts the control code in memory location pointed to by R2. The control code is then output to port 1 to set the field voltage.

12) NOCHNG subroutine In this subroutine, the Exclusive-Or instruction is used to detect if there has been a change in  $V_o$ . If  $V_o$  (new) equals  $V_o$  (old), then no adjustment of the  $V_f$  value is necessary. Here, R3 contains  $V_o$  (new) and R5 contains  $V_o$  (old).

13) DECING subroutine The title of this subroutine stands for "Decrement/Increment." It uses the two's complement technique to compare  $V_o$  (new) with  $V_o$  (old). This is required to find out if there has been any change in the value of  $V_o$  and if so, has  $V_o$  increased or decreased.

14) HYST and HYST2 subroutines The title of these subroutines

stands for "hysteresis." Their function is to add hysteresis to the adjustment of the field voltage. These subroutines filter out the sudden changes of the field voltage that can be caused from small changes in the alternator output voltage. Two's complement arithmetic is used to determine if output voltage has increased or decreased by more than a fixed amount "C." The hysteresis constant "C" in this program is assigned a value of 3 which is equivalent to 3 volts and corresponds to a power output variation of approximately 300 watts.

15) INCFV subroutine The title of this subroutine stands for "increment field voltage." In executing the HYST subroutine, if  $V_o$  (new) is greater than  $V_o$  (old) by the constant amount "C," a carry is produced which transfers the program control to execute the INCFV subroutine. As discussed in FLDVOL subroutine, register R2 contains the address of the memory location containing the field voltage control code. The value of the field voltage is incremented to the next higher step by adding the number 6H to the contents of R2 and then using the instruction "MOVP3 A,@A." The proper control code is then extracted from the table stored in page 3 of the external memory and it is output to port 1. The CORECT subroutine incorporated within the INCFV subroutine ensures that the applied field voltage does not exceed its previously set maximum limit of 68.9 volts.

16) REVOP subroutine The title of this subroutine stands for "restore the previous value (old value) of  $V_o$ ." When executing HYST or HYST2 subroutines, if  $V_o$  (new) is not greater than or less than  $V_o$  (old)

by the constant amount "C," no change in  $V_f$  is necessary and the next  $V_o$  (new) sample taken must be compared to the same  $V_o$  (old) sample. However, during the execution of the conditional tests in HYST and HYST2 subroutines, the constant value "C" is either added to or subtracted from  $V_o$  (old). Therefore, the REVOP subroutine is needed to restore  $V_o$  (old) to its original value before continuing. The storage register R5 contains the value of  $V_o$  (old).

17) DELAY subroutine The 8-bit, up-binary, counter in the 8035 is used to generate time delays required by different subroutines such as BRAKE, SAMPLE and PWRON subroutines. The operation here is basically the same as that in the SAMINT and TIMER subroutines. The "STRT T" instruction will start the counter. The counter then increments to its maximum count (FF) and overflows to zero continuing its count until stopped by a "STOP TCNT" instruction. The increment from maximum count to zero (overflow) results in the setting of an overflow-flag flip-flop. Overflows are detected by the "JTF" instruction and represent a delay of 20 ms each. Register R1 is used to accumulate 50 overflows to achieve a delay of exactly 1 second. The content of register R0 previously assigned by the calling subroutine determines the length of delay generated. For example, a 5-second delay can be generated by loading the value 5 in R0 and calling the DELAY subroutine.

#### E. Physical Description

The microprocessor-based controller was built and mounted inside a metal enclosure as shown in Figure 3.19. In order to allow for easy

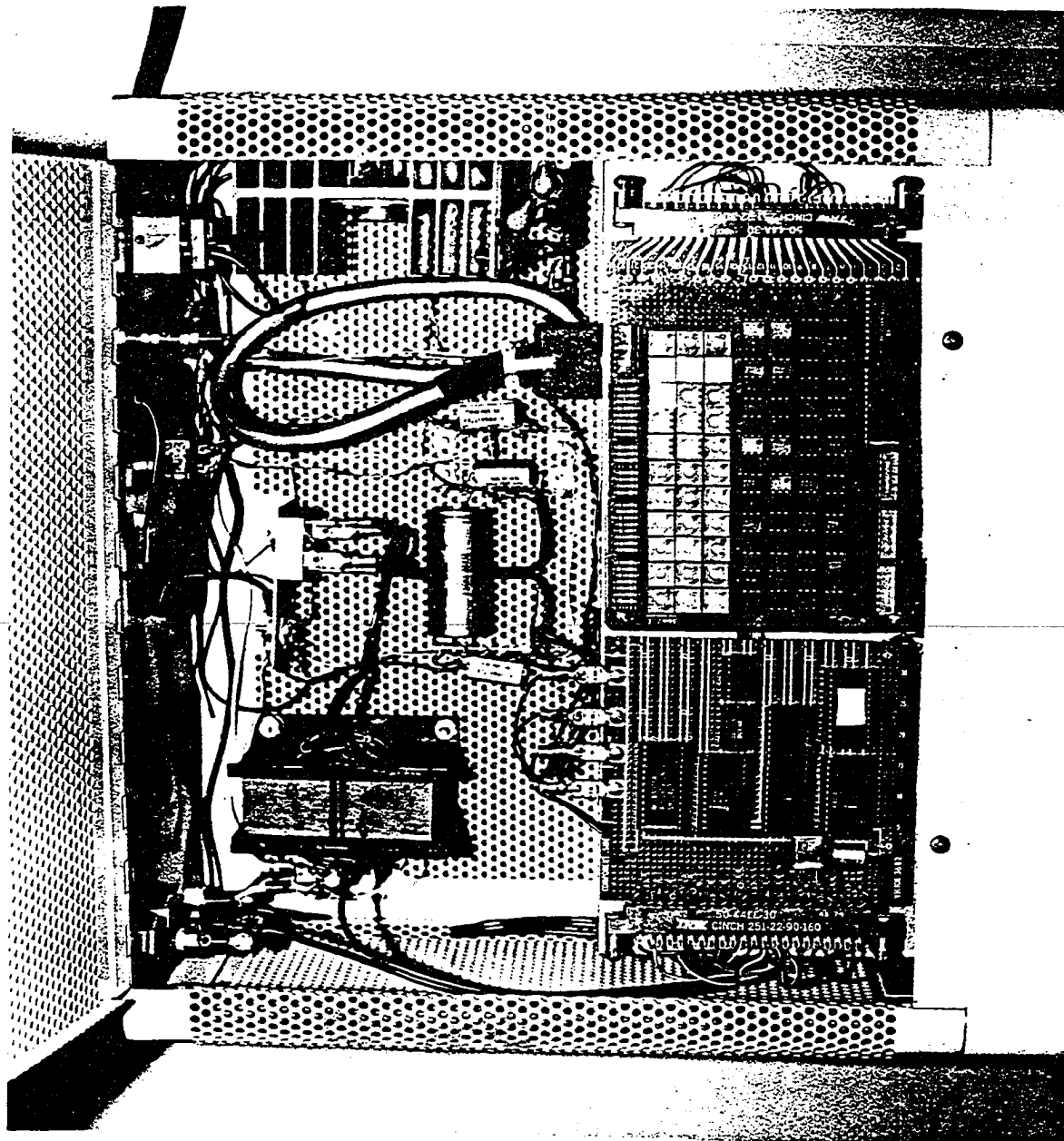
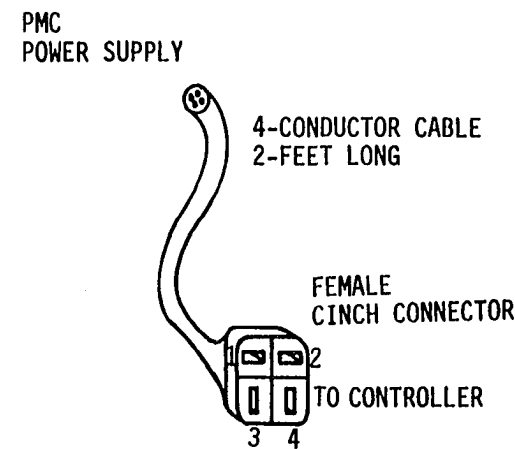
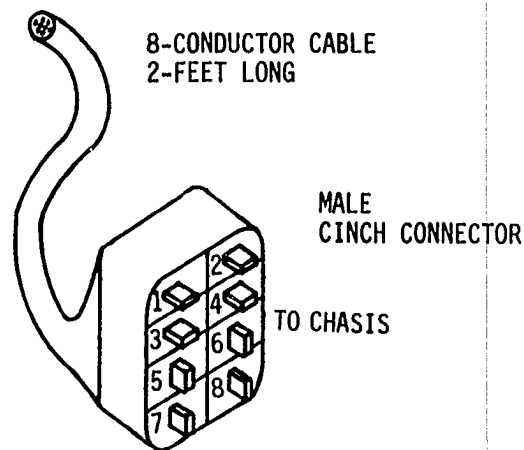


Figure 3.19. A picture of the completed microprocessor-based controller (top view)

access and trouble-shooting, when necessary, the field voltage controller board shown in Figure 3.7 and the microprocessor board shown in Figure 3.17 were mounted on a separate chassis using hinged spacers. This allows for the boards to be flipped 180 degrees so that they can be reached easily from either side. Interconnection between the two boards is done through a 10-conductor strip cable. Interconnection between the circuit boards on the chassis and the rest of the circuits inside the metal enclosure are done via an 8-conductor cable, Figure 3.20. The a.c. power is supplied to the chassis through a separate shielded cable. These cables are made long so that the chassis can be pulled out of the box without having to disconnect any of the cables. All ICs are mounted on wire-wrap sockets to allow for easy replacement. The physical layout of the mounted ICs on the boards is shown in Figures 3.7 and 3.17. The corresponding manufacturer's IC numbers and their descriptions are listed in Table 3.7 (shown in the previous section with the overall schematic diagram).

#### F. Installation

Figure 3.21 illustrates the interconnection between the microprocessor-based controller, the PMC power supply and the output voltage transducer. The PMC power supply plugs into a female socket provided in the rear panel of the controller, Figure 3.22. The signals (-S) and (-M) necessary for remote control of the PMC power supply are supplied through a 4-conductor cable shown in Figure 3.20. The output voltage from the power supply (DC+) and (DC-) is, in turn, brought



PIN #	SYMBOL	DESCRIPTION
1	+5	5V SUPPLY
2	Vo	ALT OUTPUT VOLTAGE (ANALOG)
3	S-	REMOTE CONTROL TERMINALS
4	M-	OF PMC POWER SUPPLY
5	METER+	FRONT PANEL METER (FIELD VOLTAGE)
6	NEUTRAL	A.C. NEUTRAL
7	—	SYSTEM GROUND
8	Vw	WIND SPEED (ANALOG)

PIN #	SYMBOL	DESCRIPTION
1	-DC	OUTPUT VOLTAGE TERMINALS OF THE PMC POWER SUPPLY
2	+DC	
3	S-	REMOTE CONTROL TERMINALS OF THE PMC POWER SUPPLY
4	M-	

Figure 3.20. Drawing of the cable and cinch connector interconnecting the chassis to the metal enclosure

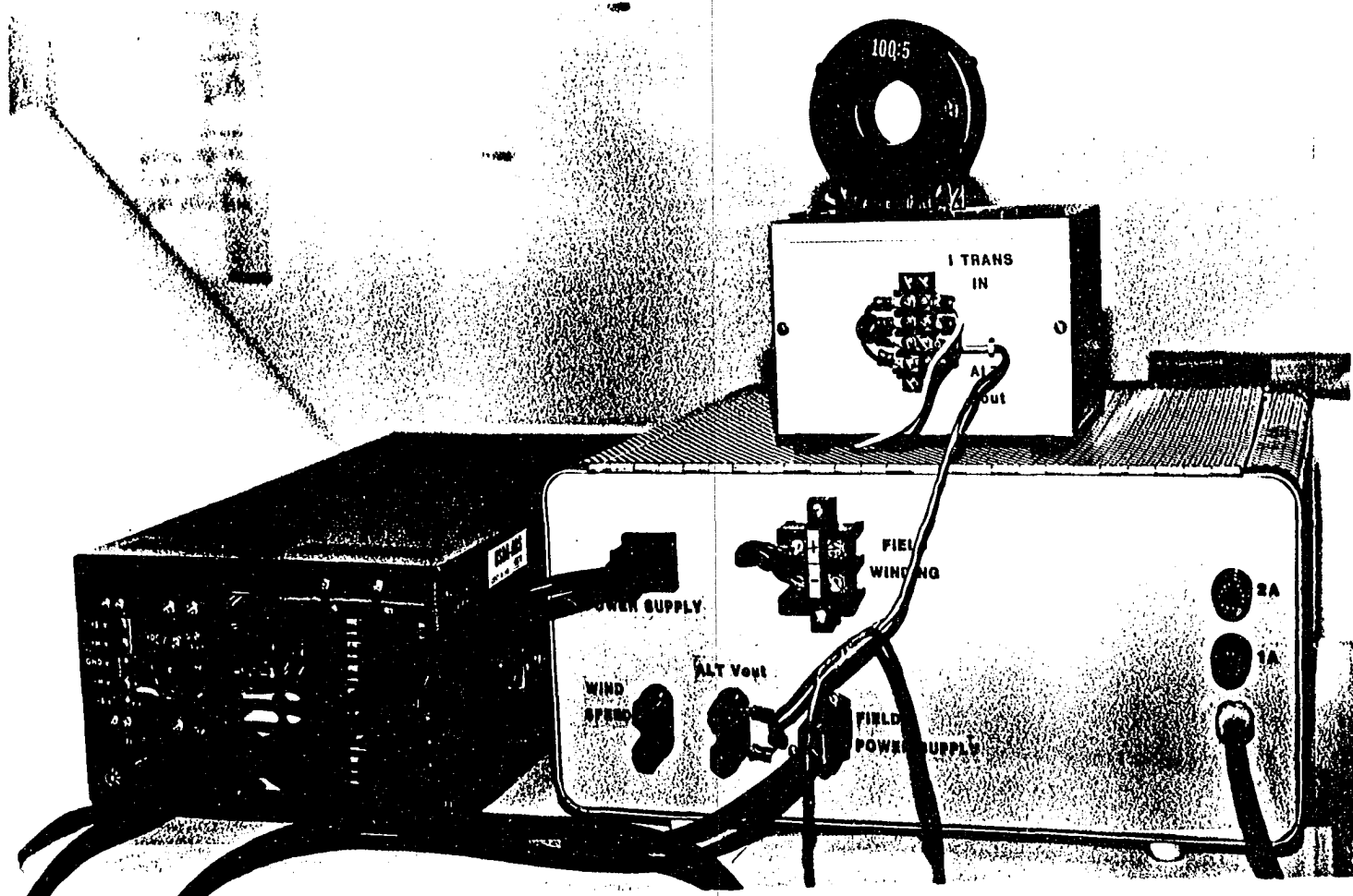


Figure 3.21. Interconnection between the controller, the Power/Mate power supply and the output voltage transducer

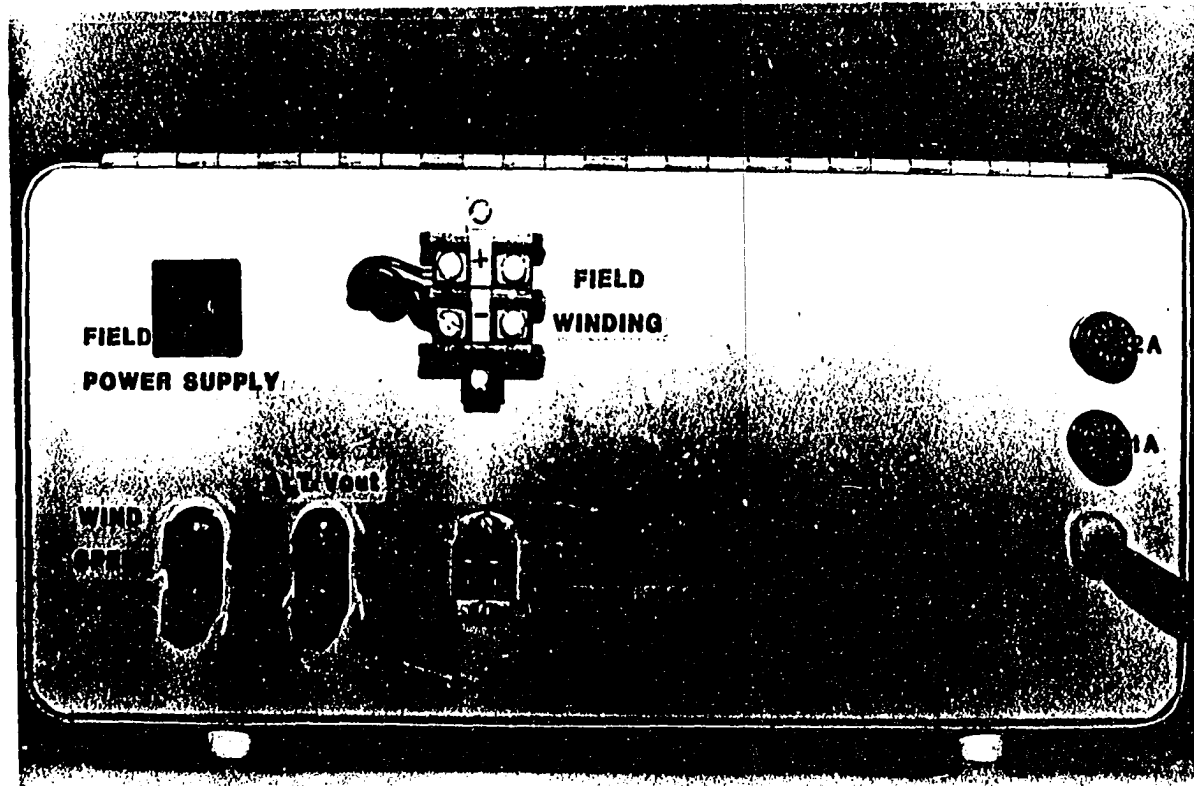


Figure 3.22. A picture showing the rear panel of the controller

through the same cable back to the controller. The power supply output voltage and the fixed 20-V regulated d.c. voltage form the desired alternator field voltage. The alternator field voltage is made available on the rear panel of the controller by means of a terminal strip. The alternator field winding is tied directly to this terminal strip. The anemometer analog signal (0-5v) is tied to a pair of terminals provided on the rear panel of the controller. The standard current transformer is placed on one of the three-phase output lines of the alternator. The output from current transformer is tied to the voltage transducer shown in Figure 3.21. The transducer analog signal (0-5v) is brought into the controller through another set of terminals provided on the rear panel of the controller.

#### G. Operation

To initiate operation of the controller, the steps listed below should be followed in order:

1. Turn on the controller (front panel switch). Note: Red neon pilot light indicates that the power has been turned on. The field voltage meter should read 20 V.
2. Press the "RESET" push-button switch on front panel. Note: The "BRAKE" light comes on indicating that the brake control is functional.
3. Turn on the PMC power supply. Note: Front panel vernier voltage control must remain in the most counter-clockwise position at all times.
4. Press "START" push-button switch. Note: The "BRAKE" light should turn off.

After the above steps have been completed, the controller should begin

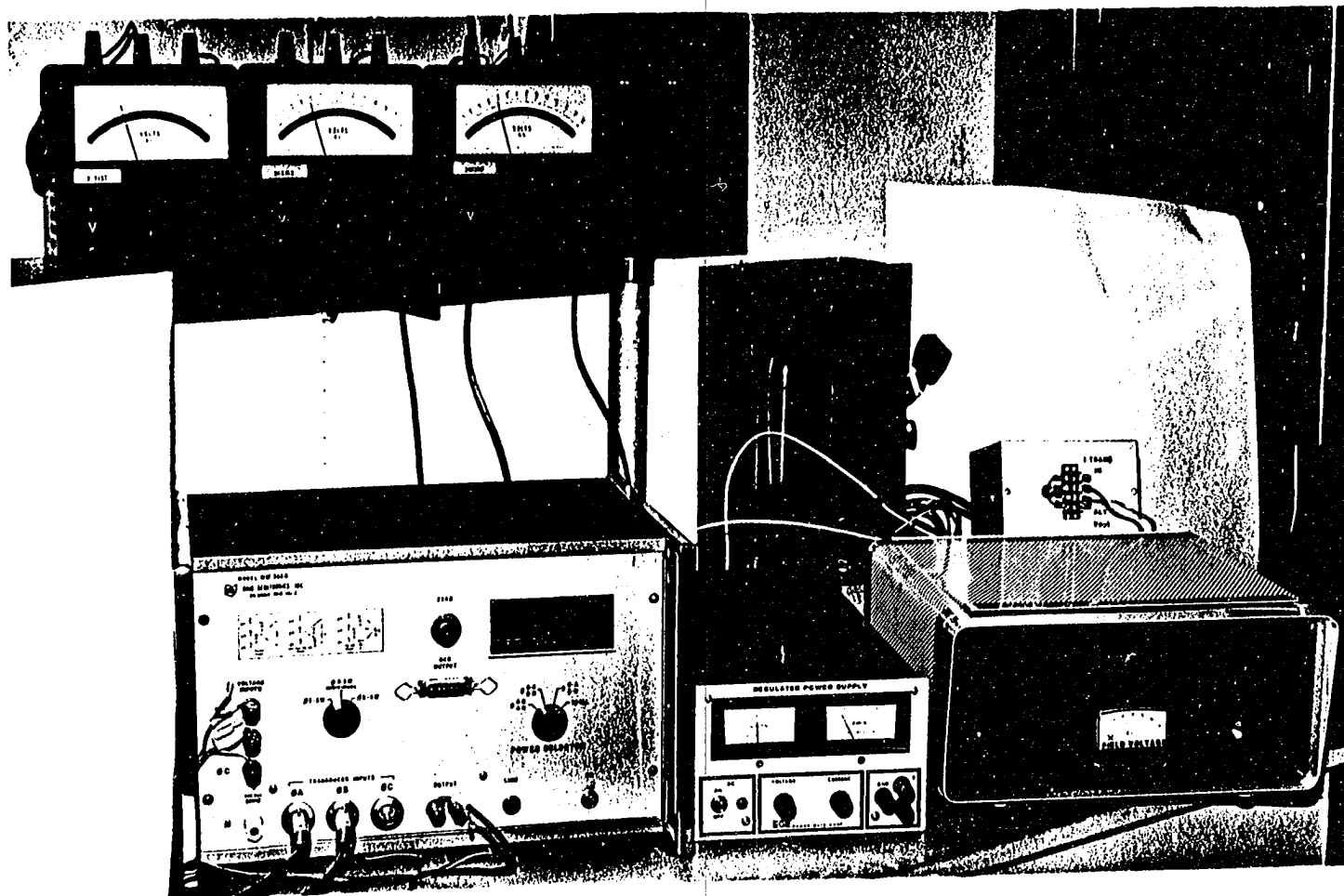


Figure 3.23. Picture showing the controller, PMC power supply, Ohio Semitronics Wattmeter and three a.c. voltmeters in operation

execution of the optimizing program to maximize the alternator output voltage. The field voltage indicator on the controller's front panel should vary in accordance to changes in the output voltage and/or wind speed.

To turn off the controller, the steps listed below should be followed:

1. Turn off the PMC power supply.
2. Turn off the controller.

#### IV. EXPERIMENTAL PROCEDURE AND RESULTS

An optimizing technique, a microprocessor-based controller and a control program for optimizing performance of wind-power systems are described in Chapter III. In this chapter, the effectiveness of the microprocessor-based controller for improving the performance of wind systems is examined. For the experimental study, two systems, a 10-kW Jacobs wind machine and a larger 17.5-kW Jacobs wind machine, were used. The description of these systems is presented in Section A.

A special method of taking performance data based on a modified "Method of Bins" has been developed. A description of this method and a data acquisition system which was employed to obtain the performance data are given in Section B. Three modes of operation under which performance data were obtained are described in Section C. Performance data for six different experiments and graphs demonstrating the improvement in performance are presented in Section D.

##### A. Test Systems

The microprocessor-based controller was added to two wind machines, a 10-kW Jacobs and a 17.5-kW Jacobs. A block diagram of the wind energy conversion system is illustrated in Figure 4.1.

The wind energy conversion system was set up to supply power to fixed-resistance heating elements arranged in a delta configuration and to a three-phase rectifier serving as input to a line-commutated synchronous inverter. The characteristics of the two wind machines used

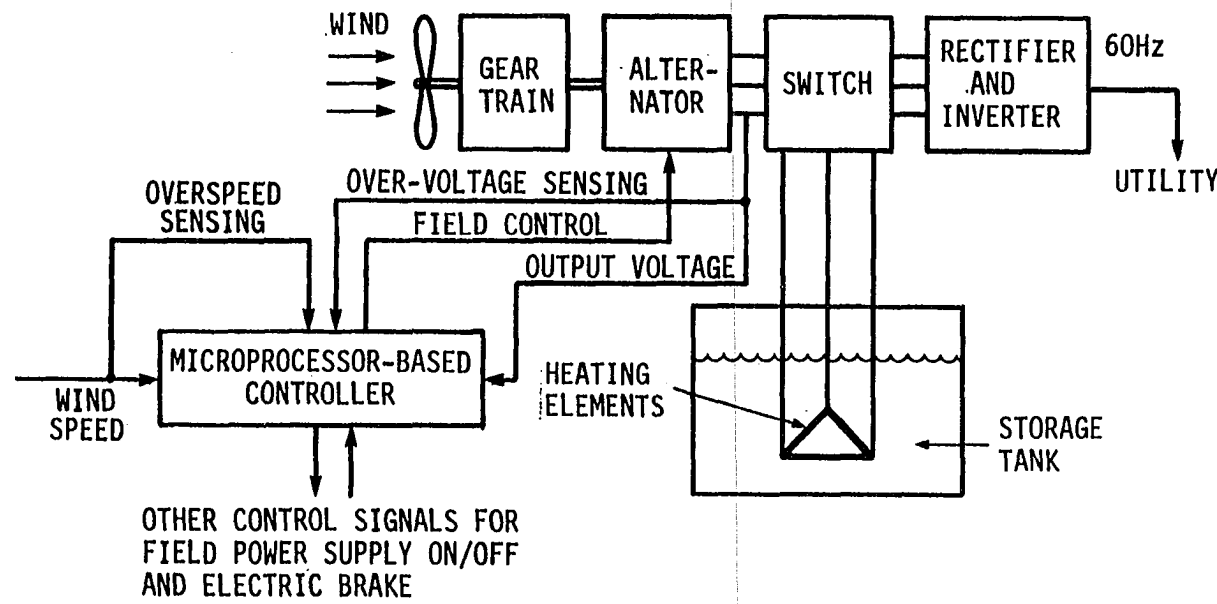


Figure 4.1. A block diagram of the wind-energy conversion system

in this study are given below:

1. 10-kW, 23-foot blade Jacobs wind system

This machine consists of a 20-kW, three-phase synchronous alternator which is driven, through gears, by a three-bladed fixed-pitch impeller, 23 feet in diameter. This unit has been designed to produce a maximum of 10 kW at 25-mph wind speeds. In wind speeds greater than 25 mph, the blades mechanically feather to limit the impeller rotational speed to avoid possible damage. The unit is mounted on top of a 100-foot self-supporting tower. Additional characteristics of this wind machine are given in Table 4.1.

Table 4.1. Characteristics of the 10-kW, 23-foot blade Jacobs wind system

Rated power output	10 kW
Alternator rated speed	1200 rpm
Rated wind speed	25 mph
Gear ratio	6:1
Blade diameter (fixed pitch)	23 ft
Output voltage (at full power)	157 volts (rms)
Alternator field resistance	61 Ω

Because the Jacobs wind system was already mounted on top of a tower, it was not possible to determine the characteristics of the alternator that is used in this system. The field voltage/output voltage characteristics given in Table 3.1 are for a similar 20-kW alternator made by the same company (Jacobs). These characteristics were used as

a guideline to determine the approximate range of the required field voltage for the 10-kW wind system. However, an exact knowledge of field-voltage/output-voltage characteristics of the wind system is not absolutely necessary because the optimizing technique adjusts the field voltage to obtain maximum output voltage without regard to the alternator characteristics.

## 2. 17.5-kW, 26-foot blade Jacobs wind system

This machine also consists of a 20-kW, three-phase synchronous alternator which is driven, through gears, by a three-bladed fixed-pitch impeller. The blade diameter for this unit is 26 feet. This system has been designed to produce a maximum of 17.5 kW at 27-mpm wind speeds. In wind speeds greater than 27 mph, the blades mechanically feather to avoid impeller rotational over speed. The unit is mounted on top of an 80-foot guyed tower. Additional characteristics of this wind system are given in Table 3.2 in Chapter III.

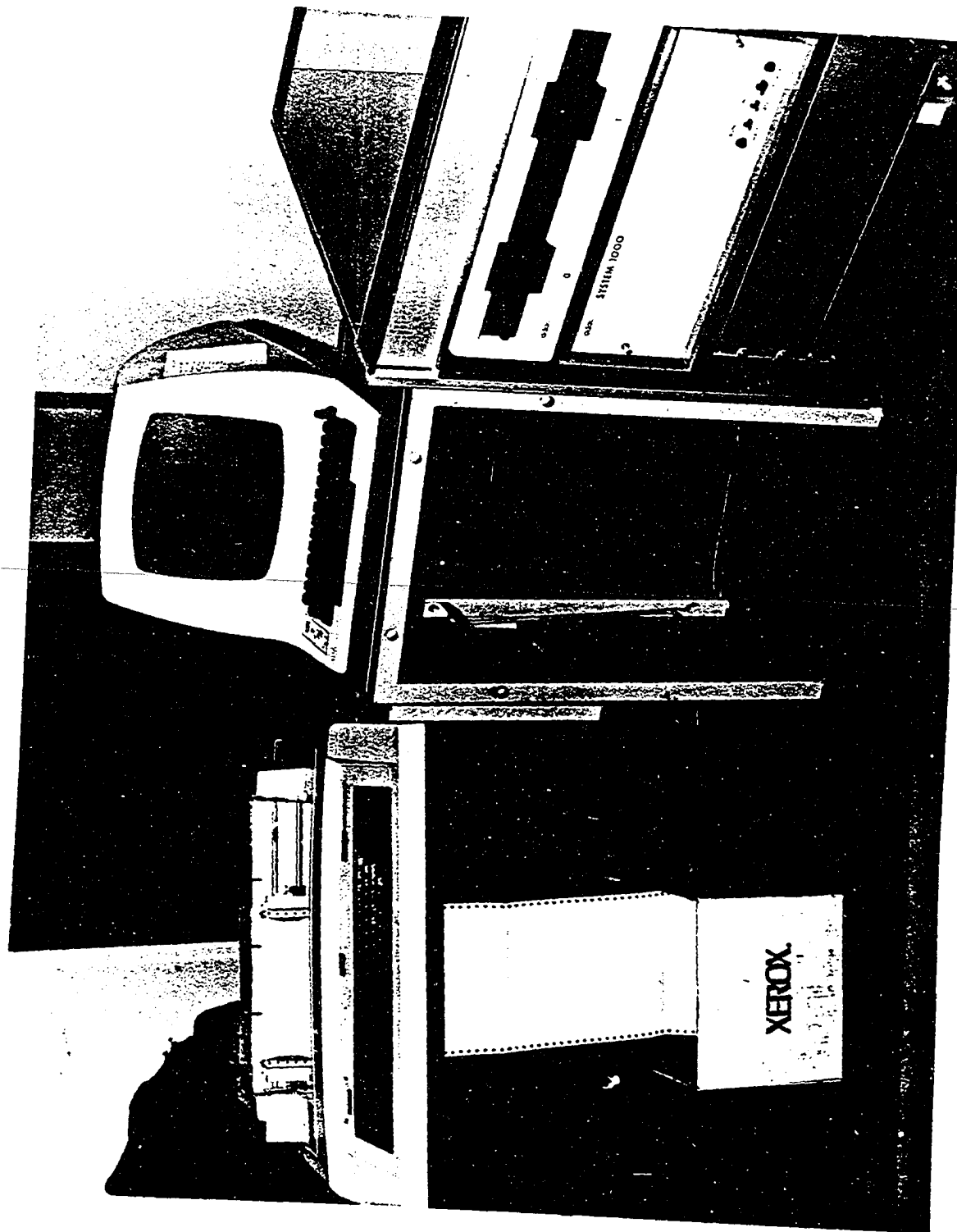
### B. Method Used for Collection of Performance Data

In order to compare the wind system's performance, with and without the microprocessor-based controller, ideally, two identical wind systems with the same exact characteristics would be required, and both systems would be tested at the same time under identical test conditions. However, this is costly and redundant. Therefore, to make possible comparison of the wind system under different modes of operation and for different test periods, a method to obtain consistent and

reliable data is necessary. Hence, a method for taking performance data based on a modified "Method of Bins" [3] was developed. In this method, the range of wind speeds that might be expected to occur during the course of a test period was divided into wind-speed "bins" of one m/s width. Each bin had two cumulative registers. One was a simple counter that was incremented each time a sampled wind speed fell within the range of the bin's width. The second register contained the cumulative sum of the WECS power output readings so that average power for each wind-speed bin could be determined. Data samples were taken only if wind speed and power readings were basically steady for a predetermined period. For the data reported in Section C, a sampling period of 1 sec was used for each test period and each data point represents an average of readings from 5 or 10 sequential samples in which wind speed and associated WECS power output did not change more than 5% for the period. This method of taking performance data has consistently given more reliable data than other methods such as the common procedure of recording instantaneous samples of wind speed and power in bins and averaging bin data.

Performance data were obtained by means of the data-acquisition system shown in Figure 4.2. The data-acquisition system consisted of an Adac system 1000 minicomputer with dual disc drives, an Adac 32-channel A/D converter (only three channels were used to sample the wind speed rotational speed and power output of the WECS), an ADM 3A video display terminal, a LA36 DECwriter and a Fortran program implementing the modified "Method of Bins."

**Figure 4.2.** Data-acquisition system



### C. Modes of Operation

To investigate the effect of the microprocessor-based controller for improving the performance of wind systems, the Jacobs wind machines described in Section A were operated in three different modes and performance data were obtained in each case. The three modes of operation, under which performance data were obtained, are described below.

#### 1. Operation in fixed-field mode

The performance of the wind systems was first evaluated under fixed-field conditions. From the knowledge of alternator output-voltage/field-voltage characteristics for the wind system, a nominal field voltage value corresponding to the average of the wind speeds normally encountered was determined. This value was found to be 35 volts for both units. A variable power supply was used to apply the proper field voltage to the field winding of the alternator. Each wind system was operated in fixed-field mode for approximately one month and performance data were collected.

#### 2. Operation with a synchronous inverter

To establish a second base line for comparison of the wind system's performance with and without the microprocessor-based controller, the 10-kW wind system was operated for approximately one month with a synchronous inverter and performance data were collected under the same conditions as for the fixed-field mode. The synchronous inverter consisted of a three-phase rectifier that feeds the rectified voltage from the alternator to a thyristor bridge to produce utility compatible AC

power. A synchronous inverter for the 17.5-kW system was not available.

### 3. Operation in controlled mode

Following the collection of data for fixed-field and synchronous inverter modes, the microprocessor-based controller was added to each wind system and the performance again evaluated. Each wind system was operated for approximately one month in a microprocessor-controlled mode and performance data were collected under the same conditions as for synchronous inverter and fixed-field modes.

## D. Results

Because all data were not collected under similar temperature and barometric pressure conditions, for each separate test period the average power reading in each bin was corrected to sea level in accordance to the procedure recommended by American Wind Energy Association (AWEA) [3]. This allowed data from separate test periods to be combined, which is a necessity if the performance is to be obtained over a wide range of wind speeds and environmental conditions. The method used to correct the data is described below.

### 1. Data correction method

For each test period, air density was first calculated by averaging the recorded values of air temperature and barometric pressure and then applying the following formula:

$$\rho_T = 1.226 \left( \frac{288.13}{T} \right) \left( \frac{B}{760} \right)$$

where

$\rho_T$  = test air density,  $\text{kg/m}^3$

T = average air temperature,  $^{\circ}\text{K}$   
 $(^{\circ}\text{K} = ^{\circ}\text{C} + 273.13)$

B = average barometric pressure, mm Hg

The corrected average power output for each bin was then calculated by:

$$P_s = P_T \left( \frac{\rho_s}{\rho_T} \right)$$

where

$P_s$  = power corrected to sea level

$P_T$  = uncorrected average power

$\rho_s$  = standard air density,  $\text{kg/m}^3$

$\rho_T$  = test air density,  $\text{kg/m}^3$

## 2. Performance data

Data collected for the fixed field, synchronous inverter, and controlled mode were corrected by the method described in Section D.1. Only bin data for which eight or more samples had been obtained were used to ensure the reliability of the data. Next, the corrected data from separate test periods were combined for each mode of operation and are presented in Tables 4.2-4.7.

## 3. Performance improvement

The data shown in Tables 4.2-4.4 have been plotted in Figure 4.3. The three superimposed graphs in Figure 4.3 represent the power output

Table 4.2. Performance data for 10-kW Jacobs wind system operated in fixed-field mode,  $V_f = 35$  V

Wind speed m/s	Number of samples	Measured output power (kW)	Impeller rpm	Measured $C_p$	Tip speed/wind speed
3.5	25	0.121	73.4	0.12	7.69
4.0	193	0.192	79.3	0.125	7.28
4.5	487	0.573	75.8	0.266	6.18
5.0	448	0.926	83.4	0.313	6.12
5.5	606	1.512	94.3	0.384	6.29
6.0	862	2.116	108.5	0.414	6.64
6.5	573	2.612	117.6	0.402	6.64
7.0	369	3.368	127.2	0.415	6.67
7.5	209	3.903	138.9	0.391	6.80
8.0	181	4.264	156.9	0.352	7.19
8.5	169	4.330	170.6	0.298	7.37
9.0	104	4.521	184.2	0.261	7.51
9.5	91	4.890	196.4	0.241	7.59
10.0	100	5.65	203.0	0.239	7.45
10.5	154	6.054	203.9	0.221	7.13
11.0	210	6.897	209.3	0.219	6.98
11.5	204	6.981	209.5	0.194	6.69
12.0	186	6.910	214.5	0.169	6.56

Table 4.3. Performance data for 10-kW Jacobs wind system operated in synchronous-inverter mode

Wind speed m/s	Number of samples	Measured output power (kW)	Impeller rpm	Measured $C_p$	Tip speed/wind speed
3.5	33	.425	110.73	0.419	11.61
4.0	211	.553	107.4	0.360	9.85
4.5	332	.696	105.9	0.320	8.64
5.0	298	.898	103.7	0.304	7.61
5.5	460	1.362	106.3	0.346	7.10
6.0	196	1.822	129.0	0.357	7.89
6.5	88	2.294	134.2	0.353	7.58
7.0	132	3.141	143.9	0.387	7.55
7.5	112	3.404	147.3	0.341	7.21
8.0	176	3.949	159.7	0.326	7.33
8.5	235	4.606	171.6	0.317	7.41
9.0	106	5.537	178.5	0.321	7.28
9.5	98	6.837	184.3	0.337	7.12
10.0	75	8.163	192.3	0.345	7.06
10.5	68	9.094	197.5	0.332	6.90
11.0	45	9.790	209.4	0.328	6.99
11.5	48	10.162	210.6	0.282	6.72
12.0	37	10.052	210.8	0.246	6.45

Table 4.4. Performance data for 10-kW Jacobs wind system operated in controlled mode, hysteresis constant  $C = 3$

Wind speed m/s	Number of samples	Measured output power (kW)	Impeller rpm	Measured $C_p$	Tip speed/ wind speed
3.5	110	0.455	82.0	0.448	8.60
4.0	285	0.629	83.0	0.416	7.62
4.5	630	0.941	89.4	0.437	7.29
5.0	735	1.316	98.0	0.445	7.19
5.5	669	1.787	103.6	0.450	6.92
6.0	663	2.228	112.3	0.436	6.87
6.5	625	2.684	116.0	0.413	6.55
7.0	670	3.53	131.0	0.435	6.85
7.5	830	4.203	136.9	0.421	6.70
8.0	220	5.027	143.6	0.415	6.59
8.5	135	6.264	156.9	0.431	6.78
9.0	163	7.213	162.3	0.418	6.62
9.5	212	8.811	176.7	0.434	6.83
10.0	185	10.26	184.9	0.433	6.79
10.5	97	11.283	187.0	0.412	6.54
11.0	88	11.842	190.4	0.376	6.32
11.5	46	12.68	197.8	0.352	6.31
12.0	39	12.50	197.4	0.305	6.04

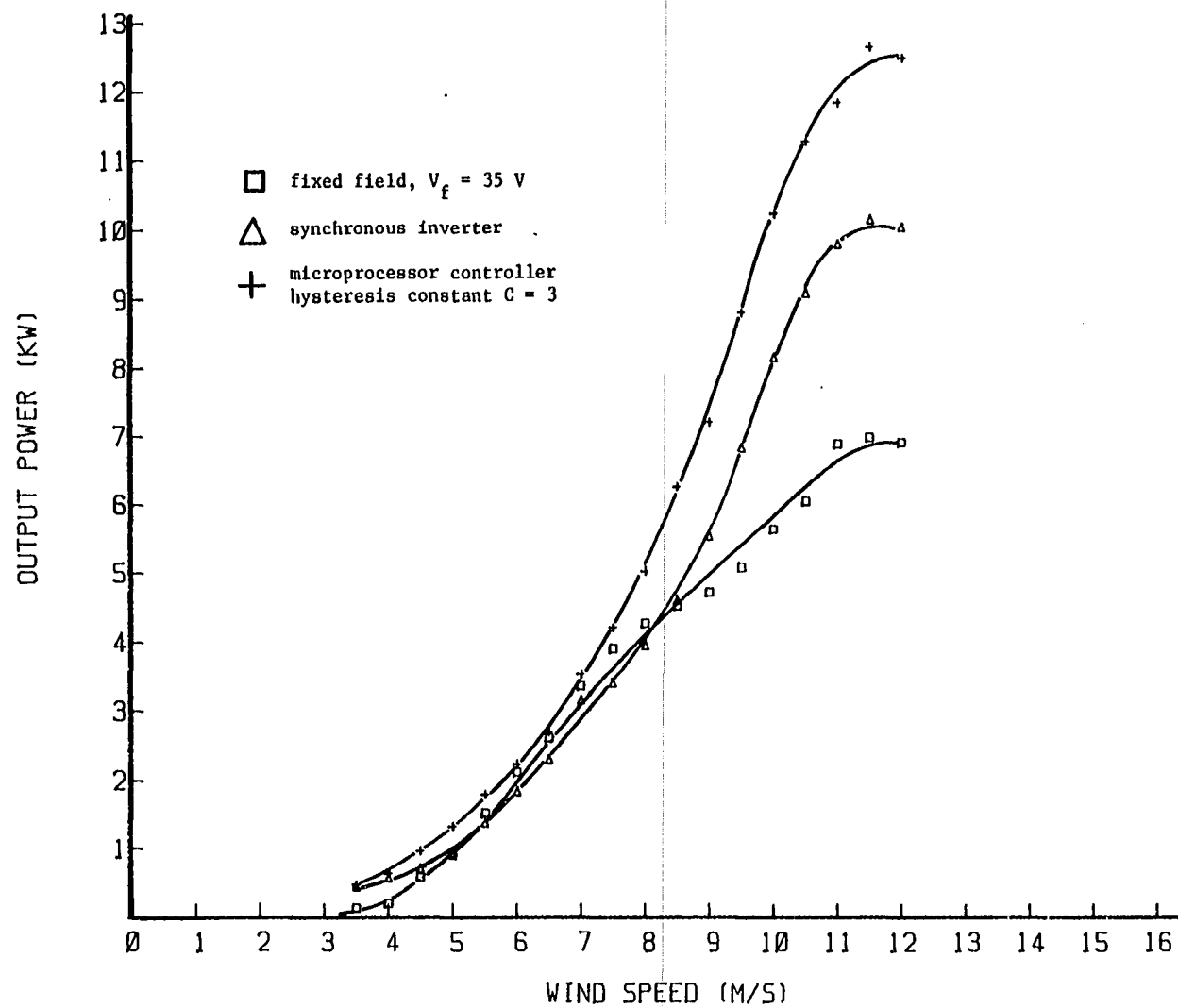


Figure 4.3. 10-kW wind system power output in relation to wind speed

of the 10-kW wind system as a result of fixed-field, synchronous-inverter, and controlled modes of operation.

Operation in the controlled mode has resulted in performance improvements over the fixed-field mode of 7 to 80% in a range of wind speeds from 5 to 9.5 m/s and performance improvements as high as 92% were obtained at higher wind speeds when feathering of the blades occurred. Performance improvements over the synchronous inverter mode of 13.7 to 31.8% were obtained in a range of wind speeds from 4 to 10.5 m/s.

The data shown in Tables 4.5 and 4.6 have been plotted in Figure 4.4. The two superimposed graphs in Figure 4.4 represent the power output of the 17.5-kW wind system as a result of fixed-field and controlled modes of operation. Operating the 17.5-kW wind system in the controlled mode has resulted in performance improvements over the fixed-field mode of operation of 7% to 69% in a range of wind speeds from 4 to 9.5 m/s. Performance improvements as high as 142% were obtained at higher wind speeds when feathering of the blades occurred.

In maximizing the output voltage by using the optimizing technique, it was found that the hysteresis constant "C" has an effect on the performance of the wind system. The hysteresis constant "C" is equivalent to the amount of change in the output voltage for which an increment or decrement in the field voltage is made. The 17.5-kW wind system was operated in the controlled mode using two different hysteresis constants. The data obtained are shown in Tables 4.6 and 4.7 and have been plotted

Table 4.5. Performance data for 17.5-kW wind system operated in fixed-field mode,  $V_f = 35$  V

Wind speed m/s	Number of samples	Measured output power (kW)	Impeller rpm	Measured $C_p$	Tip speed/wind speed
3.5	22	0.288	51.4	0.222	6.09
4.0	32	0.511	80.05	0.264	8.30
4.5	36	0.791	79.3	0.287	7.31
5.0	68	1.304	84.3	0.345	6.99
5.5	113	1.967	93.1	0.391	7.02
6.0	196	2.723	104.3	0.417	7.22
6.5	386	3.496	116.9	0.421	7.46
7.0	525	4.304	128.0	0.415	7.59
7.5	470	5.243	138.4	0.411	7.66
8.0	354	5.411	157.4	0.349	8.16
8.5	220	5.60	171.6	0.302	8.37
9.0	168	5.79	186.4	0.263	8.59
9.5	119	6.51	190.6	0.251	8.33
10.0	79	6.635	196.5	0.220	8.15
10.5	74	6.727	197.5	0.192	7.80
11.0	58	7.205	206.1	0.179	7.77
11.5	49	7.228	207.9	0.157	7.50
12.0	46	7.198	207.4	0.138	7.17
12.5	45	7.214	209.4	0.122	6.97

Table 4.6. Performance data for 17.5-kW Jacobs wind system operated in controlled mode, hysteresis constant  $C = 3$

Wind speed m/s	Number of samples	Measured output power (kW)	Impeller rpm	Measured $C_p$	Tip speed/wind speed
3.5	36	0.553	75.2	0.427	8.91
4.0	80	0.857	89.7	0.443	9.3
4.5	158	1.226	93.6	0.445	8.63
5.0	92	1.754	97.2	0.464	8.07
5.5	220	2.163	100.6	0.431	7.58
6.0	160	2.857	110.1	0.438	7.62
6.5	433	3.625	118.2	0.437	7.55
7.0	440	4.384	126.6	0.423	7.52
7.5	205	5.315	130.1	0.417	7.20
8.0	167	6.751	144.2	0.436	7.48
8.5	129	8.105	152.4	0.436	7.44
9.0	74	9.50	157.0	0.431	7.24
9.5	65	11.0	161.4	0.425	7.05
10.0	43	12.63	168.9	0.418	7.01
10.5	33	14.56	180.0	0.416	7.11
11.0	32	16.43	189.8	0.409	7.16
11.5	45	17.48	197.3	0.380	7.12
12.0	26	18.05	203.1	0.345	7.02
12.5	15	18.08	202.5	0.306	6.72

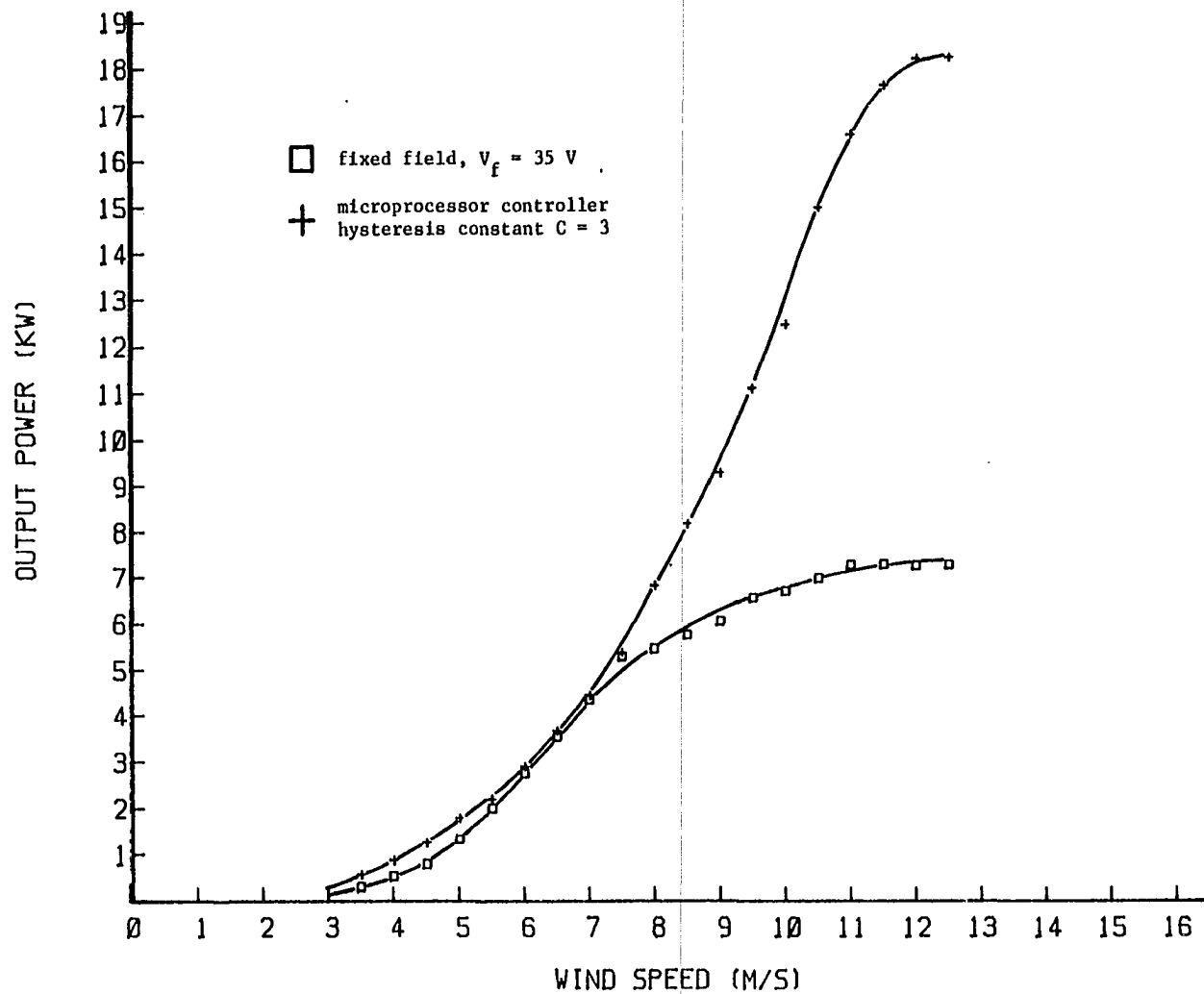


Figure 4.4. 17.5-kW wind system power output in relation to wind speed

in Figure 4.5. As shown in Figure 4.5, the performance has decreased when a small hysteresis constant is used. The performance decrease was only 6% at 7.0 m/s, but at higher wind speeds such as 11.0 m/s the performance decreased by 13%. This is because a small hysteresis constant results in rapid increments of the field voltage and causes a reaction which effectively does not allow the unit to come up to optimum speed.

The ability to adjust the hysteresis constant to an optimum value by software emphasized the advantage of using the microprocessor to implement the optimizing technique. A hysteresis constant of three was found to work best for both the 10-kW and 17.5-kW wind systems. A hysteresis constant of three is equivalent to a change in the output voltage of approximately three volts or a change in the output power of approximately 300 watts for the systems tested.

The data plotted in Figures 4.3 and 4.4 indicate that the field control, using the optimizing technique, can produce substantial improvement in wind systems performance. Furthermore, improvement in performance achieved for the two separate wind systems indicates that the developed optimizing technique is machine-independent and can be applied to any typical wind system in which the alternator is connected to a fixed-resistance load or to a synchronous inverter producing utility-compatible AC power.

Table 4.7. Performance data for 17.5-kW Jacobs wind system operated in controlled mode, hysteresis constant  $C = 2$

Wind speed m/s	Number of samples	Measured output power (kW)	Impeller rpm	Measured $C_p$	Tip speed/wind speed
3.5	29	0.527	79.9	0.406	9.47
4.0	94	0.84	92.2	0.434	9.56
4.5	189	1.15	90.3	0.417	8.33
5.0	382	1.61	91.3	0.426	7.58
5.5	404	2.016	95.8	0.401	7.23
6.0	678	2.62	104.2	0.401	7.21
6.5	615	3.178	108.7	0.383	6.94
7.0	659	4.12	119.9	0.397	7.11
7.5	391	4.84	123.4	0.379	6.83
8.0	255	5.702	129.5	0.368	6.72
8.5	240	6.583	135.3	0.354	6.60
9.0	139	8.054	145.1	0.365	6.69
9.5	186	9.352	150.9	0.361	6.59
10.0	98	11.110	161.9	0.376	6.72
10.5	60	13.021	169.7	0.372	6.71
11.0	46	14.51	175.2	0.360	6.61
11.5	48	15.60	181.0	0.339	6.53
12.0	36	17.23	188.3	0.33	6.51
12.5	25	17.40	196.5	0.295	6.49

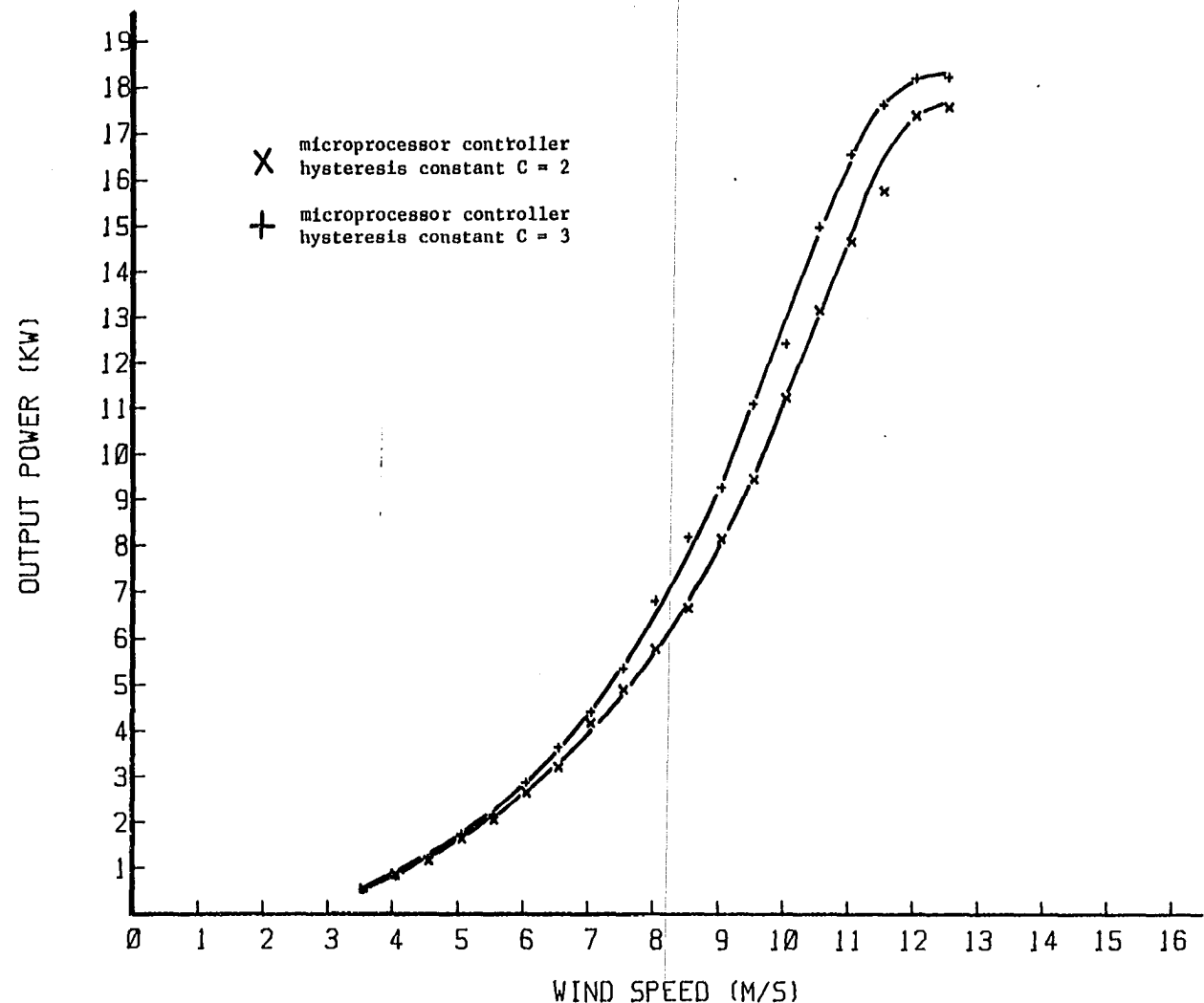


Figure 4.5. 17.5-kW wind system power output in relation to wind speed

## V. CONCLUSIONS

Theoretically, a maximum of only 59.3% of the power in the wind is obtainable by a windmill and in practice only 30-40% is actually obtained using the most efficient windmills [10]. Therefore, it is extremely desirable to have the most efficient system possible over a wide range of wind speeds.

A fixed-pitch windmill often does not provide optimum output power since it operates most efficiently only at its design tip-speed ratio. Therefore, a fixed-pitch turbine connected to drive an alternator is only optimally efficient over a narrow range of wind speeds.

Several prior art devices have attempted to overcome the above problem. These devices have generally resulted in complicated designs applicable to specific wind systems and have not necessarily extracted maximum energy from the wind.

The major objectives of this dissertation have been:

1. To develop an optimizing technique which maximizes the efficiency of fixed-pitch wind systems over a wide range of wind speeds.
2. To design and build a microprocessor-based controller that implements the optimizing technique and is machine independent (i.e., the controller is adaptable to different wind systems).
3. To investigate the effectiveness of the microprocessor-based controller for improving the performance of fixed-pitch wind machines.

Efforts and accomplishments concerning the research objectives have been presented in the previous chapters. Subsequently, the follow-

ing conclusions are drawn based on the results presented in Chapter IV.

1. The microprocessor-based controller can be used effectively to improve the performance and total output power of WECS over a wide range of wind speeds. Maximum performance improvement achieved was 69% at a wind speed of 9.5 m/s. Minimum performance improvement achieved was 7% at a wind speed of 7 m/s. Performance improvements as high as 142% were obtained over fixed-field conditions when feathering of the blades occurred.
2. The improvements in overall performance indicate that the microprocessor-based controller can make a major contribution to economic feasibility because the average annual output of the WECS can be substantially increased.
3. By demonstrating the improvement in performance of two different wind systems, not only the validity of the optimizing technique has been proven but also the optimizing technique is machine independent.
4. Use of the microprocessor in the design of the controller has allowed easy implementation of the optimizing technique. In addition, the microprocessor has provided brake and power supply control functions as well as over-voltage and over-speed sensing.
5. The alternator-output-voltage signal is the only parameter necessary for the optimizing technique. Therefore, the microprocessor-based controller can operate without the need for an anemometer. This is important when the anemometer fails to operate properly due to icing, lightning damage or other reasons.
6. It was found that the hysteresis constant "C" (i.e., amount of change in the output voltage for which an increment or decrement in the field voltage is made) has an effect on the performance. A small hysteresis constant results in rapid increments or decrements of the field voltage. This interacts with the inertial response time of the wind system and may cause a decrease in performance. An optimum value for C exists for which the wind system performs with maximum efficiency. This value can be found experimentally. A hysteresis constant of three was found to work best for both the 10-kW and 17.5-kW Jacobs wind systems. Performance improvements of 7 to 15% were achieved when the hysteresis constant was changed from two to three.

## VI. SUGGESTIONS FOR FUTURE STUDY

When using the microprocessor-based controller to maximize the power output of WECS, it was found that the value of the hysteresis constant has an effect on the performance of the wind system. To make the controller easily adaptable to different wind systems, a method needs to be developed to adjust the hysteresis constant and sampling interval without reprogramming the EPROM containing the control program.

To ensure safe operation of the WECS under all conditions, it would be desirable to develop some scheme for detecting controller malfunction.

---

## VII. BIBLIOGRAPHY

1. Alberts, J. R. "Field control for wind-driven generators." United States Patent No. 2,339,749 (January 1944).
2. Bartlett, A. Albert. "Forgotten fundamentals of the energy crisis." Am. J. Physics 46(9) (September 1978):876-889.
3. Bergey, L. S. "Performance rating document." American Wind Energy Association, Cooperative Agreement No. DE-FC04-80ALLs926, 1982.
4. Bolton, H. R. and Nicodemore, V. C. "Operation of self-excited generators for windmill application." Proc. IEE 126, No. 9 (September 1979):815-820.
5. Bright, C. "Power generating apparatus." United States Patent No. 3,974,394 (August 1976).
6. Claytor, E. M. "Wind-driven generator control system." United States Patent No. 2,179,679 (November 1939).
7. Claytor, E. M. "Load matching device for wind generators." United States Patent No. 2,230,526 (February 1941).
8. De Renzo, D. J. Wind power recent developments. Newark, New Jersey: Noyes Data Corporation, 1979.
9. Fenwal Electronics Thermistor Manual. Farmingham, Massachusetts: Fenwal Electronics, Inc., 1979.
10. Golding, E. W. The Generation of Electricity by Wind Power. New York: E and F. N. Spon, 1976.
11. Harner, K. I., Kos, J. M. and Patrick, J. P. "Wind turbine generator pitch control system." United States Patent No. 4,160,170 (June 1979).
12. Jacobs Wind Energy Systems Instruction Manual. Minneapolis, Minnesota: Jacobs Wind Electric Co., 1981.
13. Jayadev, T. S. "Wind mills stage a comeback." IEEE Spectrum 13 (November 1976):45-49.
14. Lapin, L. L. Statistics for Modern Business Decisions. New York: Harcourt Brace Jovanovich, Inc., 1978.

15. Lawson-Tancred. "Method and apparatus for generating electricity from a fixed-pitch wind wheel." United States Patent No. 4,280,061 (July 1981).
16. Lehman, R. Alternative Energy Technologies and Their Use in California's Agricultural Sector. A report by The Assembly Select Committee on Energy Alternatives in Agriculture, May 1982.
17. MCS-48 User's Manual. Santa Clara, California: Intel Corporation, 1979.
18. Minchinton, W. "Wind power." History Today 30 (March 1980):31-36.
19. Moran, K. E., Korzeniewski, E. C. "Load control for wind-driven electric generators." United States Patent No. 4,095,120 (June 1978).
20. National Semiconductor Linear Databook. Sunnyvale, California: National Semiconductor Corp., 1980.
21. Pal Dharam, Huang K. T. "Automatic electrical load matching for wind generators." United States Patent No. 4,205,235 (May 1980).
22. Park, J. "The wind power book." Palo Alto, California: Cheshire Books, 1981.
23. Putnam, P. C. Power from the Wind. New York: Van Nostrand Reinhold Co., 1948.
24. Richie, J. D. Sourcebook for Farm Energy Alternatives. New York: McGraw-Hill, Inc., 1983.
25. Soderholm, L. H. "A field control for maximizing performance of wind-driven alternators." Proc. Amer. Wind Energy Assoc. Conf. (1982):156-158.
26. Soderholm, L. H. and Andrew, J. F. "Wind-electric power." American Society of Agricultural Engineers, ASAE Paper No. 74-3503, Annual meeting, 1974.
27. Soderholm, L. H. and Andrew, J. F. "Field control for wind-driven generators." United States Patent No. 4,331,881 (May 1982).
28. Taylor, R. H. Alternative Energy Sources for the Centralized Generation of Electricity. Great Britain: Adam Higler Book Co., 1983.

120b

29. Thermistors for Measurement and Control Catalog. Niagra Falls, New York: National Lead Co., 1976.
30. Wakerly, L. F. Microcomputer Architecture and Programming. New York: John Wiley and Sons, Inc., 1981.

## VIII. ACKNOWLEDGMENTS

I would like to express my sincere appreciation to Dr. Leo H. Soderholm for making possible the work described on the preceding pages and for his constant helpful directions and valuable suggestions. I also would like to thank Dr. Terry A. Smay for his assistance and encouragement, and for serving as my major advisor; Dr. Arthur V. Pohm, Dr. Robert E. Post, Dr. Charles T. Wright, Jr., Dr. David Carlson, and Dr. Allan G. Potter, members of my committee, for the help they have given.

I acknowledge gratefully the help given by my friends, in particular Ms. Flora K. Yuen, and Mr. Thomas L. Grove. Finally, many thanks go to my family for their constant encouragement and support.

---

## IX. APPENDIX A

The procedure to fit the field voltage/wind speed data of Table 3.1 by a parabola is described in this appendix [13]. The following is the expression for a parabolic trend curve:

$$Y = a + bX + cX^2 \quad (8.1)$$

The method of least squares was extended to find the values for the constants  $a$ ,  $b$ , and  $c$  in equation 8.1. The constant values were determined by solving a set of simultaneous equations shown below:

$$\Sigma Y = na + c\Sigma X^2 \quad (8.2)$$

$$\Sigma X^2 Y = a\Sigma X^2 + c\Sigma X^4 \quad (8.3)$$

$$b = \frac{\Sigma XY}{\Sigma X^2} \quad (8.4)$$

where

$$x = X - \bar{X}$$

$X$  = wind speed, mph

$$\bar{X} = (X_{\max} - X_{\min})/2$$

$Y$  = field voltage, volts

$n$  = number of steps

Calculations were done using a Fortran program shown in Figure 8.1.

The following parabolic equation was found representing the data shown in Table 3.1:

$$Y = 21.31 + 0.07X + 0.0569X^2 \quad (8.5)$$

where

Y = field voltage (volts)

X = wind speed (mph)

```

C CURVE.FOR
C DECEMBER 21, 1984
C
C THIS PROGRAM USES THE EXTENDED METHOD OF LEAST SQUARES TO
C DETERMINE THE VALUES OF THE CONSTANTS A, B, AND C IN THE
C PARABOLIC EQUATION Y=A+BX+CX**2.
C
C LOGICAL*1 FILNAM(11),ERR
C TYPE 20
20 FORMAT(//,' THIS PROGRAM IS TO FIT THE FIELD VOLTAGE/WIND')
TYPE *, ' SPEED DATA BY THE PARABOLIC CURVE Y=A+BX+CX**2.'
TYPE 40
40 FORMAT('ENTER THE NUMBER OF DATA POINTS TO BE READ. ',$,)
ACCEPT 60, JDATPT
45 TYPE 50
50 FORMAT('ENTER THE MINIMUM WIND SPEED FROM YOUR DATA.',$,)
ACCEPT 120, E
IF(E.GT.0.1) GOTO 70
TYPE 100
TYPE *, 'YOU FORGOT THE DECIMAL. ENTER AGAIN.'
GOTO 45
60 FORMAT(I4)
70 TYPE 80
80 FORMAT('ENTER THE DATA FILE NAME TO BE READ.(DATA FORMAT IS',
     ' F8.4) ',$,)
Q CALL GETSTR(5,FILNAM,10,ERR)
TYPE 100
100 FORMAT('*****')
TYPE *, 'INSERT DISK WITH DATA FILE IN DISK DRIVE BY1'
PAUSE 'WHEN READY HIT "RETURN"'
OPEN(UNIT=1,NAME=FILNAM,TYPE='OLD',READONLY)
X2SUM=0
X2YSUM=0
YFVSUM=0
XSUM=0
X4SUM=0
D=(JDATPT-1)/2.           ! D=(MAXIMUM - MINIMUM WIND SPEED)/2
DO 150 I=0,JDATPT-1
READ(1,120) YFVOLT
120 FORMAT(F8.4)

```

```

YFVSUM=YFVSUM+YFVOLT
X=I-D
XSUM=XSUM+X
XYSUM=XYSUM+(X*YFVOLT)      ! X*YFVOLT=XY
X2=X**2
X2SUM=X2SUM+X2
X2YSUM=X2YSUM+(X2*YFVOLT)    ! X2*YFVOLT=X2Y
X4SUM=X4SUM+(X2**2)          ! X2**2=X4
150  CONTINUE
TYPE 100
TYPE 160
160  FORMAT('0'                 SUM OF VARIABLES')
TYPE 180
180  FORMAT('0FLD VOLTAGE      X      XY      X2',
           'X2Y      X4')
200  TYPE 200,YFVSUM,XSUM,XYSUM,X2SUM,X2YSUM,X4SUM
FORMAT('0',4X,F8.4,4X,F9.2,2X,F9.2,2X,F9.2,2X,F9.2)
B=XYSUM/X2SUM
AN=(YFVSUM*X4SUM-X2SUM*X2YSUM) ! A NUMERATOR
AD=(JDATPT*X4SUM-X2SUM**2)     ! A OR C DENOMINATOR
CN=(JDATPT*X2YSUM-X2SUM*YFVSUM) ! : NUMERATOR
F=D+E
A=AN/AD
C=CN/AD
TYPE 220
FORMAT('0THE EQUATION FOR THE CURVE IS:')
TYPE 240,C,(-2*F*C+B),(-B*F+A+C*F**2)
240  FORMAT('0Y =',F9.4,' X**2 +',F9.2,' X +',F9.2)
TYPE 260
260  FORMAT(1,'0Y = FIELD VOLTAGE')
TYPE 280
280  FORMAT('0X = WIND SPEED (MPH)')
STOP
END

```

X. APPENDIX B

---

FILE: CONTROL.MEMR HEWLETT-PACKARD: 8040B Answer) cr

Fri, 4 Jan 1905, 9:38

LOCATION OBJECT CODE LINE SOURCE LINE

```

1 "804B"
2 x
3 x
4 x
5 x THIS IS A CONTROL PROGRAM WRITTEN IN MCS-48 ASSEMBLY LANGUAGE.
6 x THIS PROGRAM IS PLACED ON A 2716 EPROM AND IS RUN BY
7 x AN "8035" MICROPROCESSOR. PORT 1, P1(0-4) ARE ASSIGNED
8 x TO SELECT THE PROPER FIELD VOLTAGE . PORT 2, P2(0-3) ARE
9 x USED TO EXPAND I/O PORTS.
10 x PORT 2, P2(4) CONTROLS THE BRAKE PILOT LIGHT.
11 x P2(4) LOW = LIGHT OFF. P2(4) HIGH = LIGHT ON.
12 x PORT 2, P2(5) SELECTS BETWEEN INPUT 0 AND 1 OF THE MUX ON
13 x THE ADC0809 A/D CONVERTER.
14 x PORT 2, P2(6) IS TIED TO START CONVERSION(SC) LINE OF
15 x THE A/D. IN ORDER TO CONVERT, SC LINE MUST GO THROUGH A
16 x TRANSITION FROM LOW TO HIGH AND THEN BACK TO LOW AGAIN.
17 x PORT 2, P2(7) CONTROLS THE DC POWER SUPPLY NEEDED FOR
18 x THE FIELD. P2(7) LOW = POWER SUPPLY OFF. P2(7) HIGH = ON.
19 x
20 x
21 x
22 x
23 x
24 x
25 x *-----*-----*-----*-----*
26 x * P27      P26      P25      P24 *-----*
27 x *-----*-----*-----*-----*-----*
28 x *-----*-----*-----*-----*-----*
29 x *-----*-----*-----*-----*-----*
30 x *-----*-----*-----*-----*-----*
31 x
32 x
33 x
34 x
35 x
36 x BECAUSE A "COMPARE INSTRUCTION IS NOT AVAILABLE FOR THE
37 x 8035 MICROPROCESSOR, THE COMPARE OPERATION WAS IMPLEMENTED
38 x BY SUBTRACTION USING 2'S COMPLEMENT ADDITION AND BY USING
39 x CONDITIONAL JUMPS ON THE RESULTING CARRY OR ABSENCE OF CARRY.
40 x IN THE EXAMPLE BELOW IF THE CONTENT OF ACCUMULATOR IS <= VALUE
41 x 3BH, THEN A CARRY IS PRODUCED WHEN THE "ADD" INSTRUCTION IS
42 x EXECUTED. OTHERWISE, IF CONTENT OF ACCUMULATOR IS > THE VALUE
43 x 3BH, NO CARRY IS PRODUCED AND A JUMP TO BRAKE ROUTINE IS MADE.
44 x EXAHPLE:
45 x ADD A, #3BH ;IF CONTENT OF ACCUMULATOR IS > 3BH, THEN
46 x JNC BRAKE ;JUMP TO BRAKE ROUTINE. IF NOT CONTINUE.

```

## LOCATION OBJECT CODE LINE SOURCE LINE

58 \*\*\*\*\*  
59 \* MAIN BODY OF THE PROGRAM IS LISTED BELOW STARTING  
60 \* AT MEMORY LOCATION 0000H.  
61 \*\*\*\*\*  
62 \*  
63 \*  
64 \*  
65 \*  
66 ORG 00H  
0000 0410 67 JHP BEGIN  
68 ORG 07H ;TIMER INTERRUPT VECTOR (ON-BOARD TIMER OVERFLOW  
0007 440F 69 JHP TIMER ;CAUSES A JUMP TO SUBROUTINE AT LOCATION 7 IN  
70 ORG 10H ;MEMORY.)  
0010 5400 71 BEGIN CALL START  
0012 943B 72 CALL INTLZ4  
0014 35 73 BEGIN1 DIS TCNTI  
0015 5420 74 CALL SAMPLE  
0017 5475 75 CALL OVBRK  
0019 E688 76 JNC BRAKE  
001B B621 77 JFO AHEAD  
001D 541A 78 CALL INTLZ1  
001F 0423 79 JMP AHEAD1  
0021 9432 80 AHEAD CALL INTLZ3  
0023 5420 81 AHEAD1 CALL SAMPLE  
0025 C684 82 JZ PWROFF  
0027 5456 83 CALL OSBRAK  
0029 E688 84 JNC BRAKE  
002B 545D 85 CALL MNWND  
002D F684 86 JC PWROFF  
002F 5467 87 CALL PWRON  
88  
0031 A5 89 CLR F1  
0032 5480 90 CALL SAMINT  
0034 9400 91 CALL FLDVOL  
0036 9427 92 BACK2 CALL INTCHK  
0038 C614 93 JZ BEGIN1  
003A 942C 94 CALL INTLZ2  
003C 5420 95 CALL SAMPLE  
003E 9441 96 CALL NOCHNG  
0040 C636 97 JZ BACK2  
0042 9448 98 CALL DECINC  
0044 F664 99 JC HY3T1  
0046 946C 100 CALL HYST2  
0048 E680 101 JNC REVOP2  
004A 9411 102 CALL DECFV  
004C 9427 103 BACK1 CALL INTCHK  
004E C614 104 JZ BEGIN1  
0050 942C 105 CALL INTLZ2  
0052 5420 106 CALL SAMPLE  
0054 9441 107 CALL NOCHNG  
0056 C64C 108 JZ BACK1  
0058 9448 109 CALL DECINC  
005A F670 110 JC HYST3  
005C 946C 111 CALL HYST2  
005E E67C 112 JNC REVOP1  
0060 9450 113 CALL INCfv  
0062 0436 114 JHP BACK2

## LOCATION DIRECT CODE LINE SOURCE LINE

	115	
0070 9454	116 HYST1	CALL HYST
0071 F670	117 INC	TT INC
0072 9451	118	CALL REVOP
0073 0436	119	JMP BACK2
0074 9450	120 INC	CALL INCIV
0075 0436	121	JMP BACK2
	122	
0076 9464	123 HYST3	CALL HYST
0077 F678	124	JC DEC
0078 9474	125	CALL REVOP
0079 044C	126	JMP BACK1
0080 9411	127 DEC	CALL DECFV
0081 044C	128	JMP BACK1
	129	
0082 9474	130 REVOP1	CALL REVOP
0083 044C	131	JMP BACK1
	132	
0084 9474	133 REVOP2	CALL REVOP
0085 0436	134	JMP BACK2
	135	
0086 5434	136 PWROFF	CALL PWROF
0087 0414	137	JMP BEGIN1
	138	
0088 5441	139 BRAKE	CALL BRAK
0089 0414	140	JMP BEGIN1
	141	
	142	
	143 *	
	144 *	
	145 *	
	146 *	
	147 *	
	148 *	
	149 *	
	150 *	
	151 *	
	152 x	
	153 *	
	154 *	
	155 *	
	156 *	
	157 *	
	158 *	
	159 *	
	160 *	
	161 *	
	162 *	
	163 *	
	164 *	
	165 *	
	166 *	
	167 *	
	168 *	
	169 *	
	170 *	
	171 *	

## LOCATION OBJECT CODE LINE SOURCE LINE

```

172 **** ALL THE SUBROUTINES ARE LISTED BELOW STARTING
173 * AT MEMORY LOCATION 0200H.
174 ****
175 ****
176 *
177 *
178 *
179 *
180     ORG 200H
181
0200 D5      182 START    SEL RB1   ;THE MINIMUM WIND SPEED(VW) AT WHICH THE POWER
0201 BA21    183 MOV R2,$21H ;SUPPLY IS TURNED ON IS SET AT 4.0 MPH.
0203 C5      184 SEL RE0
0204 85      185 CLR F0
0205 A5      186 CLR F1
0206 231F    187 MOV A,$1FH ;TURN BRAKE LIGHT ON FOR
0208 3A      188 OUTL P2,A ;OPERATION CHECK.
0209 2300    189 MOV A,$00H ;FIELD VOLTAGE (VF) IS SET TO ZERO.
0208 39      190 OUTL P1,A
020C 560C    191 DETECT   JTI DETECT ;WAIT FOR START SWITCH TO BE DEPRESSED.
020E 83      192 RET
193
020F 25      194 TIMER    EN TCNTI
0210 C5      195 SEL RB0
0211 1E      196 INC R6   ;WIND SPEED (VW) SAMPLING INTERVAL
0212 2332    197 MOV A,$50 ;TIMER ROUTINE.
0214 DE      198 XRL A,R6 ;FOR A 6 MHZ CLOCK, 50 TIMER INTERRUPTS = 1 SEC.
0215 C61B    199 JZ DECR7
Q 0217 93      200 RETR
0218 CF      201 DECR7   DEC R7
0219 93      202 RETR
203
021A D5      204 INTLZ1  SEL RB1   ;THIS ROUTINE WHEN EXECUTED BEFORE THE SAMPLE
021B B64F    205 MOV R0,$4FH ;ROUTINE, INITIALIZES THE SAMPLE ROUTINE TO
021D B70F    206 MOV R1,$0FH ;TAKE A SAMPLE FROM CHANNEL 0 (VW) OF THE ADC
021F 93      207 RETR   ;WITH POWER AND BRAKE OFF.
208
0220 D5      209 SAMPLE   SEL RB1
0221 FB      210 MOV A,R0
0222 3A      211 OUTL P2,A
0223 F9      212 MOV A,R1   ;A SAMPLE IS TAKEN UNDER THE CONDITIONS SPECIFIED
0224 3A      213 OUTL P2,A ;BY REGISTERS R1 AND R2.
0225 C5      214 SEL RB0   ;THE DIGITIZED SAMPLE IS STORED IN R3.
0226 B601    215 MOV R0,$01H
0228 9477    216 CALL DELAY
022A 262A    217 CONVRT JNTO CONVRT
022C 0C      218 MOVD A,P4
022D 0C      219 MOVD A,P4
022E AB      220 MOV R3,A
022F DD      221 MOVD A,P5
0230 47      222 SWAP A
0231 4B      223 ORL A,R3
0232 AB      224 MOV R3,A
0233 B3      225 RET
226
0234 B638    227 PWR0F   JFO GOON3
0236 4439    228 JHP GOON4

```

FILE: CONTRL.MEPR            HEWLETT-PACKARD: 804P Asembler  
 LOCATION OBJECT CODE LINE       SOURCE LINE

```

    0238 95        229 GOON3 CPL F0
    023F 2300      230 GOON4 MOV A,$00H ;SET VF=0
    023F 39        231 OUTL P1,A
    023C 9438      232 CALL INTLZ4
    023E BA21      233 MOV R2,$21H ;SET MINIMUM VW TO TURN THE POWER ON AT 4.0 MPH.
    0240 83        234 RET
    235
    0241 5467      236 BRAK CALL PWRON
    0243 231F      237 MOV A,$1FH ;APPLY FULL VF.
    0245 39        238 OUTL P1,A
    0246 7650      239 JF1 GOON2
    0248 85        240 CPL F1
    0249 BB0A      241 MOV R0,$0AH ;10 SEC. DELAY.
    024B 9477      242 CALL DELAY
    024D 239F      243 MOV A,$FFH ;TURN THE BRAKE ON
    024F 3A        244 OUTL P2,A
    0250 D5        245 GOON2 SEL RB1
    0251 BBFF      246 MOV R0,$0FFH ;INITIALIZE FOR SAMPLING CHANNEL 1 WITH
    0253 B9BF      247 MOV R1,$0BFH ;POWER AND BRAKE ON.
    C 0255 83       248 RET
    249
    O 0256 37       250 OSBRAK CPL A ;OVER SPEED ROUTINE.
    O 0257 17       251 INC A ;CHECK FOR MAXIMUM VW OF 29.0 MPH.
    O 0258 AB       252 MOV R3,A
    O 0259 97       253 CLR C ;3B= 59*5/255= 1.152V, i.e. 1.152V/40mV/mph=29 MPH,
    O 025A 033B     254 ADD A,$3BH ; 10
    C 025C 83       255 RET
    256
    C 025D FB       257 MINWND MOV A,R3 ;CHECK FOR MINIMUM VW CONDITION.
    025E 97        258 CLR C
    025F F7        259 RLC A ;MULTIPLY BY CONSTANT 4.0 FOR BETTER RESOLUTION
    0260 97        260 CLR C ;AND FOR PROGRAMMING EASE.
    0261 F7        261 RLC A
    0262 AC        262 MOV R4,A
    0263 97        263 CLR C
    0264 D5        264 SEL RB1
    0265 6A        265 ADD A,R2
    0266 83        266 RET
    267
    C 0267 B674     268 PWRON JFO CONTNU
    0269 95        269 CPL F0
    026A 238F     270 MOV A,$0FH ;TURN POWER ON.
    026C 3A        271 OUTL P2,A
    026D BB05     272 MOV R0,$0SH ;DELAY 5.0 SEC. FOR POWER SUPPLY STABILIZATION.
    026F 9477     273 CALL DELAY
    0271 D5        274 SEL RB1 ;HYSTERESIS FOR TURN ON AND OFF CONDITION.
    0272 BA1C     275 MOV R2,$1CH
    0274 83        276 CONTNU RET
    277
    C 0275 C678     278 OVBRAK JZ ZROCHK ;OVER VOLTAGE ROUTINE.
    0277 07        279 DEC A ;CHECK FOR MAXIMUM OUTPUT VOLTAGE OF 4.2 VOLTS.
    0278 17        280 ZROCHK INC A
    0279 AD        281 MOV R5,A ;0D6H =214 ,(214/255)*5 = 4.2 VOLTS
    027A 37        282 CPL A 10
    027B 17        283 INC A
    027C 97        284 CLR C
    027D 03D6     205 ADD A,$0D6H
  
```

Fri, 4 Jan 1985, 9:39 PAGE 5

LOCATION	OBJECT CODE	LINE	SOURCE LINE
027F 83	286	RET	
	287		
0280 C5	288	SAHINT SEL R80	
0281 AF15	289	MOV R7,\$15H	
0283 BE00	290	MOV R6,\$00H	
0285 45	291	STOP TCNT ;SET UP TIMER FOR SAMPLING INTERVAL	
0286 27	292	CLR A ;OF 10 SEC.	
0287 62	293	MOV T,A	
0288 25	294	EN TCNTI	
0289 55	295	STRI T	
028A 83	296	RET	
	297		
	298	ORG 400H	
	299		
0400 BA25	300	FLDVOL MOV R2,\$25H	
0402 FC	301	HERE MOV A,R4	
0403 97	302	CLR C	
0404 6A	303	ADD A,R2	
0405 F60D	304	JC FLDSET ;SET R2 =25H , "H STANDS FOR A HEX VALUE"	
0407 FA	305	MOV A,R2 ;FOR i =0,31	
0408 D306	306	ADD A,\$6H ;R2=R2 + 6IH	
040A AA	307	MOV R2,A ;IF VW (= R2 THEN JUMP TO FLDSET	
040B B402	308	JMP HERE ;IF NOT JUMP TO HERE.	
040D FA	309	FLDSET MOV A,R2	
040E E3	310	MOV P3 A,EA	
040F 39	311	OUTL P1,A	
0410 83	312	RET	
	313		
0411 23FA	314	DECVF MOV A,\$-6H	
0413 6A	315	ADD A,R2 ;DECREMENT VF.	
0414 AA	316	MOV R2,A	
0415 37	317	CPL A	
0416 17	318	INC A ;CHECK FOR MAX VF.	
0417 97	319	CLR C	
0418 03DF	320	ADD A,\$0DFH	
041A E65D	321	JNC CORECT	
041C FA	322	MOV A,R2	
041D D31F	323	XRL A,\$1FH ;CHECK FOR MIN VF.	
041F 960D	324	JNZ FLDSET	
0421 2306	325	MOV A,\$6H	
0423 6A	326	ADD A,R2	
0424 AA	327	MOV R2,A	
0425 B40D	328	JMP FLDSET	
	329		
0427 27	330	INTCHK CLR A	
0428 DF	331	XRL A,R7 ;CHECK TO SEE IF 10 SEC. IS UP,	
0429 C62C	332	JZ INTLZ2 ;IF YES, TAKE A NEW VW SAMPLE.	
0428 83	333	RET	
	334		
042C D5	335	INTLZ2 SEL RB1 ;THIS ROUTINE WHEN EXECUTED BEFORE	
042D B8EF	336	MOV R0,\$0DEFH ;SAMPLE ROUTINE CAUSES A SAMPLE	
042F B9AF	337	MOV R1,\$0AFH ;TO BE TAKEN FROM CHANNEL 1 WITH POWER	
0431 93	338	RETR ;ON AND BRAKE OFF.	
	339		
0432 F5	340	INTLZ3 SEL RB1 ;THIS ROUTINE WHEN EXECUTED BEFORE	
0433 B8CF	341	MOV R0,\$0CFH ;SAMPLE ROUTINE CAUSES A SAMPLE	
0435 B9BF	342	MOV R1,\$0FH ;TO BE TAKEN FROM CHANNEL 0 WITH POWER	

LOCATION	OBJECT CODE	LINE	SOURCE LINE
	0437 93	343	RETR ;ON AND BRAKE OFF.
		344	
	0438 05	345 JNTL74	SEL R81 ;THIS ROUTINE WHEN EXECUTED BEFORE
	0439 006F	346 MOV R1,16FH	;SAMPLE ROUTINE CAUSES A SAMPLE TO
	043H 022F	347 MOV R1,02FH	;BE TAKEN FROM CHANNEL 1 WITH POWER
	043D 230F	348 MOV A,00FH	;OFF AND BRAKE OFF.
	043F 3A	349 OUT_ P2,A	
	0440 93	350 RETR	
		351	
	0441 C644	352 NUCING	J2 SKIP
	0443 07	353 DEC A	;Von (NEW SAMPLE OF V <sub>o</sub> ) IS COMPARED
	0444 17	354 SKIP INC A	;WITH Vop (PREVIOUS SAMPLE OF V <sub>o</sub> ),
	0445 AB	355 MOV R3,A	;TO SEE IF THERE HAS BEEN A CHANGE
	0446 DD	356 XRL A,R5	;IN Von.
	0447 83	357 RET	
		358	
C	0448 FB	359 DECINC	MOV A,R3
C	0449 2D	360 XCH A,R5	
C	044A AB	361 MOV R3,A	
C	044B 37	362 CPL A	;CHECK TO SEE WHETHER Von IS GREATER
C	044C 17	363 INC A	;THAN OR LESS THAN Vop.
C	044D 97	364 CLR C	
C	044E 6D	365 ADD A,R5	
C	044F 83	366 RET	
C		367	
O	0450 2306	368 INCFV	MOV A,#+6H
O	0452 6A	369 ADD A,R2	;INCREMENT VF.
O	0453 AA	370 MOV R2,A	
O	0454 37	371 CPL A	
O	0455 17	372 INC A	
O	0456 97	373 CLR C	
O	0457 03DF	374 ADD A,00FH	;CHECK FOR MAXIMUM VF. THERE IS NO NEED TO CHECK
O	0459 E65D	375 JNC CORECT	;FOR MINIMUM VF HERE, BECAUSE THE PROGRAM ALWAYS
O	045B 840D	376 JHP FLDSET	;INITIALLY INCREMENTS THE VF WHEN Von > Vop.
O		377	
	045D BADF	378 CORECT	MOV R2,00FH
	045F 23DF	379 MOV A,00FH	
	0461 E3	380 MOVP3 A,RA	;SETS UP MAXIMUM LIMITS FOR VF.
	0462 39	381 OUTL P1,A	
	0463 83	382 RET	
		383	
	0464 FB	384 HYST	MOV A,R3
	0465 0303	385 ADD A,#3	;CHECK TO SEE IF Von >= Vop+3.
	0467 37	386 CPL A	;i.e. CHECK TO SEE IF V <sub>o</sub> HAS INCREASED BY
	0468 17	387 INC A	;THREE VOLTS.
	0469 97	388 CLR C	;i.e. CHECK TO SEE IF POWER OUTPUT HAS INCREASED
	046A 6D	389 ADD A,R5	;BY AT MOST 300 WATTS.
	046B 83	390 RET	
		391	
	046C FD	392 HYST2	MOV A,R5
	046D 0303	393 ADD A,#3	;CHECK TO SEE IF Von < Vop-3.
	046F 37	394 CPL A	;i.e. CHECK TO SEE IF V <sub>o</sub> HAS DECREASED BY
	0470 17	395 INC A	;THREE VOLTS.
	0471 97	396 CLR C	;i.e. CHECK TO SEE IF POWER OUTPUT HAS DECREASED
	0472 6B	397 ADD A,R3	;BY AT MOST 300 WATTS.
	0473 83	398 RET	
		399	

## LOCATION OBJECT CODE LINE SOURCE LINE

0474 FB	400	REVOP	MOV A,R3
0475 AD	401		MOV RS,A
0476 83	402		RET
	403		
0477 27	404	DELAY	CLR A
0478 B900	405		MOV R1,\$00H
047A 62	406		MOV T,A
047B 55	407		STRY T
047C 1680	408	IN	JTF OUT
047E 847C	409		JMP IN
0480 19	410	OUT	INC R1
0481 2332	411		MOV A,\$50
			;EXAMPLE FOR A 5.0 SEC. DELAY,
0483 D9	412		XRL A,R1
0484 967C	413		JNZ IN
0486 EB77	414		DJNZ R0,DELAY
0488 65	415		STOP TCNT
0489 83	416		RET
	417		
	418		
0325 00FFFFFF	419		ORG 325H
	420		HEX 00,FF,FF,FF,FF,01,FF,FF,FF,FF,02,FF,FF,FF,FF
	421		ORG 337H
0337 03FFFFFF	422		HEX 03,FF,FF,FF,FF,04,FF,FF,FF,FF,05,FF,FF,FF,FF
	423		ORG 349H
0349 06FFFFFF	424		HEX 06,FF,FF,FF,FF,FF,07,FF,FF,FF,FF,FF,08,FF,FF,FF
	425		ORG 35BH
035B 09FFFFFF	426		HEX 09,FF,FF,FF,FF,FF,0A,FF,FF,FF,FF,0B,FF,FF,FF
	427		ORG 36DH
036D 0CFFFFFF	428		HEX 0C,FF,FF,FF,FF,FF,0D,FF,FF,FF,FF,FF,0E,FF,FF,FF
	429		ORG 37FH
037F 0FFFFFFF	430		HEX 0F,FF,FF,FF,FF,FF,10,FF,FF,FF,FF,11,FF,FF,FF
	431		ORG 391H
0391 12FFFFFF	432		HEX 12,FF,FF,FF,FF,FF,13,FF,FF,FF,FF,14,FF,FF,FF
	433		ORG 3A3H
03A3 15FFFFFF	434		HEX 15,FF,FF,FF,FF,FF,16,FF,FF,FF,FF,17,FF,FF,FF
	435		ORG 3B5H
03B5 18FFFFFF	436		HEX 18,FF,FF,FF,FF,FF,19,FF,FF,FF,FF,1A,FF,FF,FF
	437		ORG 3C7H
03C7 1BFFFFFF	438		HEX 1B,FF,FF,FF,FF,FF,1C,FF,FF,FF,FF,1D,FF,FF,FF
	439		ORG 3D9H
03D9 1EFFFFFF	440		HEX 1E,FF,FF,FF,FF,FF,1F

Errors= 0